DISSERTATION

A RETINAL CONTRIBUTION TO CHRONIC OPIOID-INDUCED SLEEP/WAKE DYSFUNCTION

Submitted by

Nikolas Bergum

Department of Biomedical Sciences

In partial fulfillment of the requirements

For the Degree of Doctor of Philosophy

Colorado State University

Fort Collins, Colorado

Fall 2023

Doctoral Committee:

Advisor: Jozsef Vigh

Soham Chanda
Shane Hentges
Brent Myers

ABSTRACT

A RETINAL CONTRIBUTION TO CHRONIC OPIOID-INDUCED SLEEP/WAKE DYSFUNCTION

Light is among the most important environmental factors that regulate mammalian sleep/circadian behaviors. Melanopsin-expressing intrinsically photosensitive retinal ganglion cells (ipRGCs) transmit environmental light information to key sleep/circadian centers in the brain through a process known as photoentrainment. Interestingly, past studies have revealed that ipRGCs express μ-opioid receptors (MORs), the primary molecular target for opioid analgesics. Furthermore, MOR agonists can directly inhibit ipRGC firing. Therefore, we hypothesize that opioid drugs acting on MORs expressed by ipRGCs could disrupt ipRGC-mediated regulation sleep/wake rhythms in response to environmental light/dark cycles. To test this idea, we need to confirm that morphine reaches the mouse retina following systemic delivery. To accomplish this, tissue (retina, brain and serum) was collected from mice following intraperitoneal morphine administration. Importantly, results from this study show that systemically administered morphine selectively accumulates in the mouse retina, but not the serum or the brain. To test the role that MORs expressed by ipRGCs play in opioid-induced dysregulation of sleep/circadian behaviors, we used mini-telemetry devices to assess how chronic morphine alters their sleep/wake behavior in mice. Importantly, we performed these experiments in wildtype mice along with mice lacking MORs exclusively in ipRGCs (McKO). Results from these studies reveal that McKO animals exhibit decreased morphine-induced locomotion compared to controls, which implicates MORs expressed by ipRGCs as a mediator of opioid-induced sleep-wake alterations. Finally, we tested

whether ipRGCs developed cellular tolerance to MOR agonists following chronic exposure to morphine. The lack of cellular tolerance development at the level of solitary ipRGCs provides a potential cellular correlate for the persistent sleep/wake dysfunction commonly attributed to chronic opioid exposure. Taken together, these findings support the idea that opioid accumulation in the eye persistently activate MORs on ipRGCs, continuously altering the ability of ipRGCs to transmit light information to the brain's sleep/wake circuitry. This alteration in photic input to the brain could underlie some of the sleep/wake problems associated with long-term opioid use.

ACKNOWLEDGEMENTS

There are too many people I want to thank for their help and support throughout my graduate studies, however, in the interest of brevity I will do my best to appropriately thank those that have been most instrumental in my personal and professional growth over the past few years.

First, I want to thank family and friends for their love and support over the years; without which this would not have been possible. Next, I want to express my gratitude to MCIN/BMS faculty, staff, and students for providing a rich and supportive environment that has allowed me to develop as a scientist and a person. The value of everyone's camaraderie and support can truly not be overstated.

Additionally, I would like to extend a special thanks to the members of my committee. I want to thank Dr. Shane Hengtes for sparking my interest in opioid pharmacology and to Dr. Soham Chanda for giving me the opportunity to patch my first cell. I would like to express my gratitude to Dr. Brent Myers for his invaluable input on the behavioral studies presented in this document as well as for his patience with regard to my between-experiment shenanigans. Finally, I want to thank Dr. Jozsef Vigh for taking a chance on me, allowing me to join his lab and giving me tools to ask exciting scientific questions. I have thoroughly enjoyed working under his supervision and I value our spirited discussions and shared enthusiasm for neuroscience and electrophysiology.

I also want to take this opportunity to recognize my lab partners-in-crime: Sebastian Pace and Casey-Tyler Berezin. I cannot imagine graduate school without your scientific input and emotional support.

TABLE OF CONTENTS

Chapter 1 – Introduction[1]

1.1 Overview of opioid-induced sleep/wake dysfunction

Chronic opioid use has been shown to disrupt healthy sleep/wake behavior, which often manifests as insomnia and daytime fatigue (Hartwell et al., 2014; Hallinan et al., 2019; Rosen et al., 2019; Huhn and Finan, 2021). The sleep problems associated with chronic opioid use are a significant risk factor for drug abuse, relapse and depression (Garnaat et al., 2017; Tripathi et al., 2020). Chronic pain patients are especially susceptible to the negative consequences associated with opioid-induced sleep problems, as sleep loss can exacerbate existing pain symptoms (Roehrs et al., 2006). Despite the breadth of literature documenting the negative effects of opioid drugs on sleep, the mechanism by which opioids disrupt sleep remains poorly understood. Sleep's essential role in the successful treatment of both pain and opioid use disorders highlights the importance of developing a mechanistic understanding of how opioid drugs disrupt healthy sleep/wake behaviors.

Opioid drugs such as morphine exert much of their clinically relevant actions via activation of the μ-opioid receptor (MOR), with lesser contributions from interactions with the κ- (KOR) and δ-opioid receptors (DOR) (Andersen et al., 2003). These are G-protein coupled receptors that associate with inhibitory G-proteins to inhibit neuronal firing and adenylate cyclase-mediated signaling (Contet et al., 2008; Kieffer and Evans, 2009; Pasternak and Pan, 2013; Williams et al., 2013). While the MOR is credited with mediating the analgesic and hedonic

---

[1] Bergum N, Berezin CT, Vigh J. A retinal contribution to opioid-induced sleep disorders? *Front Neurosci*, 16, 981939. doi: 10.3389/fnins.

properties of opioids, the KOR is implicated in the dysphoria sometimes associated with opioid well as their anxiolytic properties (Kieffer and Evans, 2009). While it is important to consider use (Kieffer and Evans, 2009). DORs have also been linked to the hedonic value of opioids as the potential contributions of all opioid receptor classes when dissecting the mechanisms that underlie chronic opioid-related sleep/wake problems, the effects of opioid drugs are primarily mediated by acting at the MOR.

Many of the sleep centers in the brain express opioid receptors and thus have the potential to contribute to opioid-induced sleep/wake changes (Eacret et al., 2020). Homeostatic as well as circadian components underlie an organism's sleep drive (Deboer, 2018). The homeostatic drive for sleep builds the longer that the organism is awake, while circadian sleep regulation is often entrained to external factors, perhaps most notably environmental light (LeGates et al., 2014). Importantly, light has been shown to directly influence sleep onset as well as sleep homeostasis (LeGates et al., 2014).

Given the importance of light in regulating sleep/wake behavior, this review assesses how opioid drugs alter the light-mediated regulation of sleep/wake behavior. Specifically, we examine the evidence that light-sensitive sleep/circadian centers within the central nervous system (CNS) contribute to the development of opioid-related sleep disturbances. In mammals, the retina is responsible for conveying environmental light into neuronal signals that can be interpreted by the brain for both image forming and non-image forming visual functions. Non-image forming visual functions, such as the light-mediated regulation of sleep/wake behavior, are dependent on intrinsically photosensitive retinal ganglion cells (ipRGCs) (Tsai et al., 2009; Schmidt et al., 2011; LeGates et al., 2014). Six subtypes of ipRGCs exist in mice (M1-M6), with each subtype exhibiting specific morphological and physiological properties as well as

behavioral roles (Schmidt et al., 2011; Hu et al., 2013; LeGates et al., 2014; Li and Schmidt, 2018; Aranda and Schmidt, 2021). Similarly, five ipRGC subtypes (M1-M5) have been identified in rat and evidence suggests that M1-M4 subtypes exist in the human retina (Aranda and Schmidt, 2021). Critically, mouse studies have demonstrated that ipRGCs project to a number of brain regions that are involved in both the circadian and homeostatic regulation of sleep/wake cycles (Hattar et al., 2006; Chen et al., 2011; Schmidt et al., 2011; LeGates et al., 2014). For the purposes of this review, we will focus on M1 ipRGCs and their projection areas (Figure 1.1) given their functional role in the light-mediated regulation of sleep/wake behavior (Hattar et al., 2006; Schmidt et al., 2011; LeGates et al., 2014; Li and Schmidt, 2018; Aranda and Schmidt, 2021).

Many clinical studies have noted the negative impact that chronic opioid use can have on sleep/wake behavior (Huhn and Finan, 2021). Opioid receptors have been shown to be highly expressed in many regions of the brain that are involved in sleep/wake including circadian and sleep centers in the hypothalamus, as well as the locus coeruleus and the dorsal raphae nucleus (Eacret et al., 2020). Due to widespread opioid receptor expression within the brain's complex sleep/wake circuitry, it is daunting to try and elucidate a comprehensive mechanism by which opioids disrupt sleep/wake. However, many animal studies point to opioid-induced alterations in an animal's ability to synchronize their sleep/wake behaviors to the environmental light cycles (ie. photoentrainment) (Cutler et al., 1999; Mistlberger and Holmes, 1999; Byku and Gannon, 2000; Meijer et al., 2000; Tierno et al., 2002; Vansteensel et al., 2003, 2005; Pačesová et al., 2015, 2016). Specifically, opioid drugs have been shown to shift the onset of circadian behavior (phase-shift), desynchronizing an animal's sleep/wake activity with respect the environmental light cycle (Meijer et al., 2000; Vansteensel et al., 2005; Pačesová et al., 2015). While several

studies attribute the opioid-induced phase-shifts to drug effects on sleep and circadian centers within the hypothalamus (Meijer et al., 2000; Vansteensel et al., 2005; Pačesová et al., 2015), the exact mechanism by which opioids can alter photoentrainment remains unclear.

In this review, we assess the evidence that opioids could alter sleep/wake behavior by acting directly on M1 ipRGCs and their projection regions involved in the light-mediated regulation of sleep/wake cycles. These projection regions can be distinguished based on their function within the context on sleep/wake regulation through parallel pathways (Zhang et al., 2021). ipRGCs photoentrain circadian centers such as the suprachiasmatic nucleus (SCN) of the hypothalamus to synchronize sleep/wake cycles to environmental light conditions (Schmidt et al., 2011; LeGates et al., 2014; Rupp et al., 2019; Aranda and Schmidt, 2021). Additionally, the acute light-induced regulation of sleep depends on ipRGC inputs to the preoptic area (POA) of the hypothalamus (Schmidt et al., 2011; LeGates et al., 2014; Rupp et al., 2019; Aranda and Schmidt, 2021; Zhang et al., 2021).

1.2 Intrinsically photosensitive retinal ganglion cells (ipRGCs)

While there is no clinical evidence that opioids alter image forming visual functions, Grace et al., 2010 showed that pupillary light reflex (PLR) was altered in buprenorphine-treated patients. Since PLR has been shown to be ipRGC-dependent (Lucas et al., 2001, 2003; Güler et al., 2008), this suggests that opioids could alter ipRGC activity in humans. In support of this idea, M1-M3 ipRGCs have been shown to express MORs in rodents (Cleymaet et al., 2019) and MOR-selective agonist [D-Ala2, N-MePhe4, Gly-ol]-enkephalin (DAMGO) reduced ipRGC-mediated PLR in mice (Cleymaet et al., 2021). Moreover, MOR-selective antagonist D-Phe-Cys-Tyr-D-Trp-Arg-Thr-Pen-Thr-NH2 (CTAP) as well as selective ablation of MORs from ipRGCs enhanced dim light-evoked PLR (Cleymaet et al., 2021). Thus, both clinical and preclinical

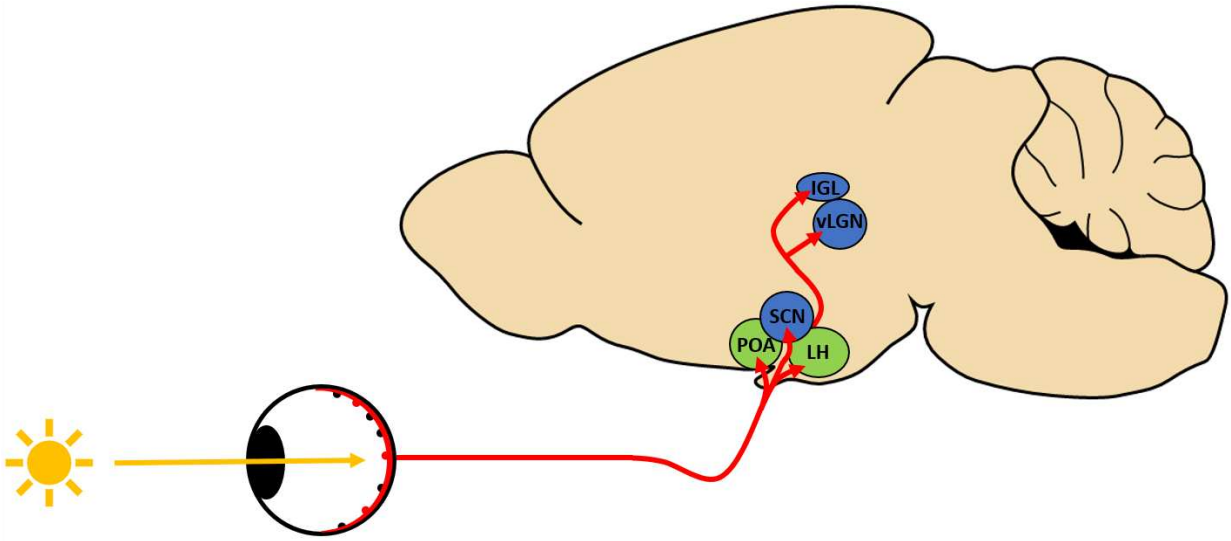

Figure 1.1 Schematic depicting intrinsically photosensitive retinal ganglion cell (ipRGC) projection regions implicated in light-induced regulation of sleep/wake behavior. ipRGCs (red) send light information via the retinohypothalamic tract to sleep/circadian centers in the hypothalamus (POA: Preoptic area, SCN: suprachiasmatic nucleus, LH: lateral hypothalamus) as well as to specific thalamic targets (IGL: inner geniculate leaflet, vLGN: ventrolateral geniculate nucleus). Many of these regions express opioid receptors that could underlie the opioid-induced alterations in photoentrainment. Blue: circadian photoentrainment centers; green: regions involved in light-induced sleep.

studies point to a potential opioid-mediated effect on ipRGC function. Importantly, functional studies revealed that light-evoked ipRGC firing activity is suppressed by application of the MOR-selective agonist DAMGO via modulation of voltage-gated potassium and calcium currents (Cleymaet et al., 2019). This would suggest that opioid drugs can, in fact, modulate ipRGC activity via direct interactions with MORs expressed by ipRGCs. Significantly, behavioral studies also suggest that MORs expressed by ipRGCs play a role in regulating sleep/wake homeostasis via their interactions with the circadian oscillations in retinal β-endorphin expression (Berezin et al., 2022). These findings point to the idea that opioid-induced alteration of ipRGC activity impacts an organism's ability to transmit environmental light information to the brain's sleep/circadian centers.

1.3 Circadian photoentrainment

1.3.1 Suprachiasmatic nucleus of the hypothalamus

Perhaps the region that has been most heavily implicated with the phase-shifting activity of opioid drugs is the SCN, however its exact role remains controversial (Meijer et al., 2000; Vansteensel et al., 2005; Pačesová et al., 2015, 2016). Fentanyl (a potent MOR agonist) has been shown shift the circadian phase of wheel-running activity (Meijer et al., 2000), presumably by altering light input, firing rate and circadian gene expression of hamster SCN neurons (Vansteensel et al., 2005). Interestingly, acute but not chronic morphine exposure resulted in a shift in Per1 gene expression within the rat SCN (Pačesová et al., 2015, 2016).

Other studies have found that DOR agonists, not MOR or KOR agonists, induced a non-photic phase shift in hamsters (Byku and Gannon, 2000; Byku et al., 2000; Tierno et al., 2002). Byku et al., 2000 showed punctate DOR-labeling surrounding cells in the hamster SCN, indicative of DOR expression within presynaptic axon terminals. These studies suggest that DOR-preferring enkephalins released from the IGL onto the SCN underlie the ability of DOR-selective agonists to advance the circadian phase in hamsters (Byku and Gannon, 2000; Tierno et al., 2002).

Contrastingly, (Cutler et al., 1999) reported that hamster SCN neurons were mostly unresponsive to MOR agonist morphine and enkephalins (which are known agonists of both MORs and DORs). Some studies assessing opioid receptor expression within the CNS corroborate this finding, as MORs and DORs were shown to be undetectable or lowly expressed within the mouse and rat SCN (with some evidence of KOR expression with the ventral SCN) (Mansour et al., 1994a, 1994b; Erbs et al., 2015). While these studies offer different explanations for the SCN's role in mediating opioid-related changes in sleep/wake rhythms, this structure is

likely involved either directly or indirectly. Based on the evidence discussed here, opioids appear to alter gene expression and neuronal activity within the SCN. However, the SCN's involvement in opioid-induced sleep/wake disturbances may not be as significant as contributions from other hypothalamic sleep centers that more robustly express opioid receptors.

1.3.2 Inner geniculate leaflet of the thalamus

The IGL contains enkephalinergic interneurons as well as neuropeptide Y (NPY)-producing neurons that synapse on the SCN (Palus et al., 2017). In rat, enkephalins inhibited synaptic transmission in the IGL and robustly hyperpolarized IGL neurons (Palus et al., 2017). Critically, this opioid-induced inhibition was blocked by both MOR- and DOR-selective antagonists (Palus et al., 2017). This suggests that both enkephalinergic and NPY-ergic rat IGL neurons express functional MORs and DORs, which makes them susceptible to opioid-induced alterations in neuronal activity (Palus et al., 2017). There is also evidence of MORs in the IGL of mice and DORs in the hamster IGL (Byku et al., 2000; Erbs et al., 2015). Taken together, it is probable that the IGL at least partially mediates the phase-advances associated with systemic opioid administration.

1.3.3 Ventral lateral geniculate nucleus of the thalamus

M1 ipRGCs have also been shown to the vLGN of the thalamus, another region implicated in circadian photoentrainment (Li and Schmidt, 2018; Aranda and Schmidt, 2021). While there is not much functional work regarding opioid receptor activity within this region, there is evidence suggesting the expression of MORs, but not DORs within the vLGN of the thalamus (Mansour et al., 1994b; Erbs et al., 2015). Thus, this region could also play a role in the opioid-driven alterations in sleep/wake.

1.4 Acute light-induced sleep

Acute light-induced regulation of sleep in mice has been shown to be mediated by ipRGC inputs to the hypothalamus, specifically the preoptic area (POA) and the lateral hypothalamus (LH) (Hattar et al., 2006; Lupi et al., 2008; Muindi et al., 2014; Li and Schmidt, 2018).

1.4.1 Preoptic area (POA) of the hypothalamus

The preoptic area, specifically the ventrolateral preoptic area (VLPO), has been studied extensively in regard to its role in sleep (Saper et al., 2010). In rodents, the POA contains neurons that robustly express MOR and KOR, as well as DOR to a lesser degree (Mansour et al., 1994a, 1994b; Erbs et al., 2015). In rats, MOR and KOR mRNA is expressed in many (>85%) of the sleep-promoting neurons in the VLPO (Greco et al., 2008). Indeed, behavioral experiments corroborate this finding, as an infusion of a MOR- and KOR-selective agonists into the VLPO increased wakefulness in rats (Greco et al., 2008). In line with this, another group found that morphine microinjections into the VLPO increased wakefulness and suppressed sleep in rats (Wang et al., 2013). This study also characterized the electrophysiological properties of VLPO neurons, specifically showing that sleep-promoting VLPO neurons were sensitive to morphine-induced inhibition of action potential firing (Wang et al., 2013). The application of MOR- and KOR-selective antagonists confirmed the contributions of both receptor subtypes in the morphine-mediated suppression of firing activity (Wang et al., 2013). These findings provide strong evidence suggesting opioid-induced inhibition of VLPO neurons may underlie the wake-promoting effects of opioid drugs in rats.

Notably, this region contains two separate populations of Gamma Aminobutyric Acid (GABA)-ergic neurons that are thought to be important mediators of sleep. Galanin-expressing GABAergic neurons in the POA are thought to be involved in the homeostatic regulation of

sleep (Ma et al., 2019), however these neurons do not receive photic input from ipRGCs (Zhang et al., 2021). The GABAergic neurons in the POA that have been shown to be light responsive are mostly corticotropin-releasing hormone-expressing cells (Zhang et al., 2021). Thus, further research must be done to dissect how opioids affect the light-responsive and/or homeostatic sleep-active neurons within this brain region to improve our understanding of how (chronic) opioids alter photoentrainment circuitry.

1.4.2 Lateral hypothalamus (LH)

The lateral hypothalamus (LH) has been heavily implicated in both sleep and opioid use disorders (Harris et al., 2005; Tsujino and Sakurai, 2013), making it a logical therapeutic target for substance use disorders (Matzeu and Martin-Fardon, 2020). Orexin-producing neurons in the LH project both to the ventral tegmental area (VTA) and the paraventricular nucleus of the thalamus (PVT), which are involved in reward/addiction and sleep/wake, respectively (Harris et al., 2007; Eacret et al., 2020). Moreover, many of these orexin-expressing LH neurons have been shown to express MORs in rodents (Mansour et al., 1994a, 1994b; Georgescu et al., 2003; Peckham and Traynor, 2006; Erbs et al., 2015). Interestingly, chronic morphine exposure decreased MOR mRNA expression in the LH, while precipitated withdrawal increased MOR mRNA expression (Zhou et al., 2006)(Zhou et al., 2006). Notably, moderate levels of KOR mRNA, but only low levels of DOR mRNA were detected in the LH (Mansour et al., 1994a).

Both endogenous opioid peptides and opioid drugs can suppress excitatory inputs to LH neurons as well as directly inhibit the firing of LH orexin/hypocretin neurons (Li and van den Pol, 2008). Interestingly, chronic opioid exposure also increased the number of orexin-producing neurons in mouse, rat, as well as human subjects (Thannickal et al., 2018; James et al., 2019). Importantly, chronic morphine reduced the opioid-mediated suppression of spike frequency in

LH neurons, suggesting that chronic exposure leads to cellular tolerance (Li and van den Pol, 2008). This reduction in the effects of morphine on LH neurons suggests that it is unlikely LH neurons underlie the persistent sleep disturbances associated with chronic opioid use. Additionally, LH neurons receive input from light responsive GABAergic neurons in the POA (Sherin et al., 1998; Zhang et al., 2021). As cells in both of these regions robustly express opioid receptors, characterization of opioid receptor expression within light-responsive POA projections to the LH would further clarify the roles of these regions in the context of opioid-induced alterations in sleep/wake behavior.

1.5 Discussion

For opioid drugs to able to suppress ipRGC activity, they must deposit in the retina following systemic exposure. Previous studies have also shown that opioids deposit in the mammalian retina/VH following systemic administration (Husain et al., 2012; Gottås et al., 2016; Maskell et al., 2016; Bergum et al., 2022a). Recently, our group found that morphine similarly deposits in

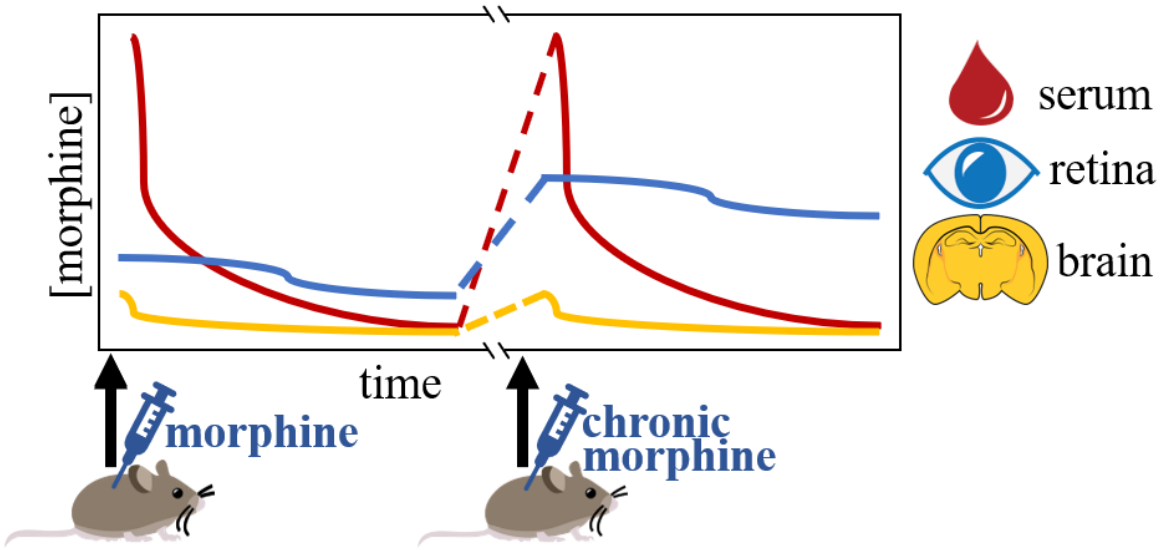

Figure 1.2 Graphical representation of the pharmacokinetic evidence for a retinal contribution to chronic opioid-induced sleep/wake disturbances (as presented in Bergum et al., 2022a). Morphine levels in the retina appear to accumulate following chronic systemic exposure, while levels in both the serum and hypothalamus remain the same.

the mouse retina following systemic injection (Bergum et al., 2022a). Surprisingly, our detailed study showed that retinal morphine levels greatly exceeded the concentrations detected in the hypothalamus (Figure 1.2). In addition to this, we observed sustained increases in morphine levels in the retina compared to the hypothalamus following systemic administration (Bergum et al., 2022a). Retinal morphine levels remained elevated up to 11 hours following systemic exposure, while levels in the hypothalamus dropped to near undetectable levels just 3 hours after administration (Bergum et al., 2022a). This evidence suggests that morphine can persistently activate retinal targets, while morphine's effect on hypothalamic sleep/circadian centers is restricted to just a few hours following systemic administration. Morphine's influence on retinal MOR-expressing cells is further enhanced when we consider that chronic systemic morphine led to morphine accumulation in the mouse retina, but not the hypothalamus (Bergum et al., 2022a). Notably, similar morphine accumulation was not detected in the hypothalamus, indicating that even chronic morphine only alters the activity of opioid receptor-expressing cells within hypothalamic sleep/circadian centers transiently following each systemic exposure (Figure 1.2). Forensic toxicological studies have shown the postmortem vitreous humor samples taken from overdose victims suggest that opioids and their metabolites enter the posterior compartment of the eye (including the retina) following systemic exposure (Wyman and Bultman, 2004). Taken together, these findings provide a strong pharmacokinetic basis for the significant contribution of MOR-expressing ipRGCs in terms of the dysregulation of photoentrainment that is associated with chronic opioid use.

This introduces a novel retinal route by which opioids could persistently alter sleep/wake behavior. This is especially exciting because retinal neurons are far more accessible for targeted interventions compared to sleep/wake centers in the brain. Targeting sleep centers in the brain to

treat opioid-related sleep problems is exceedingly difficult due to the number of brain regions involved in both sleep/wake as well as other opioid-mediated effects on the body. However, the retina represents a unique CNS structure that lies outside the cranial vault, making it far more accessible for targeted therapeutic interventions.

Chapter 2 - Morphine Accumulates in the Retina Following Chronic Systemic Administration[2]

2.1 Introduction

Opioids are some of the most effective analgesics and are therefore commonly used to treat both acute and chronic pain (Williams et al., 2013). Despite their analgesic efficacy, opioid use has a plethora of negative, on-target side effects, including respiratory depression and gastrointestinal problems, as well as a high abuse liability (McQuay, 1999; Benyamin, 2008; Williams et al., 2013). Therefore, developing a better understanding of how opioids deposit in different tissues could elucidate the mechanisms underlying the sometimes-disparate effects of opioid drugs. Understanding drug pharmacokinetics is essential for optimizing treatment options and minimizing risk for patients (Struys et al., 2011).

Morphine is the prototypical opioid against which other opioid drugs are compared (McQuay, 1999; Gharavi et al., 2015; Sheth et al., 2018). It can be administered via several different routes (oral, intravenous, intrathecal, etc.) for perioperative and postoperative pain management (Sheth et al., 2018). Morphine exerts its analgesic effects primarily via interactions with the μ-opioid receptor, with lesser contributions from its binding to the κ- and δ-opioid receptors (Andersen et al., 2003). Moreover, morphine is a major pharmacologically active metabolite of other opioids such as heroin and codeine (Lötsch, 2005; Andersen et al., 2009; Karinen et al., 2009; Maskell et al., 2016, 2019). Thus, studying the pharmacokinetics of morphine in different tissues provides information about the drug's metabolism at different sites of action.

---

[2] Bergum N, Berezin CT, Dooley G, Vigh J. Morphine Accumulates in the Retina Following Chronic Systemic Administration. *Pharmaceuticals*, 15(5), 527. doi: 10.3390/ph15050527.

For morphine to exhibit its antinociceptive effect, it must access opioid receptors located in the central nervous system (CNS) by crossing the tightly regulated blood brain barrier (BBB) (Chaves et al., 2017; Schaefer et al., 2017). As a polar molecule, morphine trafficking across selective barriers such as the BBB is relatively poor. Thus, only a fraction of the morphine present in serum reaches the brain to affect the CNS neurons that mediate opioid-induced antinociception, locomotor activity, and respiratory depression (Oldendorf, 1977; Groenendaal et al., 2007; Boström et al., 2008; Viscusi and Viscusi, 2020). Therefore, it is important to determine the amount of morphine that reaches the target neurons in the CNS to determine appropriate dosages.

Morphine's uptake into the CNS is lower than other opioids due to its low lipid solubility (Oldendorf, 1977). Due to morphine's hydrophilicity, it is thought that morphine transport across the BBB is primarily mediated by ATP-binding cassette (ABC) transporters and solute carrier (SLC) transporters (Gharavi et al., 2015; Yang et al., 2018). Of these transporters, P-glycoprotein (P-gp) is the best studied in regard to its role in mediating morphine efflux from the CNS (Gharavi et al., 2015; Chaves et al., 2017; Yang et al., 2018). Indeed, genetic and pharmacological manipulations of P-gp expression/function show an inverse relationship between P-gp expression/function and the deposition of morphine in the brain (Letrent et al., 1999; Dagenais et al., 2004; Hamabe et al., 2007; L. Mercer and Coop, 2011; Yang et al., 2018). The inner blood–retinal barrier (iBRB), the retinal analog of the BBB, expresses the same transporters found at the BBB, which are similarly thought to regulate drug transport between the retina and systemic circulation (Bévalot et al., 2016; Díaz-Coránguez et al., 2017; Liu and Liu, 2019). Interestingly, the relative expression of P-gp has been shown to be lower in the iBRB

compared to the BBB (Li et al., 2021). However, whether reduced P-gp expression in the retina has functional consequences with regard to retinal morphine deposition remains unknown.

In forensic toxicology, the vitreous humor (VH) of the eye is often used to determine if an opioid overdose contributed to fatality (Scott and Oliver, 1999; Wyman and Bultman, 2004; Sanches et al., 2012; Rees et al., 2013; Bévalot et al., 2016; Gottås et al., 2016). Opioid drugs/metabolites in the VH are protected from postmortem degradation and redistribution in the eye, making it an ideal sample for postmortem toxicological investigations (Scott and Oliver, 1999; Wyman and Bultman, 2004; Sanches et al., 2012; Bévalot et al., 2016). Since these VH samples are mostly collected postmortem from victims of opioid-related deaths, the pharmacokinetics of opioid drugs within the VH are relatively poorly understood compared to other tissues such as the brain and blood (Dahlström and Paalzow, 1975; Scott and Oliver, 1999; Kalvass et al., 2007; Rees et al., 2013; Gottås et al., 2016; Maskell et al., 2016, 2019). Thus, the mechanism that underlies the persistence of opioid drugs (and their metabolites) in the VH is unclear (Hosoya and Tachikawa, 2009; Bévalot et al., 2016).

The present study examines the pharmacokinetics of morphine in the brain (hypothalamus) and retina/VH following systemic administration. Mice have been used extensively to study the analgesic and psychomotor effects of morphine (and other opioid drugs), as well as to examine the pharmacokinetics of opioids in the serum and brain (Handal et al., 2002; Andersen et al., 2009; Koek et al., 2012; Koek, 2014). Thus, we measured the morphine content of mouse retina/VH samples following intraperitoneal (i.p.) morphine injection(s) using liquid chromatography–tandem mass spectrometry (LC-MS/MS). Using this method, we were able to establish a pharmacokinetic profile for morphine in mouse retina/VH. Moreover, we measured the morphine content of the serum and hypothalamus samples from these same mice to

directly compare the pharmacokinetics of morphine in the blood, brain, and retina/VH. Consistent with forensic toxicological findings, these experiments show that morphine persists in the retina/VH for up to 11 h following a systemic injection. Additionally, morphine can accumulate in the retina/VH upon repeat systemic exposure. Significantly, morphine levels in the retina/VH exceed the concentrations found in the brain at all time points. Indeed, the retina shows reduced expression of the morphine extruder P-gp compared to the hypothalamus, which could explain the persistent high morphine levels in the retina following systemic exposure. Given the evidence that some retinal neurons express opioid receptors (Husain et al., 2009; Cleymaet et al., 2019), the accumulation of morphine in the retina could result in changes in image-forming, as well as non-image-forming, visual functions. Thus far, no visual deficits have been reported that would directly implicate opioid-induced interference with image-forming visual circuitry. However, pupillary light reflex (PLR) is altered in opioid-tolerant patients (Grace et al., 2010). Similarly, mice intraocularly injected with the MOR-selective agonist [D-Ala2, N-MePhe4, Gly-ol]-enkephalin (DAMGO) exhibit deficits in PLR (Cleymaet et al., 2021). These observations support the idea that morphine accumulation in the retina could have functional consequences within the eye.

2.2 Results

2.2.1 Morphine Deposits in Mouse Retina Following Systemic Exposure

To examine the pharmacokinetics of morphine in mouse retina, we injected mice with 20 mg/kg morphine i.p. at light onset (Zeitgeber Time (ZT) 0). Whole retina and serum samples were then collected from mice sacrificed at 0.5 (n = 8), 1 (n = 14), 2 (n = 11), 3 (n = 14), 5 (n = 10), 7 (n = 8), 9 (n = 16), and 11 (n = 13) hours following the i.p. injection. The morphine content of these samples was measured using LC-MS/MS. Serum morphine peaked around

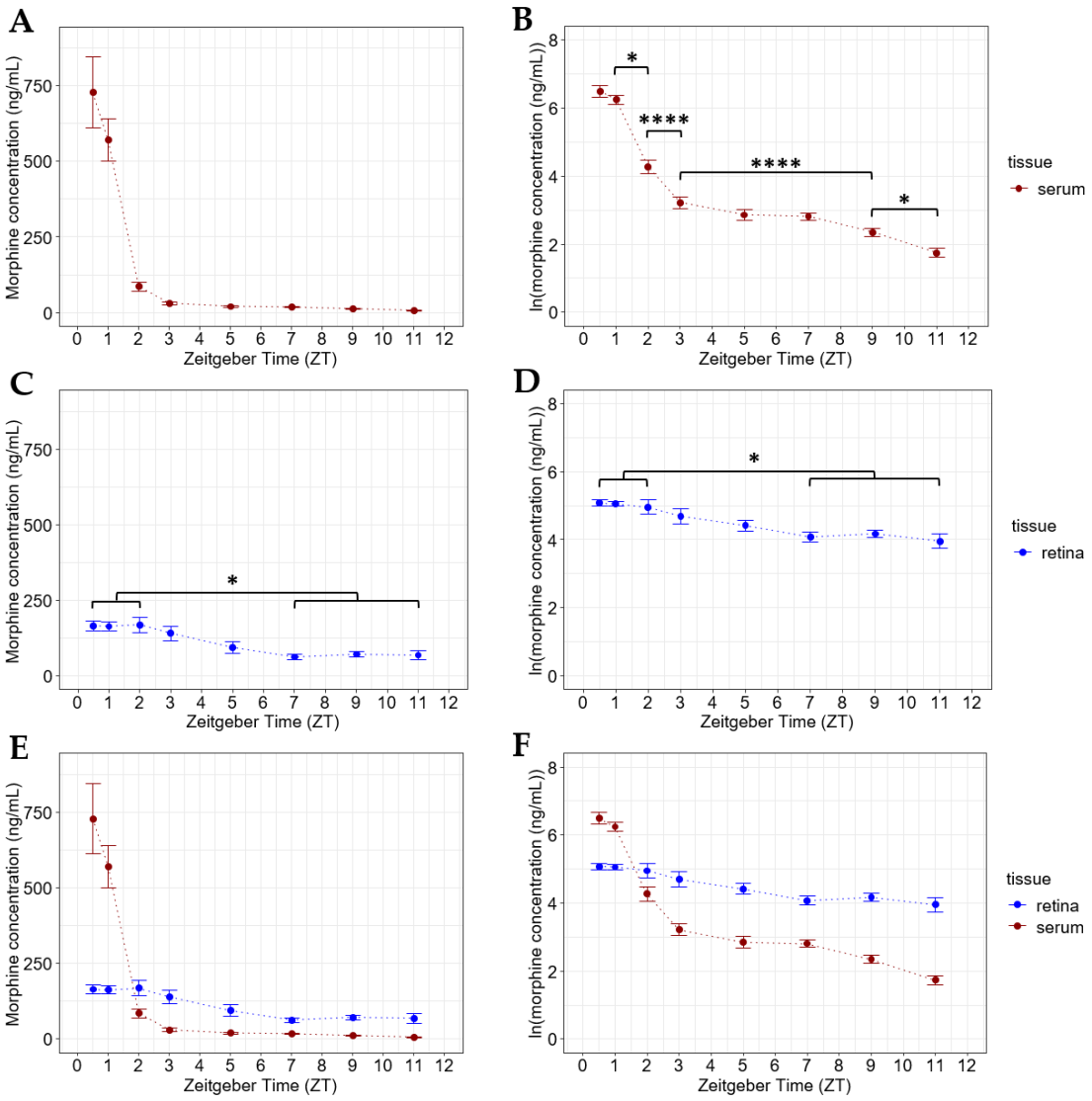

Figure 2.1 Morphine deposits in the retina following systemic exposure. (**A**) Serum morphine concentrations and (**B**) natural logarithmic (ln) transformation of serum morphine concentrations collected from mice sacrificed at specified time points following a 20 mg/kg i.p. morphine injection at light onset (ZT 0). One-way ANOVA with a Tukey post hoc adjustment was performed on an ln scale to compare serum concentrations from animals sacrificed at different time points (* = $p < 0.05$, **** = $p < 0.0001$). (**C**) Retinal morphine concentration and (**D**) ln transformation of retinal morphine collected from the same mice (as in **A** and **B**) sacrificed at specified time points following a 20 mg/kg i.p. morphine injection at light onset (ZT 0). One-way ANOVA with a Tukey post hoc adjustment was performed on an ln scale (* = $p < 0.05$). (**E**) Serum and retinal morphine concentrations and (**F**) ln transform of serum and retinal morphine concentrations collected from mice sacrificed at specified time points following a 20 mg/kg i.p. morphine injection at light onset (ZT 0). Retina and serum samples were collected from the same mice (as in **A**–**D**) within each time point. (**F**) Significant differences exist within each plotted time point between the retinal and serum concentrations ($p < 0.001$). Two-way ANOVA with a tissue *x* ZT interaction and a Tukey post hoc adjustment was performed on an ln scale. Data are presented as the mean ± SEM, with 8–16 mice per group.

0.5–1 h post-injection, before dropping to low levels (< 50 ng/mL) after just 3 h (Figure 2.1A,B). These findings are consistent with past studies that examined the serum pharmacokinetics of morphine in mice (Handal et al., 2002; Andersen et al., 2009; Koek et al., 2012). Importantly, while morphine levels peaked at 0.5–1 h post-injection, serum morphine levels were lowest (3.3 ng/mL) 11 h following the injection (Figure 2.1B).

From these same mice, we collected whole retina/VH samples and measured their morphine content using LC-MS/MS. Given the proximity of the VH to the retina, as well as the small volume of the mouse VH, we were unable to reliably separate the VH from the retina. Thus, the retina samples tested contained both retina and VH. Henceforth, when referring to retina, this represents samples that contain both retina and VH. Interestingly, we detected morphine in the retina of these mice 0.5–11 h following the 20 mg/kg i.p. injection at ZT 0 (Figure 2.1C,D). In contrast to the serum morphine levels from these animals, the retinal morphine levels were highest between 0.5–2 h following the injection before slowly dropping and stabilizing around 70 ng/mL (Figure 2.1C,D). When comparing the serum and retina morphine pharmacokinetics (from samples collected from the same animals), we observed that the serum morphine exceeded the retinal morphine concentration 0.5–1 h following the injection. However, the serum morphine levels soon dropped and remained lower than the morphine concentration in the retina for the remainder of the detection period (Figure 2.1E). There were statistically significant differences ($p < 0.001$) between the serum and retinal morphine concentrations at each time point (Figure 2.1F). Perhaps the most striking finding is that morphine persists in the retina at around 70 ng/mL long after it has dropped to < 10 ng/mL in the serum (Figure 2.1E,F).

2.2.2 Morphine accumulates in Mouse Retina Following Repeated Systemic Exposure

After establishing the pharmacokinetics of morphine in the retina relative to serum following a single systemic injection, we wanted to assess the pharmacokinetics of morphine in these tissues following a subsequent, as well as after chronic, i.p. morphine injections. To assess this, we first collected serum and whole retina samples at various time points (ZT 13: $n = 9$, ZT 14: $n = 8$, ZT 15: $n = 8$, and ZT 23: $n = 8$) from mice treated with 20 mg/kg morphine i.p. at both light onset (ZT 0) and light offset (ZT 12). Like the single injection data, the serum morphine levels exceeded the retinal morphine concentrations an hour (ZT 13) after the second i.p. injection (Figure 2.2A–C). Additionally, the serum morphine dropped significantly below the retinal morphine concentrations 2 h (ZT 14) after the second injection (Figure 2.2C) and remained below the retina morphine levels for the remainder of the detection period (Figure 2.2A–C). Interestingly, when comparing retinal morphine levels both 1 (ZT 13) and 11 (ZT 23) hours after the second morphine injection, we saw an increase ($p < 0.05$) compared to the retinal morphine levels from samples collected 1 (ZT 11) and 11 (ZT 23) hours after just a single i.p. morphine injection (Figure 2.2D). Contrastingly, there were no significant differences (1 h: $p = 0.8238$, 11 h: $p = 0.547$) detected in the serum morphine levels at these same time points when comparing one versus two morphine injections (Figure 2.2D). Next, we wanted to assess how chronic morphine treatment would affect the deposition of morphine in the retina. The chronic morphine paradigm consisted of twice daily 20 mg/kg i.p. morphine injections (at ZT 0 and ZT 12) for 5 or 12 days (McLane et al., 2017). On day 6 or day 13, retina and serum samples were collected from these mice at the specified time points after a final 20 mg/kg i.p. injection at ZT 0. Morphine measurements from these mice revealed increases in retinal morphine concentrations (at all comparable time points) between the mice treated with just a single morphine injection

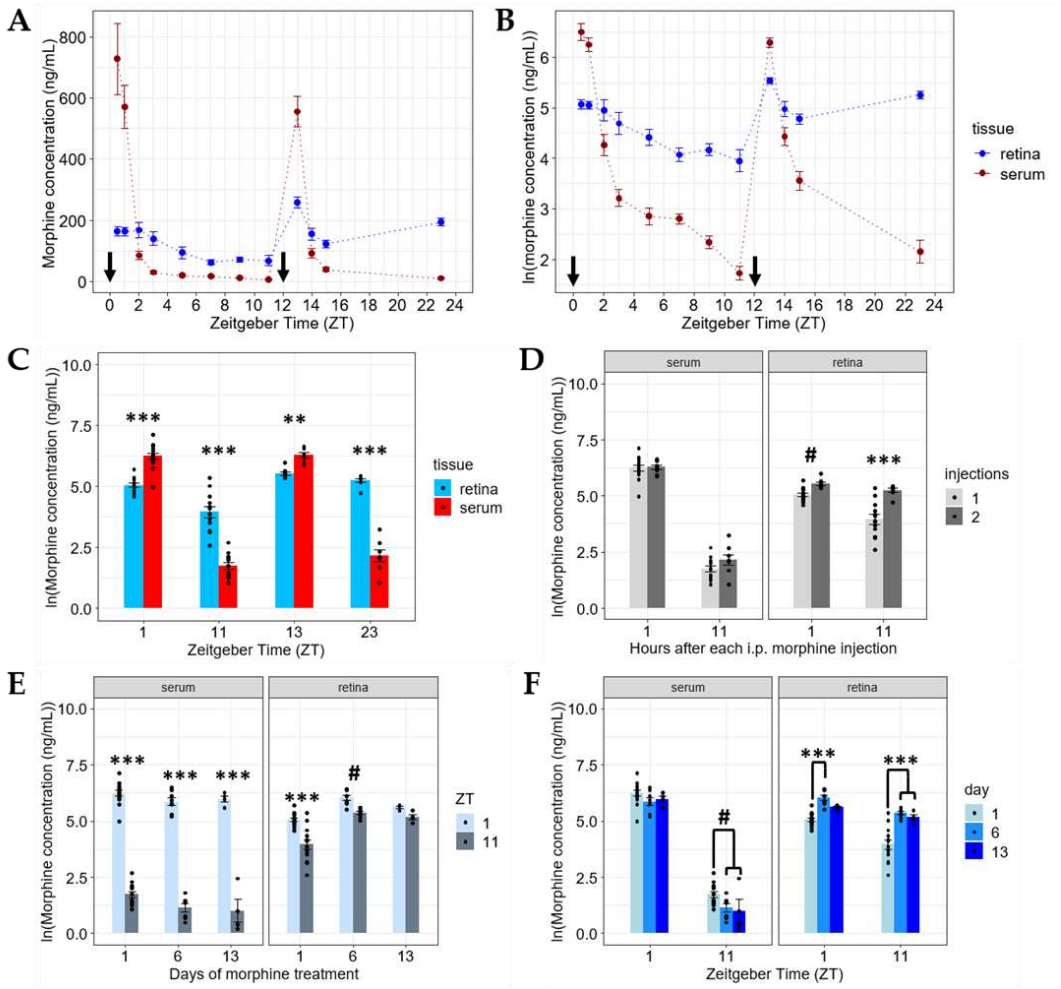

Figure 2.2 Morphine accumulates in the retina following repeated systemic exposure. (**A**) Morphine pharmacokinetics in retina and serum following 20 mg/kg i.p. morphine injections at ZT 0 and ZT 12 (indicated by arrows). (**B**) Morphine concentrations in retina and serum following systemic injections at ZT 0 and ZT 12 (indicated by arrows) on the natural logarithmic (ln) scale. Significant differences exist between the retina and serum within each measured time point ($p < 0.01$). Two-way ANOVA was used with a Tukey post hoc adjustment for the ln scale. (**C**) Morphine concentration in the serum is higher than in the retina 1 h (ZT 1 and ZT 13) after 20 mg/kg i.p. morphine injections at ZT 0 and ZT 12 (at the selected time points from the data shown in **B**). However, the retinal morphine levels exceed the serum levels at 11 h after systemic exposure (ZT 11 and ZT 23). Two-way ANOVA with a tissue *x* ZT interaction and a Tukey post hoc adjustment was performed on the ln scale. (**D**) Serum morphine pharmacokinetics remain the same at 1 and 11 h after one and two 20 mg/kg i.p. morphine injections, while the retinal morphine levels increased following the second injection at those same time points. Three-way ANOVA with a tissue *x* hours post-injection *x* injection number interaction and a Tukey post hoc adjustment was performed on the ln scale. (**E**,**F**) Morphine appears to accumulate in the retina following 6 or 13 days of chronic systemic morphine treatment, while the serum pharmacokinetics remain similar for ZT 1 and ZT 11. Three-way ANOVA with a tissue *x* ZT *x* day interaction using a Tukey post hoc adjustment was performed on the ln scale. (# = $p < 0.05$, **= $p < 0.001$, *** = $p < 0.0001$). Data are presented as the mean ± SEM.

(day 1) and mice chronically treated with morphine (day 6 and day 13) (Figures 2.2F and S1B). Moreover, the difference in retinal morphine between 1–2 h (Figure 2.2F: Day 6 ZT 1: $n = 8$, Day 13 ZT 1: $n = 4$; Figure S1B: Day 13 ZT 2: $n = 4$) and 9–11 h (Figure 2.2F: Day 6 ZT 11: $n = 7$, Day 13 ZT 11: $n = 4$; Figure S1B: Day 13 ZT 9: $n = 4$) disappeared after 13 days of chronic morphine exposure, while the serum pharmacokinetics remained similar (Figures 2.2E and S1B). Intriguingly, the chronic-morphine-treated animals (day 6 & day 13) showed a modest, yet significant decrease ($p < 0.05$) in serum morphine concentration both 9 (ZT 9) and 11 (ZT 11) hours after the final morphine injection (when compared to day 1 levels) (Figures 2.2F and S1B).

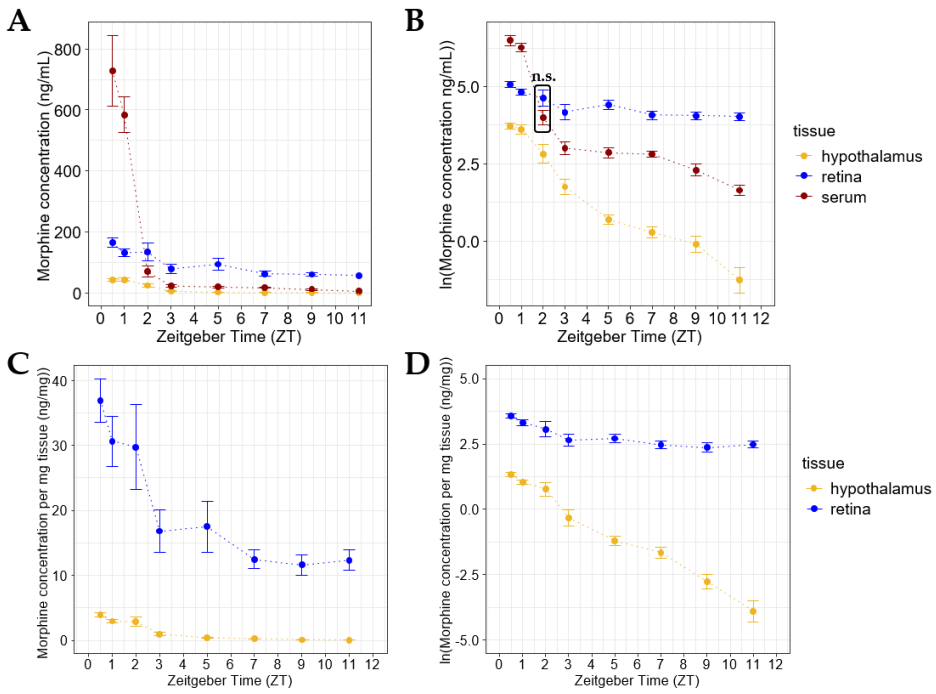

Figure 2.3 Morphine deposits more in the retina than in the hypothalamus following systemic administration. (**A**) Retinal morphine concentrations exceed hypothalamic morphine concentrations at all measured time points following a single i.p. morphine injection. (**B**) Morphine concentrations between the hypothalamus, retina, and serum were all significantly different at each measured time point following a single i.p. morphine injection ($p < 0.001$), except for comparison shown in the box at ZT 2 (n.s. = not significantly different). Two-way ANOVA with a Tukey post hoc adjustment was performed on a natural logarithmic (ln) scale (**C**,**D**). Morphine concentration in the retina exceeds that detected in the hypothalamus when normalized against tissue weight at each measured time point following a single i.p. morphine injection ($p < 0.0001$). (**D**) Two-way ANOVA with a Tukey post hoc adjustment was performed on an ln scale. Data are presented as the mean ± SEM, with 6–10 mice per group

2.2.3 Morphine Concentration in Mouse Retina Exceeds the Hypothalamic Morphine Concentration Following Systemic Exposure

Since retinal morphine levels seem to increase upon repeated systemic exposure, we wanted to compare the deposition of morphine in the retina to the brain. We chose to compare the retina to the hypothalamus, as the hypothalamus has been shown to have the highest concentration of morphine following systemic exposure (when compared to other brain regions) (Bhargava et al., 1992). Using solid phase extraction followed by LC-MS/MS, we were able to reliably measure the morphine content of brain tissue, including the hypothalamus and cortex. Despite the hypothalamus' proximity to the median eminence, we did not detect any differences in morphine deposition between the hypothalamus and the cortex (Figure S2). Interestingly, the hypothalamic morphine concentration was lower than both the retinal and serum morphine levels at 0.5 (n = 8), 1 (n = 17), 2 (n = 10), 3 (n = 7), 5 (n = 10), 7 (n = 8), 9 (n = 8), and 11 (n = 6) hours after a single i.p morphine injection at ZT 0 (Figure 2.3A,B). When the morphine concentrations of the retina and hypothalamus were normalized to their weights, the retinal morphine concentrations still vastly exceeded the morphine levels detected in the hypothalamus (Figure 2.3C,D). Additionally, the retinal morphine concentration per tissue weight remained much higher ($p < 0.0001$) than the hypo-thalamic morphine concentration in samples collected 1, 2, and 3 h after a second i.p. morphine injection at ZT 12 (Figure S3).

2.2.4 Morphine Accumulates in Mouse Retina but not in the Hypothalamus

After observing the significant difference in morphine penetrance within two CNS tissues (retina and brain) after a single systemic injection, we measured the levels of morphine in the retina and hypothalamus after 6 days of chronic morphine treatment. The retinal morphine content exceeded the morphine concentrations in the hypothalamus; furthermore, chronic

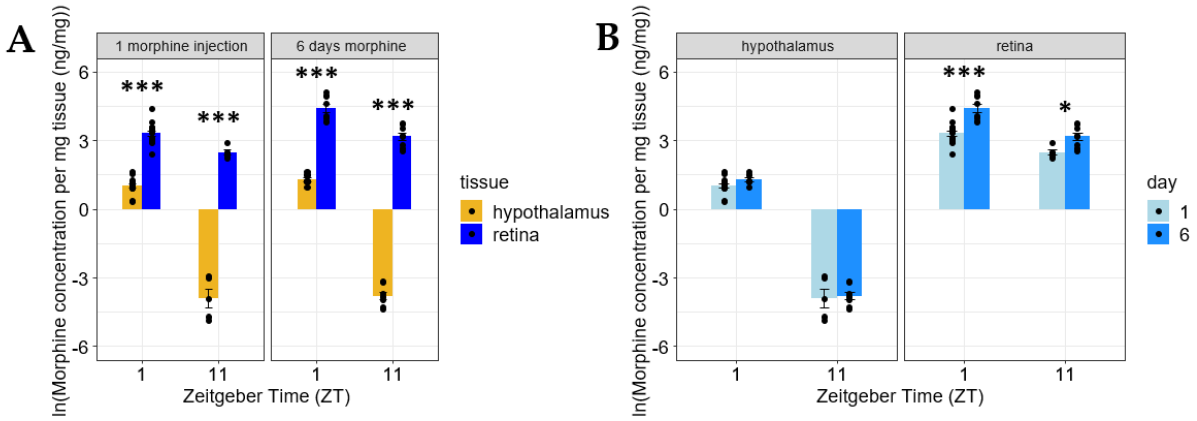

Figure 2.4 Morphine accumulates in the retina, but not the hypothalamus. (**A**) Retinal morphine concentrations exceed hypothalamic morphine concentrations at 1 (ZT 1) and 11 (ZT 11) hours following chronic morphine exposure (6 days of morphine treatment). (**B**) Morphine accumulates in the retina, but not the hypothalamus following chronic morphine exposure. Two-way ANOVA with a Tukey post hoc adjustment was performed on a natural logarithmic (ln) scale. Data are presented as the mean ± SEM with 5-17 mice per group (* = $p < 0.01$, *** = $p < 0.0001$).

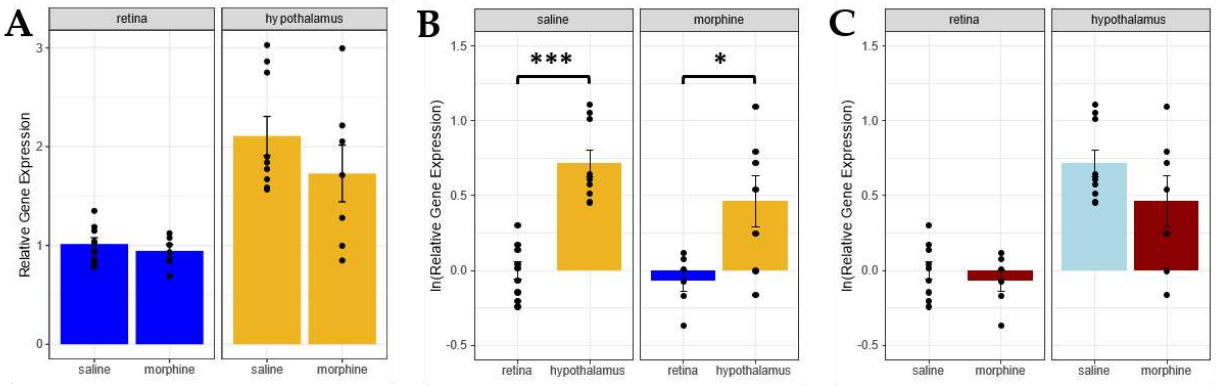

Figure 2.5 Reduced P-gp expression in the retina may underlie retinal morphine accumulation. P-pg mRNA expression (**A**) and natural logarithm (ln) (**B**) of P-gp mRNA expression is lower in the retina than in the hypothalamus at one hour (ZT 1) after an i.p. morphine injection at ZT 0. (**C**) Chronic morphine exposure does not affect P-gp mRNA expression in either tissue depositions at ZT 1. Two-way ANOVA with a Tukey post hoc adjustment was performed on an ln scale. Data are presented as the mean ± SD (* = $p < 0.01$, *** = $p < 0.0001$).

morphine exposure appeared to exacerbate the differences in morphine concentrations between these tissues (Figure 2.4A). These analyses revealed that chronic morphine administration preserved the differences in morphine concentrations between the retina and hypothalamus at both 1 (Day 6 ZT 1: $n = 8$) and 11 (Day 6 ZT 11: $n = 8$) h after the ZT 0 systemic injection. Intriguingly, morphine seems to accumulate in the retina following chronic systemic exposure, while morphine levels in hypothalamus ap-pear to remain the same (Figure 2.4B). Figure S4B even shows that at ZT9 following chronic morphine exposure, hypothalamic morphine levels drop following 13 days of chronic morphine, while the retinal morphine concentration is significantly larger ($p < 0.01$) than the single injection levels following chronic administration.

2.2.5 Reduced P-gp Expression in the Retina May Underlie Retinal Morphine Accumulation

P-gp's role in transporting morphine from the brain into systemic circulation is well established (Letrent et al., 1999; Dagenais et al., 2004; Hamabe et al., 2007; L. Mercer and Coop, 2011; Yang et al., 2018). Significantly, this important transporter is also expressed in the iBRB, albeit at lower levels than in the brain (Chapy et al., 2016; Li et al., 2021). Thus, we wanted to assess the role of P-gp within the context of differential morphine deposition in the retina versus the hypothalamus following systemic exposure. To investigate the role of P-gp in morphine transport within these different CNS tissues, we injected mice with 20 mg/kg morphine ($n = 7$) or sa-line ($n = 9$) i.p. at ZT 0 and ZT 12 for 6 days. Retina and hypothalamus samples were collected from these mice and total RNA from these tissues was extracted for quantitative reverse-transcription PCR (qRT-PCR) analysis. The expression of *Abcb1a* (gene transcript coding for P-gp) mRNA, relative to the reference genes B-actin and Tbp, was calculated using the saline retina samples as the control. Relative gene expression analyses revealed that *Abcb1a*/P-gp mRNA expression in the retina was lower than the expression in the hypothalamus

(Figure 2.5A,B). Importantly, chronic morphine exposure did not alter the expression of *Abcb1a*/P-gp mRNA in the brain (hypothalamus) or retina (Figure 2.5C).

2.3 Discussion

The data presented provide an in depth look at morphine pharmacokinetics in the retina, as well as in the serum and hypothalamus, for longer durations than previously reported. Consistent with past findings, these data suggest that morphine levels in the serum peak within the first hour after i.p. administration, and then drop rapidly to low levels within 1–2 h following the injection (Pacifici et al., 2000; Handal et al., 2002; Koek et al., 2012). While the serum pharmacokinetics of past studies focused on the serum morphine levels within the first 3 h after injection, this study measured serum morphine up to 11 h following injection. Analysis of this data showed consistent decreases in serum morphine content up to 11 h after the initial injection.

As previously mentioned, opioid metabolites are routinely detected from postmortem human VH samples; however, these samples are often collected from overdose victims following the administration of a fatal opioid dose (Scott and Oliver, 1999; Wyman and Bultman, 2004; Sanches et al., 2012; Rees et al., 2013; Bévalot et al., 2016; Gottås et al., 2016). While it is unclear whether sub-lethal opioid doses similarly accumulate in human VH/retina, animal studies suggest that sub-lethal doses of opioids accumulate in the mammalian VH/retina following systemic exposure (Husain et al., 2012; Gottås et al., 2016; Maskell et al., 2016). While the current study differs in species, treatment, and methodology, it builds on this past work by providing an examination of morphine pharmacokinetics within mouse retina following both acute and repeated systemic morphine administration.

To our knowledge, no study has measured retinal morphine levels in mice following systemic exposure. Therefore, we developed and validated a method for detecting morphine

levels within the retina/VH samples of systemically morphine-treated mice. The data from these experiments indicate that morphine indeed deposits in the retina following systemic exposure and even persists at elevated levels relative to the serum and hypothalamus. These findings are consistent with the idea that opioid metabolites in the VH are resistant to postmortem redistribution, and thus have an extended detection window within the VH/retina compared to other tissues (Bévalot et al., 2016; Maskell et al., 2016). In humans, morphine is metabolized into morphine-3 glucuronide (M3G) and morphine-6 glucuronide (M6G) via UDP-glucuronyl-transferase (UGT) (Sawe et al., 1985; Andersen et al., 2003; Rook et al., 2006). Of these metabolites, M3G does not contribute to morphine's analgesic effect (Gong et al., 1992; Penson, 2000; Rook et al., 2006) or to morphine-induced behavioral activation (Handal et al., 2002), while M6G does (van Dorp et al., 2006). However, mice produce little to no M6G following morphine administration (Zuccaro et al., 1997; Handal et al., 2002; Andersen et al., 2009).

Importantly, following a second systemic injection, the morphine levels in the retina seem to accumulate, while the pharmacokinetics of serum morphine in the same animals remain relatively constant when compared 1 and 11 h after one or two injection(s). This retinal accumulation following repeated systemic exposure is further evidenced when comparing retina samples collected at ZT 1 and ZT 11 after a single injection to samples collected at ZT 1 and ZT 11 from animals following chronic systemic morphine exposure. Interestingly, the levels of morphine in the serum after 11 h (ZT 11) appear to be even lower in animals chronically treated with morphine than after a single i.p. morphine injection. While few other studies have examined the long-term serum pharmacokinetics of morphine, we suspect that this may be due metabolic adaptations (i.e., increased UGT2B activity) that mice undergo in response to a chronic morphine paradigm (Andersen et al., 2003; Ochiai et al., 2016).

Morphine deposition and transport into the brain has been extensively studied as it is necessary for the analgesic efficacy of morphine (Chaves et al., 2017; Schaefer et al., 2017). Since mice are used extensively as a mammalian model for opioid-related biomedical research, the pharmacokinetics of morphine and other opioids in the mouse brain has been well characterized (Zong and Pollack, 2000; Guillot et al., 2007; Andersen et al., 2009; Koek et al., 2012; Boix et al., 2013; Ollikainen et al., 2019). Although we initially suspected that the hypothalamus might have increased morphine penetrance due to its proximity the median eminence (Chapy et al., 2016; Haddad-Tóvolli et al., 2017), we found no difference in morphine concentrations compared to cortices harvested from the same animals (Figure S1). With that being said, the data we obtained regarding the pharmacokinetics of morphine in the brain were consistent with past findings, with peak concentrations of hypothalamic morphine levels detected around 30 min to 1 h following the time of injection (Andersen et al., 2009; Koek et al., 2012). Nonetheless, this study offers a more in depth look at the brain pharmacokinetics of morphine up to 11 h following systemic administration. In many ways, the pharmacokinetics of morphine in the hypothalamus mirror that of the serum, as both serum and brain morphine concentrations peak about an hour after systemic exposure and continuously drop over time. Contrastingly, the retinal morphine concentration remains high compared to the serum and hypothalamus. Perhaps most significantly, our data suggest that while the morphine appears to be accumulating in the retina/VH following chronic systemic exposure, the concentrations in the brain do not. Both CNS tissues have structurally similar barriers (the iBRB and BBB) that selectively regulate the transport of xenobiotics. Past experiments have shown that the genetic and pharmacological manipulation of P-gp alter morphine concentration within the brain (Letrent et al., 1999; Dagenais et al., 2004; Hamabe et al., 2007; L. Mercer and Coop, 2011; Yang et al., 2018). In

fact, experimental evidence suggests that P-gp expression and brain morphine levels have an inverse relationship, as increased P-gp expression results in lower levels of morphine within the brains of mice (Hamabe et al., 2007). Our data are consistent with this idea, as the relative P-gp mRNA (*Abcb1a*) expression within the retina is significantly lower than expression levels in the hypothalamus.

Initially, it was believed that chronic morphine exposure could alter the expression of P-gp mRNA at the BBB (Aquilante et al., 2000; Yousif et al., 2008). However, it was later observed that the cessation of chronic morphine treatment, rather than the chronic morphine treatment itself, likely resulted an increase in P-gp mRNA (Chaves et al., 2016). Our data support the latter of the two findings, as our chronic morphine treatment did not alter the P-gp mRNA in with either tissue. Future studies shall investigate the role of other BBB transporters (such as Breast Cancer Resistance Protein and Multidrug Resistance Protein 2) to assess their potential roles in the pharmacokinetics of morphine within both the brain and the retina.

Because the analgesic and psychomotor effects of morphine are heavily dependent on the concentration within the brain and spinal cord, the opioid pharmacokinetics within these regions have been extensively studied (Handal et al., 2002; Koek et al., 2012; Chaves et al., 2017; Schaefer et al., 2017). Contrastingly, the retina/VH has been less studied in regard to opioid pharmacokinetics as it has been primarily employed as a sample for postmortem toxicological investigations. This study presents an in-depth pharmacokinetic characterization of morphine in the retina relative to serum and hypothalamus, highlighting that morphine persists and accumulates in the retina following chronic systemic exposure. Since no visual phenotype has been reported following chronic opioid exposure, it was previously assumed that systemic opioid exposure did not affect structures in the eye. However, chronic morphine exposure was shown to

promote neovascularization in the retina, which could contribute to retinopathy in patients with sickle cell disease (Gupta et al., 2019). Although opioids often have profound deleterious effects, the administration of chronic systemic morphine protected against hypertension-mediated retinal ganglion cell death in rats (Husain et al., 2012). Additionally, rabbit studies have indicated that retinal morphine might reduce ischemia-induced retinal ganglion cell death following systemic exposure (Riazi-Esfahani et al., 2008, 2009). As these previous studies suggest, opioids may affect retinal ganglion cells through opioid receptors expressed on these cells (Husain et al., 2009). Interestingly, our group has identified a subset of intrinsically photosensitive retinal ganglion cells (ipRGCs) that express the μ-opioid receptors (MOR), which are the main molecular targets for opioid drugs such as morphine (Cleymaet et al., 2019). Moreover, these studies have shown that the MOR-selective agonist [D-Ala2, N-MePhe4, Gly-ol]-enkephalin (DAMGO) not only directly affects ipRGC firing activity via the modulation of specific ionic currents, but also that MOR activation attenuates the ipRGC-dependent PLR in mice (Cleymaet et al., 2019, 2021).

Perhaps most importantly, ipRGCs are crucial for the synchronization of sleep/circadian behavior to environmental light–dark cycles through a process known as photoentrainment (LeGates et al., 2014). These ipRGCs send environmental light information to key sleep and circadian centers located in the hypothalamus such as the suprachiasmatic nucleus (SCN) and the ventrolateral preoptic area (VLPO) (LeGates et al., 2014). Moreover, the opioid fentanyl has been shown to alter photoentrainment in hamsters, presumably though alteration of electrical activity and clock gene expression within the SCN (Byku and Gannon, 2000; Meijer et al., 2000; Vansteensel et al., 2005). Additionally, opioid-induced modulation of the VLPO increases wakefulness in rodents via MORs within this region (Greco et al., 2008; Wang et al., 2013).

Given this evidence, it is believed that chronic opioid-related sleep/wake disturbances are due to opioid-induced alterations to key sleep centers within the brain (Eacret et al., 2020; Fathi et al., 2020), while the retinal contributions to opioid-mediated sleep disruption are seldom considered. However, retinal morphine levels appear to exceed the EC_{50} for the inhibition of calcium current (an established effector of ipRGC MORs) after repeated systemic morphine exposure (Connor et al., 1999). This suggests that chronic systemic morphine exposure within these mice might activate MORs present on the ipRGCs, thus affecting their ability to transmit important environmental light information to brain's sleep/wake centers. Taken together, the present data point to an intriguing possibility that retinal morphine accumulation might contribute to chronic opioid-induced sleep/wake disturbances.

2.4 Materials and Methods

2.4.1 Animals

All animals used in these studies were handled in compliance with the Institutional Animal Care and Use Committees of Colorado State University (Protocol 18-8395A, 28 January 2019) and in accordance with the ARVO Statement for the Use of Animals in Ophthalmic and Vision Research. The animals were housed under a 12:12 light/dark (LD) cycle, with lights on at 7:00 AM (ZT 0) and lights off at 7:00 PM (ZT 12). Food and water were made available ad libitum.

2.4.2 Morphine Treatment

Mice were weighed and injected with a single i.p. dose of 20 mg/kg morphine (Morphine sulfate salt pentahydrate, Sigma-Aldrich Saint Louis, MO , USA; Prod-uct Number: M8777, dissolved in sterile saline) at light onset (ZT 0). The dosage of 20 mg/kg i.p. morphine is commonly used to assess analgesic tolerance in mice (Peart and Gross, 2004). Mice that received

two injections received a second 20 mg/kg i.p. morphine injection at light offset (ZT 12). The chronic morphine treatment paradigm consisted of 5 or 12 days of twice daily 20 mg/kg morphine (administered at ZT 0 and ZT 12), followed by a final 20 mg/kg i.p. injection at ZT 0 on day 6 or 13 of the treatment paradigm (McLane et al., 2017).

2.4.3 Tissue Sample Collection: Retina, Hypothalamus, and Serum

Mice were deeply anesthetized with isoflurane, decapitated, and trunk blood was collected into EDTA-coated tubes (BD Vacutainer K2 EDTA 7.2 mg tube 4.0 mL). Then, the hypothalamus was removed, weighed, and placed in tubes containing 100 µL 0.1 M PBS. Whole retinas were then microdissected from the eyes of each animal and placed in tubes containing 100 µL 0.1 M PBS. Notably, the retina samples tested contained both retinal tissue and VH.

2.4.4 Morphine Analysis by LC-MS/MS

2.4.4.1 Retina Batch Preparation

To prepare retina samples for analysis, 10 µL of 10 µg/mL D6-morphine internal standard solution (Morphine-D6 solution, Cerilliant, Round Rock, TX, USA) was added to whole-retina samples and matrix-matched standards. Here, matrix-matched standards were whole-retinal samples collected from untreated mice spiked with a morphine standard (Morphine solution, Sigma-Aldrich Saint Louis, MO, USA; Product Number: M-005). Subsequently, 200 µL ice-cold acetonitrile was added to the retina samples/standards and the samples/standards were sonicated at maximum power (40 kHz) for 30 min using a Branson Bransonic® (Emerson Electric Co. Saint Louis, MO, USA) 5800 Ultra-sonic bath (with bath water at room temperature). Retina samples were then spun down at 14,000 rpm for 5 min, and 100 µL supernatant was added to sample vials containing 200 µL 0.1% formic acid in water and then

transferred to autosampler vials fitted with 400 µL glass inserts. The limit of detection was 20 ng/mL morphine.

2.4.4.2 Hypothalamus Batch Preparation

To prepare hypothalamus samples for analysis, 10 µL of 1 µg/mL D6-morphine in-ternal standard solution was added to hypothalamus samples and matrix-matched standards. Here, matrix-matched standards were hypothalamus samples collected from untreated mice spiked with a morphine standard. Hypothalamus samples/standards were then homogenized for 10 s using a BeadBug™ (Benchmark Scientific, Inc. Sayreville, NJ, USA) 3 Position Bead Microtube homogenizer in 400 µL ice-cold acetonitrile. Samples were then centrifuged 14,000 rpm for 5 min and supernatant was added to Phenomenex Strata-X-Drug B solid phase columns. Columns were washed with 2 mL 0.1% formic acid in water and 2 mL methanol. Columns were then dried for 10 min prior to elution. Two successive aliquots of a solution containing 50% acetonitrile, 42% methanol, and 8% 7N ammonium in methanol were used to elute samples from the columns. Eluents were collected into a clean glass test tube and dried under nitrogen at 40 °C. Dried eluents were reconstituted with 200 µL 95:5% water:acetonitrile and transferred to autosampler vials fitted with 400 µL glass inserts. The limit of detection was 0.2 ng/mL morphine.

2.4.4.3 Serum Batch Preparation

To prepare serum samples for analysis, 10 µL of 1 µg/mL D6-morphine internal standard solution was added to serum samples and matrix-matched standards. Here, matrix-matched standards were serum samples collected from untreated mice spiked with a morphine standard. Serum samples/standards were prepared for solid phase ex-traction by adding 20 µL zinc sulfate (5% weight/volume), followed by the addition of 300 µL ice-cold acetonitrile to each tube.

Samples were then centrifuged 14,000 rpm for 5 min and supernatant was added to Phenomenex Strata-X-Drug B solid phase columns. Col-=umns were washed with 2 mL 0.1% formic acid in water and 2 mL methanol. Columns were then dried for 10 min prior to elution. Two successive aliquots of a solution containing 50% acetonitrile, 42% methanol, and 8% 7N ammonium in methanol were used to elute samples from the columns. Eluents were collected into a clean glass test tube and dried under nitrogen at 40 °C. Dried eluents were reconstituted with 200 µL 95:5% water: acetonitrile and transferred to autosampler vials fitted with 400 µL glass inserts. The limit of detection was 0.5 ng/mL morphine.

2.4.4.4 Data Acquisition and Analysis

Samples were analyzed with an Agilent 1290 UHPLC coupled to an Agilent 6460 triple quadruple mass spectrometer equipped with an Agilent Jet Stream electrospray ionization. Morphine was chromagraphically separated on a Restek Raptor biphenyl column (3.0 × 50 mm, 2.7 µm) held at 40 °C. A sample volume of 10 µL was injected into a mobile phase mixture of 95% water with 0.1% formic acid (A) and acetonitrile with 0.1% formic acid (B). The flow rate of 0.4 mL/min was kept consistent throughout the run time. The mobile phase composition was held at 3% B for 1.5 min, increased to 40% B at 3 min, and finished at 100% B at 4 min. The ionization source conditions used were as follows: positive polarity and nebulizer 40 psi; gas flow of 10 L/min at 320 °C; sheath gas flow of 12 L/min at 380 °C; capillary voltage of 3750 V; and nozzle voltage of 500 V. The ion transitions monitored were 286.2- > 152 and 128 m/z for morphine and 292.2- > 152 and 128 m/z for D6-morphine. Analytes were confirmed by retention time and the product ion ratio correlation between the sample peaks and corresponding standards (± 20%). The data collection and processing were performed by using Agilent (Santa Clara, CA, USA) Mass Hunter Quantitative software (v.B.08.01). Quantitation was performed with linear

regression using seven-point calibration curves from 0.5 ng/mL to 500 ng/mL (for hypothalamus and serum) or six-point calibration curves from 5 ng/mL to 1 µg/mL (for retina). These calibration curves were made from matrix (hypothalamus, serum, or retina tissue derived from untreated animals) spiked with morphine standards (morphine solution, Sigma-Aldrich Saint Louis, MO, USA; Product Number: M-005).

2.4.4.5 Method Validation

Prior to assessing the morphine concentrations of tissues derived from the mor-phine-treated animals, LC-MS/MS methods were validated for all three matrices (retina, serum, and hypothalamus). Matrices were validated using the following parameters: accuracy, precision, calibration model, carryover, interference, limit of quantitation (LOQ), and sample stability (see Tables S2 and S3 for validation results and acceptance criteria).

2.4.5 qRT-PCR

2.4.5.1 RNA Preparation

Male WT mice received morphine or saline as described above. One hour after the injection (ZT 1), the mice were anesthetized with isoflurane and sacrificed by decapitation. Hypothalamic tissue was dissected from the brain and immediately homogenized for RNA extraction, while retinas were microdissected in 0.1 M phosphate buffered saline (PBS; pH 7.4) and placed in RNAlater solution (Sigma-Aldrich R0901) at 4 °C until after hypothalamic RNA was extracted. Total RNA was extracted from both tissues using the RNeasy Mini Kit (Qiagen, Hilden, Germany) according to the manufacturer's instructions. Briefly, the tissues were lysed in Buffer RLT with DTT (GoldBio, St. Louis, MO, USA) by disruption with a micropipette, followed by homogenization of the solution by passing it through a 20-gauge needle five times. The lysate was centrifuged, and the supernatant was combined with 70% ethanol before being

put on the column. After RNA was eluted from the column, the concentration and quality (A260/A280) of each sample was assessed using a Nanodrop (ThermoFisher NanoDrop Lite, Waltham, MA, USA). Genomic DNA (gDNA) was digested using DNase I and RNase-free (ThermoFisher) according to the manufacturer's instructions. After DNase treatment, the RNA concentration was again measured using a Nanodrop, and RNA integrity and successful DNase treatment was assessed on a 1% agarose gel. All samples displayed strong 28S and 18S rRNA bands, no gDNA contamination, and no degradation.

2.4.5.2 Reverse Transcription

Reverse transcription of RNA was performed using the GoScript™ Reverse Transcription System (ProMega, Madison, WI, USA) according to the manufacturer's instructions. In each rotation, 200 ng RNA was used and a no-reverse-transcription (NRT) control was performed alongside each sample. cDNA was stored at −20 °C until it was used for qPCR amplification.

2.4.5.3 qRT-PCR Primer Design

Previously published primers against Abcb1a (the rodent gene for p-glycoprotein [p-gp]) in rats [58] were adapted for use for the mice. The probe sequence for Abcb1a, as well as primer and probe sequences for the reference genes β-actin and Tbp, were designed using Integrated DNA Technologies' PrimerQuest™ Tool. β-actin is a commonly used reference gene that has been used successfully in mouse retina (Sawant et al., 2017), and Tbp has been shown to be an appropriate reference gene for adult mouse retina (Adachi et al., 2015).

For each target, primers were designed to span an exon–exon junction, have melting temperatures of between 60 °C and 65 °C, have a GC content of between 45–65%, and be no more than 30 nucleotides long. Probes were designed to have melting temperatures at least 5 °C

higher than the primers, have a GC content of between 45–75%, and be no more than 30 nucleotides long. Amplicons were required to be shorter than 150 nucleotides. All other parameters were left as defaults. The multiplexed primers (500 nM) and probe (250 nM) were resuspended in an IDTE buffer (10 mM Tris, 0.1 mM EDTA in H2O) upon receipt, then stored at −20 °C. The primer and probe sequences can be found in Table S1. PCR products from each primer set were run on a 2% agarose gel to assess the specificity of the primers. For all genes, one clear band was seen with no gDNA contamination or additional products. The reaction parameters were first determined in singleplex reactions before multiplexing. For each primer set, a temperature gradient was used to deter-mine the optimal annealing temperature.

2.4.5.4 qRT-PCR Protocol

Reactions were set up using GoTaq® Probe qPCR Master Mix (ProMega) according to the manufacturer's instructions; however, because our primers and probes arrived multiplexed, only 1 µL total was used, and an additional 2 µL of nuclease-free water was added to the total 20 µL reaction mix. The cycling conditions were as follows: 2 min, 95 °C, GoTaq® DNA polymerase activation, and then 35 cycles of denaturation (95 °C, 15 s) and annealing/extension (63 °C, 30 s).

Each plate contained a standard curve run in triplicate, which included three 10-fold dilutions. Every experimental sample was run in triplicate using 2 µL of cDNA. Both reference genes were stably expressed in all samples. A NRT control and no-template control (H_2O instead of cDNA or RNA; NTC) was included in each run. No amplification was seen in any of the NRT or NTC controls. Assay plates were prepared in-lab, then run on a CFX96 Touch Real-Time PCR Detection System (BioRad, Hercules, CA, USA).

2.4.5.5 Data Analysis

The CFX Manager™ Software Version 3.1 (BioRad, Hercules, CA, USA) was used to set the threshold for each reaction (the highest R2 just above the background) and to assess the efficiency of the reaction based on the standard curve (90–110%). It was also used to normalize the data between plates when samples needed to be re-run or run on multiple plates. In these cases, at least one identical sample was run on each plate and used as an inter-run calibrator. The Cq values for each experiment were downloaded as an Excel spreadsheet and the ΔΔCt method was used for analysis (Livak and Schmittgen, 2001; Hellemans et al., 2007). For each gene, the Cq values for all samples in the control group were averaged and used as the reference to calculate the relative gene expression (RGE) in each sample. Because multiple reference genes were used, the geometric mean of those genes' relative quantities was used to calculate the RGE (Vandesompele et al., 2002).

2.4.6 Data Collection and Statistical Analysis

Data are presented as mean ± standard error of the mean (SEM) or mean ± standard deviation (SD), as specified in figure captions. The data were analyzed using One-way, two-way, or three-way ANOVA on a natural logarithmic scale to satisfy ANOVA assumptions. Data visualizations and analyses were performed using RStudio (version 4.0.0) with Tukey's post hoc adjustments for all pairwise comparisons, and $p < 0.05$ was considered significant.

2.5 Conclusions

In this study, we measured morphine concentrations in mouse retina. The data reveal that morphine deposits and accumulates in mouse retina following both acute and chronic systemic exposure. Importantly, morphine concentrations in the retina accumulate following chronic systemic administration and vastly exceed brain morphine concentrations across all sampled time points. Future studies will explore the physiological implications of retinal morphine

accumulation and how it might contribute to opioid-induced alterations in both visual functions and circadian regulation of sleep/wake behaviors.

Chapter 3 - μ-Opioid Receptors Expressed by Intrinsically Photosensitive Retinal Ganglion Cells Contribute to Morphine-Induced Behavioral Sensitization[3]

3.1 Introduction

Opioids remain some of the most powerful analgesics and are thus extensively used clinically for treating pain (Volkow et al., 2019). Therefore, it is important to carefully consider the dangerous side effects associated with their therapeutic use. While opioids are infamous for their addictive nature, their propensity to perturb sleep is often underappreciated. Both acute and chronic opioid administration have been shown to disrupt sleep/wake behaviors in patients (Dimsdale et al., 2007; Serdarevic et al., 2017; Chrobok et al., 2020). Moreover, chronic opioid use has been associated with insomnia as well as daytime drowsiness (Kay, 1975; Serdarevic et al., 2017; Chrobok et al., 2020; Fathi et al., 2020). These opioid-related sleep/wake problems often persist throughout chronic opioid treatment, which can exacerbate (existing) pain symptoms as well as the increase the risk for developing affective disorders (Kay, 1975; Hartwell et al., 2014; Cheatle and Webster, 2015; Latif et al., 2019). Additionally, sleep disturbances have been cited as a primary contributor to opioid relapse and have been linked to increased suicidality (Simmons et al., 2020; Huhn and Finan, 2021). Preclinical animal experiments have also shown that opioid administration disrupts healthy sleep/wake behaviors (Meijer et al., 2000; Vansteensel et al., 2005; Gillman et al., 2009; Glaser et al., 2012; Eacret et al., 2020). Opioid receptors are robustly expressed throughout the central nervous system (CNS), including regions of the brain implicated in sleep/wake regulation (Eacret et al., 2020). For

---

[3] Bergum N, Berezin CT, King CM, Vigh J. μ-Opioid Receptors Expressed by Intrinsically Photosensitive Retinal Ganglion Cells Contribute to Morphine-Induced Behavioral Sensitization. *Int J Mol Sci*, 23(24), 15870. doi: 10.3390/ijms232415870.

instance, opioid receptors expressed by sleep-active neurons within the ventrolateral preoptic area (VLPO) of the hypothalamus (Greco et al., 2008), commonly referred to as the sleep switch (Saper et al., 2010), have been shown to mediate opioid-induced sleep/wake changes in rats (Wang et al., 2013). Fentanyl has been shown to shift circadian rhythms in hamsters, presumably by modulating circadian pacemaker neuron signaling within the suprachiasmatic nucleus (SCN) of the hypothalamus (Meijer et al., 2000; Vansteensel et al., 2005; Gillman et al., 2009). Importantly, neurons within both the SCN and VLPO receive photic input from the retina (Lupi et al., 2008).

Recent findings from our lab have demonstrated that a subset of ganglion cells in the mouse retina, the intrinsically photosensitive retina ganglion cells (ipRGCs), express μ-opioid receptors (MORs), the main molecular target for opioid drugs (Cleymaet et al., 2019). Indeed, MOR-selective agonist [D-Ala2, N-MePhe4, Gly-ol]-enkephalin (DAMGO) can effectively suppress light-evoked ipRGC firing (Cleymaet et al., 2019). These ipRGCs provide direct light information to the brain's sleep/wake centers (e.g., SCN and VLPO), which synchronizes mammalian sleep/wake rhythms to environmental light conditions (i.e., photoentrainment) (LeGates et al., 2014). We have previously shown that endogenous opioid signaling in the retina modulates native sleep/wake behavior in mice via MORs expressed by ipRGCs (Berezin et al., 2022). Importantly, similar to opioid deposition in the human eye (Wyman and Bultman, 2004), morphine deposits in the mouse retina following systemic administration (Bergum et al., 2022a). Thus, we wanted to test if MORs expressed by ipRGCs contribute to opioid-related sleep/wake disturbances in mice by telemetrically recording locomotor activity and body temperature upon acute and chronic intraperitoneal (i.p.) injections of morphine in freely moving mice.

Results revealed that acute and chronic morphine exposure differentially altered locomotor activity and body temperature of mice lacking MORs entirely (MKO, (Matthes et al., 1996)) compared with those lacking MORs only in ipRGCs (McKO) and controls (mouse line containing a floxed version of the *Oprm1* gene, Mu^{fl}, (Weibel et al., 2013; Severino et al., 2020)). Acute morphine triggered transient hypothermia in control mice during both the subjective day and night that faded upon chronic administration. In McKO animals, transient hypothermia was observed upon both acute and chronic morphine administration in the subjective night, whereas in MKO mice, morphine had little effect on the body temperature. Both control and McKO mice exhibited increased locomotor movement following repeated i.p. morphine injections regardless of the injection time (i.e., behavioral sensitization (Kalivas and Duffy, 1987)). Moreover, their behavioral activity became increasingly entrained to the morphine injections rather than the light schedule. Consistent with past findings, the MKO mice failed to acquire morphine-induced behavioral sensitization (Tian et al., 1997; Sora and Li, 2001; Yoo et al., 2003). Nonetheless, while control and McKO mice both acquired morphine-induced behavioral sensitization, McKO mice exhibited reduced morphine-induced increases in locomotor activity compared with control littermates. Taken together, our data point to a previously unexplored retinal contribution to chronic opioid-induced disruption of photoentrainment as well as morphine-induced hypothermia.

3.2 Results

3.2.1 Prolonged morphine exposure has differential effects on locomotor activity in control, McKO and MKO

Single-housed mice were implanted with mini-telemetry transmitters to record horizontal locomotor movement and body temperature within their respective cages every minute for the

duration of the experiment. After recovery from transmitter surgeries, these mice were injected with saline twice daily at light onset (ZT 0) and light offset (ZT 12) for 6–7 days. Following the final saline injections on day 7, mice were injected with 20 mg/kg of morphine twice daily for 12 days (McLane et al., 2017; Bergum et al., 2022a). To assess the effect of acute and prolonged morphine exposure on diurnal locomotor activity, we analyzed data from the final day of vehicle/saline treatment (Saline) as well as the data from the first day of morphine treatment (Morphine Day 1), the sixth day of morphine treatment (Morphine Day 6) and the tenth day of morphine treatment (Morphine Day 10). Notably, we chose to use day 10 as the last analysis day due to substantial data loss and attrition that occurred during days 11 and 12 of the morphine treatment paradigm. Additionally, we provided a range of animals for control and McKO groups, as subject attrition and data loss led to a decrease in usable data toward the end of the study. Analysis of these data revealed that each genotype responded differently to the chronic morphine treatment paradigm. Control (n = 15) and McKO (n = 10) littermates exhibited increased locomotor activity in the dark compared with aged-matched MKO (n = 7) mice during vehicle (Saline; Control vs. MKO: t(220) = 2.821, p = 0.0157; McKO vs. MKO: t(211) = 2.634, p = 0.0182) and acute morphine (Morphine Day 1; Control vs. MKO: t(220) = 2.580, p = 0.0316; McKO vs. MKO: t(211) = 2.433, p = 0.0316) treatment (Figure 3.1A,B). Interestingly, after subchronic morphine exposure (Morphine Day 6), there were no significant differences in dark phase horizontal activity across all genotypes (Figure 3.1A,B). Intriguingly, control mice (n = 14) showed increased locomotor activity in the dark compared with McKO littermates (n = 9) after chronic morphine exposure (Morphine Day 10; Control vs. McKO: t(214) = 2.927, p = 0.0114; Figure 3.1A,B). While there were no differences between different genotypes in light phase activity during saline and acute morphine treatment, subchronic (Morphine Day 6; Control

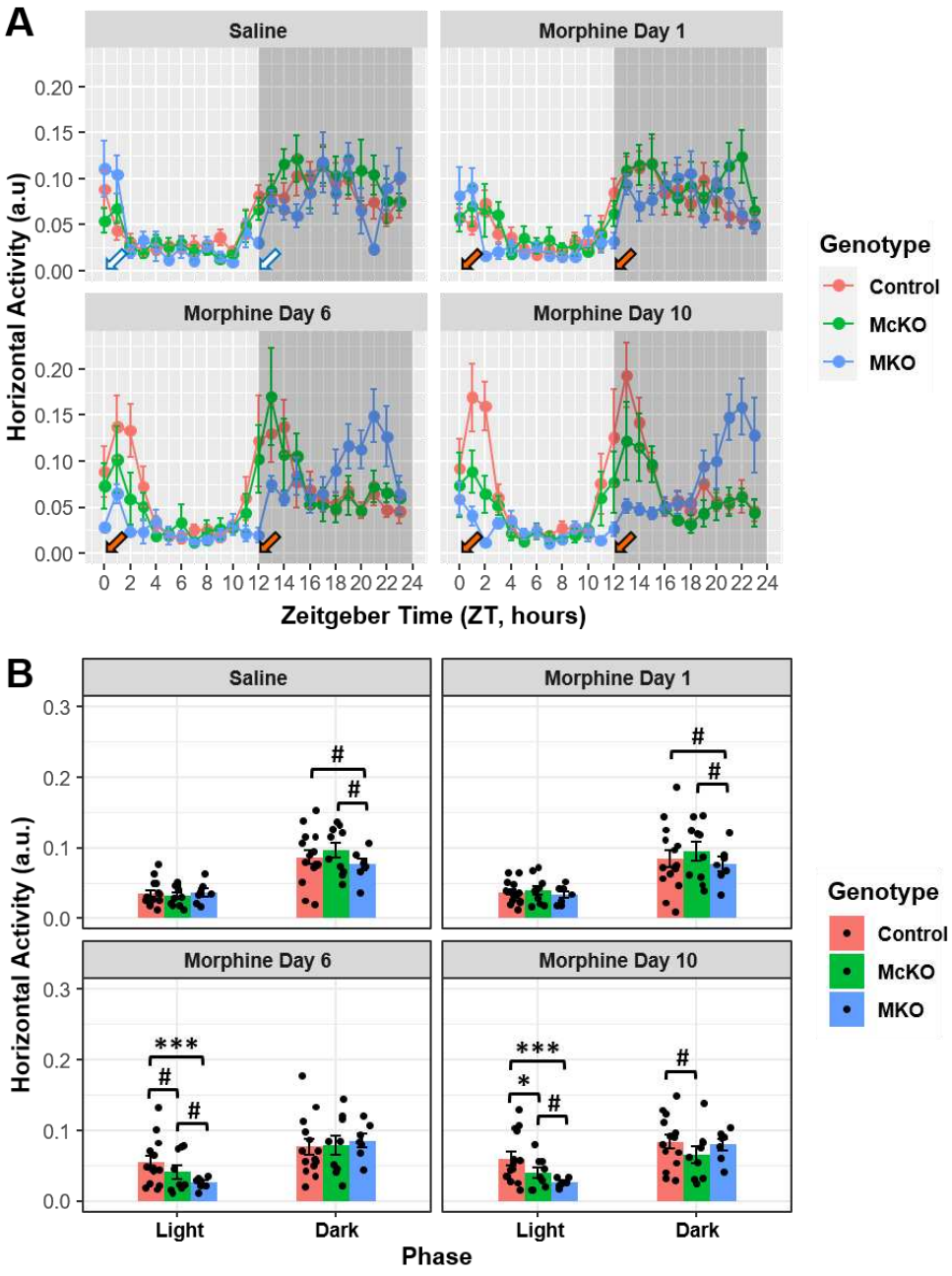

Figure 3.1 Prolonged but not acute morphine exposure differentially altered locomotor activity in Control, McKO, and MKO mice across light and dark phases. (**A**) Average behavioral activity plotted for Control (n = 14–15), McKO (n = 9–10), and MKO (n = 7) by hour (Zeitgeber Time) for different experimental days. Arrows indicate time of i.p. injection with either saline (white arrows) or 20 mg/kg of morphine (orange arrows). (**B**) Control and McKO animals exhibited increased horizontal activity compared with MKO animals. After prolonged morphine exposure, control mice exhibited increased locomotor activity compared with McKO littermates. Analysis performed using a three-way ANOVA (phase x genotype x experimental day) with a Holm–Bonferroni post hoc adjustment performed on all pairwise comparisons. (# $p < 0.05$, * $p < 0.01$, *** $p<0.0001$). Data presented as mean ± SEM.

vs. McKO: t(214) = 2.428, $p = 0.0321$; Control vs. MKO: t(219) = 4.426, $p < 0.0001$) and chronic morphine (Morphine Day 10; Control vs. McKO: t(214) = 3.206, $p = 0.0031$; Control vs. MKO: t(219) = 4.938, $p < 0.0001$) exposure increased control activity compared with McKO littermates and aged-matched MKO ($n = 7$) animals (Figure 3.1A,B). Additionally, McKO mice exhibited overall increases in dark phase locomotor activity following prolonged morphine administration (Morphine Day 6; McKO vs. MKO: t(210) = 2.276, $p = 0.0321$; Morphine Day 10; McKO vs. MKO: t(210) = 2.102, $p = 0.0368$; Figure 3.1A,B).

Interestingly, chronic morphine (Saline vs. Morphine Day 10: t(206) = −3.099, $p = 0.0133$; Morphine Day 1 vs. Morphine Day 10: t(206) = −2.912, $p = 0.0200$) treatment, but not acute or subchronic morphine exposure, increased light phase activity in control mice compared with saline treatment; there was no impact on dark phase locomotor behavior across all experimental days (Figure S5A). Conversely, McKO mice exhibited decreased dark phase locomotor activity across the morphine treatment paradigm (Saline vs. Morphine Day 10: t(206) = 3.276, $p = 0.0074$; Morphine Day 1 vs. Morphine Day 10: t(206) = 3.076, $p = 0.0119$), while their light phase locomotor activity remained unchanged (Figure S5A). As a result, diurnal differences in horizontal activity ([Activity]dark phase—[Activity]light phase) for control and McKO mice were significantly decreased following subchronic (Saline vs. Morphine Day 6; Control: t(93.5) = 4.082, $p = 0.0006$; McKO: t(94) = 2.923, $p = 0.0174$) and chronic morphine (Saline vs. Morphine Day 10; Control: t(93.5) = 3.911, $p = 0.0009$; McKO: t(94) = 4.203, $p = 0.0004$) treatment when compared with vehicle-treated activity measures (Figure S5A). Meanwhile, morphine exposure did not seem to impact locomotor activity in MKO mice, regardless of treatment day (Figure S5A,B).

Upon subchronic and chronic morphine exposure, no significant differences were observed between McKO and MKO animals. However, McKO mice did appear to gradually decrease their dark phase activity throughout the treatment paradigm, while MKO mice did not exhibit any changes in average locomotor activity in either phase (Figures 3.1 and S5). Furthermore, diurnal differences in overall horizonal activity decreased in McKO mice, but not MKO mice, following 6 and 10 days of morphine exposure (Figure S5). This suggests that these chronic morphine-induced decreases in activity across the paradigm were dependent on MOR-expressing cells outside of the retina (not ipRGCs). Perhaps more intriguingly, following subchronic and chronic morphine exposure, control mice exhibited increased activity relative to McKO littermates (Figures 3.1 and S5). While both control and McKO mice showed reduced diurnal differences in horizontal locomotor activity, these differences resulted from progressive increases in control daytime activity throughout the morphine treatment regimen (Figure S5). These findings are consistent with past work showing that morphine-pellet-implanted rats exhibited a decrease in their diurnal activity amplitudes relative to those of controls [14]. Interestingly, while overall differences in light vs. dark activity decreased throughout protracted morphine treatment, the dark phase activity remained higher than that in the light phase across all experimental conditions ($p < 0.01$, Figure S6). This indicates that while morphine's ability to alter mouse locomotor activity is robust, it is not enough to completely eliminate light's ability to entrain the circadian rhythms of locomotor activity.

3.2.2 McKO mice display diminished morphine-induced behavioral sensitization compared to control littermates

` The increase in control and McKO horizontal activity following morphine injections on day 6 and 10 was evident (Figure 5). This stereotyped increase in locomotor activity following

repeated morphine exposure has been previously termed behavioral sensitization (Kalivas and Duffy, 1987; Smith et al., 2009). This behavioral phenomenon has been well established within the field, as rodents tend to increase their locomotor response over the course of chronic opioid paradigms (Kalivas and Duffy, 1987; Yoo et al., 2003; Smith et al., 2009). To quantify morphine-induced increases in horizontal activity, we assessed horizontal locomotor activity during ZT 1, ZT 2, ZT 13, and ZT 14 (2–3 h) following a 20 mg/kg i.p. morphine injection at ZT 0 and ZT 12 (Figure 5A). Horizontal activity data were transformed (square root) to meet the normality and homogenous variance ANOVA assumptions. Notably, we excluded the first hour post-injection from our analysis, as locomotor depression has been observed in mice within the first ~30 min following systemic morphine administration, resulting in little total change in horizontal activity within the first hour (Hecht and Schiorring, 1979; Szkeley et al., 1980; Itoh et al., 1987). When we compared differences in injection-induced horizontal locomotor activity across genotype, no significant differences were detected following saline and acute morphine treatment at ZT 0 and ZT 12 (Figure 3.2A,B). However, after six days of morphine exposure, control animals exhibited increased morphine-induced behavioral activity compared with both McKO littermates and MKO mice during the light phase (Control vs. McKO: $t(221) = 2.341$, $p = 0.0403$; Control vs. MKO: $t(224) = 3.309$, $p = 0.0033$; Figure 3.2C). This effect was amplified following 10 days of morphine treatment, as control animals retained their increased morphine-related locomotor activity compared with McKO and MKO mice in the light (Control vs. McKO: $t(221) = 3.216$, $p = 0.0030$; Control vs. MKO: $t(224) = 5.527$, $p < 0.0001$; Figure 3.2D). Control mice also showed increased behavioral activity compared with MKO mice in the dark following chronic morphine exposure ($t(224) = 4.110$, $p = 0.0002$; Figure 3.2D). Additionally, during Morphine Day 10, McKO mice exhibited increased post-injection horizontal activity compared

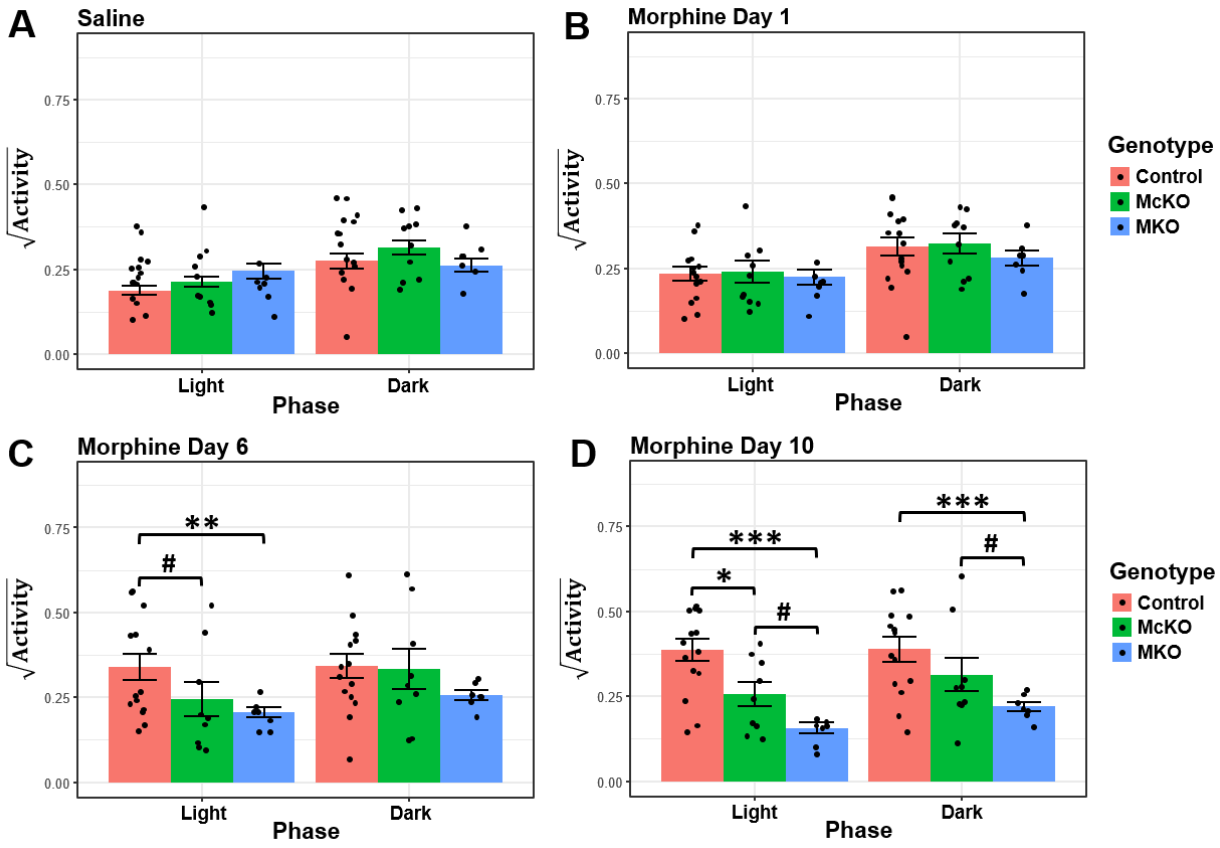

Figure 3.2 McKO mice exhibited reduced morphine-induced locomotor activation compared with control littermates following protracted morphine exposure. (A) Quantification of locomotor activity 1–2 h following saline injections at ZT0 and ZT12 for Control (n = 15), McKO (n = 10), and MKO (n = 7) mice. (B) Quantification of horizontal activity 1–2 h following initial 20 mg/kg i.p. morphine injections at ZT0 and ZT12 for Control (n = 15), McKO (n = 10), and MKO (n = 7) mice. (C) Quantification of horizontal activity 1–2 h following 20 mg/kg i.p. morphine injections at ZT0 and ZT12 for Control (n = 14), McKO (n = 9), and MKO (n = 7) mice on day 6 of the morphine treatment paradigm. (D) Quantification of horizontal activity 1–2 h following 20 mg/kg i.p. morphine injections at ZT0 and ZT12 for Control (n = 14), McKO (n = 9), and MKO (n = 7) mice on day 10 of the morphine treatment paradigm. Three-way ANOVA with a Holm–Bonferonni post hoc adjustment was performed on all pairwise comparisons (# p < 0.05, * p < 0.01, ** p < 0.001, *** p < 0.0001). Data presented as mean ± SEM.

with MKO animals in both the light (t(215) = 2.563, p = 0.0111) and the dark (t(215) = 2.446, p = 0.0305; Figure 3.2D).

Interestingly, when we compared horizontal activity across experimental days within mice of the same genotype, only control animals acquired morphine-induced behavioral

sensitization compared with vehicle injection days in both dark (Saline vs. Morphine Day 10: $t(206) = -3.427$, $p = 0.0044$) and light phases (Saline vs. Morphine Day 6: $t(206) = -4.645$, $p < 0.0001$; Saline vs. Morphine Day 10: $t(206) = -6.108$, $p < 0.0001$; Figure S7A,B). Meanwhile, McKO and MKO mice did not exhibit significant increases in post-injection locomotor activity over the course of the experiment (Figure S7C–F). While the role of MORs in the acquisition of behavioral sensitization is well-established (Tian et al., 1997; Sora and Li, 2001; Yoo et al., 2003), these data point to a potential contribution of MORs expressed by ipRGCs in morphine-induced locomotor sensitization.

3.2.3 Morphine has disparate effects on body temperature across the chronic treatment paradigm in mice differentially expressing the MOR

Body temperature data were also obtained from implanted transmitters during the chronic morphine administration protocol described above. During the last day of vehicle treatment, control mice had higher average body temperature than McKO littermates in the light phase (Control vs. McKO: $t(219) = 3.823$, $p = 0.0005$); additionally, control animals showed increased body temperature compared with MKO animals in the dark phase following treatment with saline (Control vs. MKO: $t(223) = 2.960$, $p = 0.0102$; Figure 3.3A,B). Interestingly, no significant body temperature differences between the genotypes were detected upon acute morphine exposure (Morphine Day 1) (Figure 3A,B). However, differences between the genotypes returned following 6 and 10 days of morphine treatment, as control mice again had higher average body temperature than McKO littermates during both light (Morphine Day 6: $t(217) = 3.659$, $p = 0.0010$; Morphine Day 10: $t(217) = 3.069$, $p = 0.0073$) and dark (Morphine Day 6: $t(217) = 3.338$, $p = 0.0028$; Morphine Day 10: $t(217) = 3.250$, $p = 0.0040$) phases (Figure 3.3A,B). Additionally, control mice had higher body temperature compared with MKO mice in

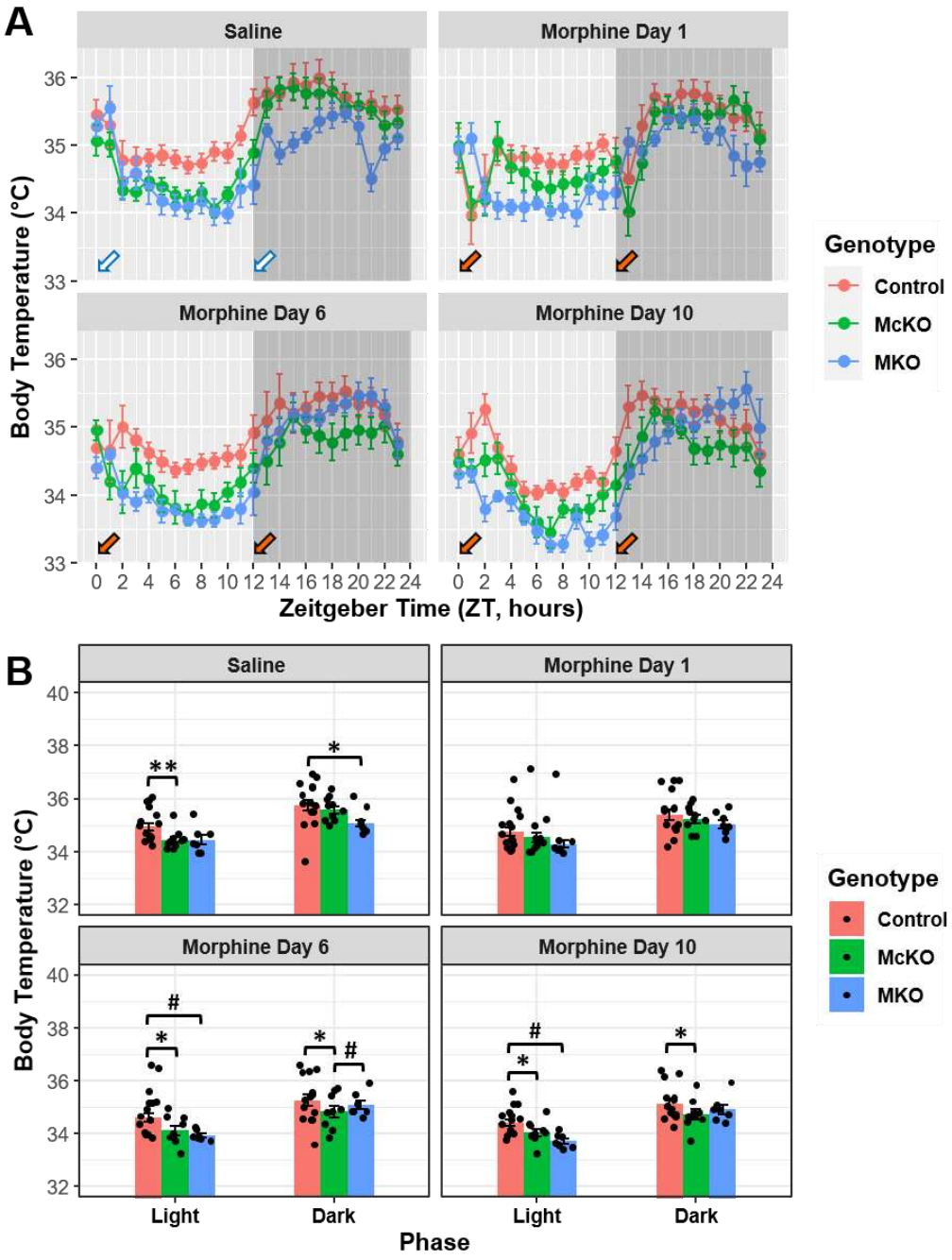

Figure 3.3 Morphine had differential effects on body temperature in control, McKO, and MKO mice across the morphine treatment paradigm. (**A**) Average body temperature plotted for control (n = 14–15), McKO (n = 9–10), and MKO (n = 7) mice by hour (Zeitgeber Time) for different experimental days. Arrows indicate time of i.p. injection with either saline (white arrows) or 20 mg/kg of morphine (orange arrows). (**B**) McKO mice had a lower mean body temperature than control littermates on all experimental days except for the first day of morphine treatment. Three-way ANOVA (phase x genotype x experimental day) with a Tukey post hoc adjustment was performed on all pairwise comparisons. (# $p < 0.05$, * $p < 0.01$, ** $p < 0.001$). Data presented as mean ± SEM.

the light phase alone ($t(223) = 2.768$, $p = 0.0122$; Figure 3A,B), and McKO mice had decreased dark phase body temperature compared with MKO mice on Morphine Day 6 ($t(212) = -2.494$, $p = 0.0268$; Figure 3.3A,B).

When we dissected the changes in body temperature across experimental days, it appeared that chronic morphine tended to decrease overall body temperature during both light and dark phases (except in the dark phase for MKO mice) (Figure S8A). In control mice, significant reductions in body temperature existed between Saline and Morphine Day 6 (light: $t(206) = 2.543$, $p = 0.0499$; dark: $t(206) = 3.448$, $p = 0.0034$) as well as Saline and Morphine Day 10 (light: $t(206) = 3.780$, $p = 0.0012$; dark: $t(206) = 4.247$, $p = 0.0002$) during both phases (Figure S8A). Similarly, McKO mice had reductions in dark phase body temperature between Saline and Morphine Days 6 ($t(206) = 4.108$, $p = 0.0003$) and 10 ($t(206) = 4.664$, $p < 0.0001$). Additionally, McKO mice exhibited significant differences between Morphine Day 1 and Morphine Day 10 in both the light ($t(206) = 2.932$, $p= 0.0225$) and dark phases ($t(206) = 2.857$, $p = 0.0189$; Figure S8A). MKO mice exhibited body temperature decreases when Saline was compared with Morphine Day 10 ($t(205) = 3.285$, $p = 0.0072$) and when Morphine Day 1 was compared with Day 10 ($t(205) = 2.615$, $p = 0.0479$) during the light phase, while MKO mice showed no such changes across experimental days in the dark phase (Figure S8A). Finally, it is important to note that nocturnal increases in overall body temperature were maintained for all experimental days across each genotype ($p < 0.01$; Figure S9).

3.2.4 Control mice, but not McKO or MKO mice, appear to develop tolerance to the hypothermic effects of morphine during chronic administration

Similar to the locomotor effects of morphine, the hypothermic response to high morphine doses has been shown to be biphasic, with a brief increase in body temperature followed by a

longer-lasting period of hypothermia upon systemic administration (Rawls and Benamar, 2011). Thus, to capture the peak of the acute morphine effect on body temperature, we looked at the window of time described above (2–3 h after i.p. morphine injections): ZT 1, ZT 2, ZT 13, and ZT 14. Analyses of this portion of the data revealed that control mice exhibited decreased body temperature in both light (Saline vs. Morphine Day 1: $t(205) = 2.757$, $p = 0.0381$) and dark (Saline vs. Morphine Day 1: $t(205) = 2.944$, $p = 0.0217$) phases following acute morphine exposure (Figure 4.4A,B). In the light phase, control mice showed a significant increase in body temperature between Morphine Day 1 and 10 ($t(206) = -2.728$, $p = 0.0381$); the body temperature was also increased (near saline baseline measurements) in the dark phase following prolonged morphine exposure (Saline vs. Morphine Day 10: $t(206) = 1.405$, $p = 0.5629$; Figure 4.4A,B). In the dark phase, McKO mice exhibited a similar reduction in body temperature compared to saline ($t(205) = 3.667$, $p= 0.0019$); however, this reduction persisted throughout the morphine treatment paradigm (Saline vs. Morphine Day 6: $t(206) = 2.959$, $p = 0.0173$; Saline vs. Morphine Day 10: $t(206) = 2.955$, $p = 0.0173$; Figure 4.4C,D). Importantly, no changes were detected in body temperature during the light phase (ZT 1 & ZT 2) in McKO animals (Figure 4.4C,D). Finally, MKO animals showed no significant changes in post-injection body temperature throughout the course of the treatment paradigm (Figure 4.4E,F).

When we assessed differences across the three genotypes, we found that during the final saline day, control mice had higher body temperature than McKO littermates during the light phase ($t(221) = 2.505$, $p = 0.0389$; Figure S10A,B). Interestingly, on the first day of morphine administration, control mice had higher body temperature compared with McKO mice during the dark phase ($t(221) = 2.926$, $p = 0.0114$; Figure S10A,B). After six days of systemic morphine

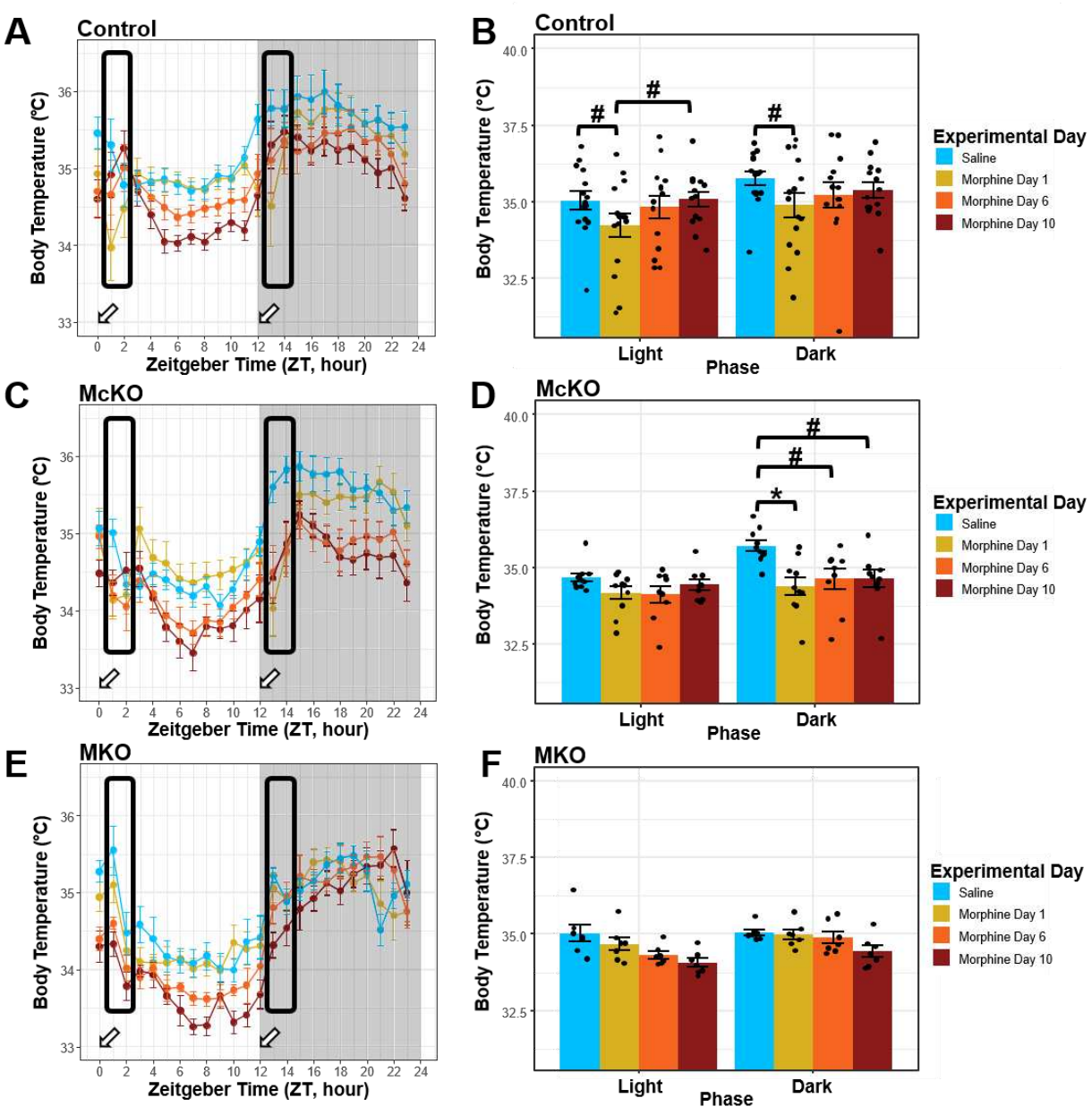

Figure 4.4 Control mice, but not McKO or MKO mice, developed tolerance to the hypothermic effects of morphine. (**A**,**B**) Control mice (n = 14–15) treated with chronic morphine exhibited morphine-induced hypothermia following acute but not chronic morphine exposure. Body temperature was measured 2–3 h following a 20 mg/kg i.p. morphine injection at ZT0 and ZT12. (**C**,**D**) McKO mice (n = 9–10) treated with morphine-induced hypothermia in the dark but not in the light. Body temperature was measured 2–3 h following a 20 mg/kg i.p. morphine injection at ZT0 and ZT12. (**E**,**F**) MKO mice (n = 7) exhibited minimal body temperature changes following both acute and chronic morphine administration. Body temperature was measured 2–3 h following a 20 mg/kg i.p. morphine injection at ZT0 and ZT12. Three-way ANOVA (phase x genotype x experimental day) with a Holm–Bonferroni post hoc adjustment was performed on all pairwise comparisons (# $p < 0.05$, * $p < 0.01$). Timing of injections indicated by the white arrows. Data presented as mean ± SEM.

exposure, control mice retained their high body temperature compared with McKO littermates in the light phase ($t(218) = 3.326$, $p = 0.0031$) while also exhibiting increased core temperature in the dark phase ($t(218) = 3.002$, $p = 0.0090$; Figure S10A,B). Lastly, on Morphine Day 10, control mice exhibited higher body temperatures than both McKO and MKO mice after morphine injection at both light (Control vs. McKO: $t(218) = 3.170$, $p = 0.0052$; Control vs. MKO: $t(224) = 2.990$, $p = 0.0062$) and dark (Control vs. McKO: $t(218) = 3.429$, $p = 0.0022$; Control vs. MKO: $t(224) = 2.822$, $p = 0.0104$) phases. These data suggest not only that MORs are required for the hypothermic effects of high doses of morphine but also that MORs specifically expressed by ipRGCs play a modulatory role in tolerance development to morphine-induced hypothermia.

3.2.5 Morphine-Induced Behavioral Alterations in McKO Animals Likely Arise from MOR Expression Changes within the Retina

In order to determine whether the reported behavioral effects observed in McKO mice were due to alterations in MOR expression within the retina, we needed to validate that *Opn4* drove Cre recombinase (Cre) expression in ipRGCs and not in key regions within the brain. To accomplish this, we immunolabeled Cre in the hypothalamus (SCN and VLPO), striatum (caudate/putamen [CP]), and the paraventricular nucleus of the thalamus (PVT). We first labeled Cre in the retina of McKO mice crossed with *Opn4*-EGFP BAC-carrying mice (in which M1-M3 ipRGCs have green somas (Cleymaet et al., 2019)). As shown in Figure S11A–C, we found strong somatic immunolabeling of Cre in McKO ipRGCs (26 cells from 2 animals, average cell volume = 213 μm^2). Notably, we considered a cell a "true positive" if 5% of the cell's volume was Cre+ and found that nearly 70% of ipRGCs were Cre+ (18/26 cells). Within cells that passed our 5% cutoff, the average Cre+ volume percentage in positive ipRGCs was 28.5% (maximum =

87.3%). Due to variable *Opn4* expression between ipRGC subtypes, only M1-M3 ipRGC subtypes can be identified in the *Opn4*-EGFP mouse (Cleymaet et al., 2019). Because we did not quantify Cre+ non-ipRGCs (Figure S11B,C), we likely underestimated the number of ipRGCs (especially in M4-M6 ipRGC subtypes) that were Cre+ in the McKO retina. To examine Cre expression in the brain, we first had to confirm that the antibody labeled Cre in the brain. To accomplish this, we sectioned the preoptic area of the hypothalamus from mice in which tdTomato was present in Cre-expressing galaninergic neurons (*Gal*-cre-tdTomato). As the preoptic area contains a high number of galanin-expressing cells (Wu et al., 2014), Cre immunolabeling in the *Gal*-cre-tdTomato brain also resulted in somatic labeling, albeit less robust than in the retina (Figure S11D–F). This was in strong contrast to the pattern of Cre immunostaining found in the McKO brain (Figure S12). In single optical sections from all analyzed brain regions, Cre appeared to be primarily localized to the outer surfaces of (i.e., surrounding) DAPI-labeled cells (Figure S12), suggesting that Cre immunoreactivity in the McKO brain primarily originated from Opn4+ ipRGC processes and not from neurons in the brain themselves. Nevertheless, as in the retina, we considered a cell a true positive if 5% of the cell's volume was Cre+. We found that in the VLPO, 1.4% of cells were Cre+ (12/869; Figure S8A–C); in the SCN, 0.89% of cells were Cre+ (4/445); in the CP, 1.7% of cells were Cre+ (15/848 cells; Figure S12D–F); and in the PVT, 3.8% of cells were Cre+ (15/398; Figure S12G–I). Although we manually segmented most DAPI cell clusters (resulting in an average cell volume of 361 μm^2; median = 341 μm^2), the maximum cell volume (1480 μm^2) indicates that some cell clusters remain, which may have led to artificially higher percentages of Cre+ cells. Given the low proportion of neurons that express Cre in the brains of McKO animals, their contributions to the behaviors described in this paper are likely small if not insignificant.

3.3 Discussion

Synchronizing circadian activity rhythms to environmental light/dark cycles is essential for an organism's ability to survive (LeGates et al., 2014). Mounting evidence points to synchronization of activity during specific light/dark phases to be crucial to optimal health of humans and rodents alike (LeGates et al., 2014). Results from the present study confirmed that chronic morphine exposure can drastically alter both circadian locomotor activity as well as body temperature rhythms (Moreton et al., 1976; Gillman et al., 2009; Glaser et al., 2012). Morphine primarily exerts its effect via MORs that are widely expressed throughout both the CNS as well as other body systems (Andersen et al., 2003). Thus, the observation that twice daily morphine exposure alters circadian behavioral/body temperature rhythms is not particularly surprising (Figures 3.1 and S5). Indeed, this effect has been extensively demonstrated in both humans and rodents (Moreton et al., 1976; Byku and Gannon, 2000; Vansteensel et al., 2005; Gillman et al., 2009; Glaser et al., 2012; Serdarevic et al., 2017; Eacret et al., 2020; Simmons et al., 2020; Huhn and Finan, 2021). However, to our knowledge, no studies have examined the role of MORs expressed by retinal neurons in the context of opioid-related circadian dysregulation (Figure S9).

3.3.1 Systemic Morphine Affects Behavioral Activity via MORs Expressed by ipRGCs

Saline-injected mice lacking MORs (MKO) exhibited decreased horizontal activity compared with control/McKO aged-matched mice (Figure 3.1B). This finding is interesting, as it is consistent with the idea that increased levels of MOR-preferring β-endorphin at night potentially contribute to regulating behavioral activity (Kerdelhue et al., 1983; Berezin et al., 2022). On the other hand, it differs from previous findings from our lab that showed decreased dark phase activity in McKO mice compared with wildtype (C57BL6/J) animals (Berezin et al., 2022). This discrepancy in findings can be potentially attributed to two factors: (1) the use of

littermate control animals (in this study) instead of wildtype mice as controls and (2) the stress of repeated injections utilized in the present study. Stress has been shown to alter circadian rhythms in both humans and rodents (Koch et al., 2017). Thus, it is possible that the stress of repeated injections in the present study was enough to mask the decreases in nocturnal activity between McKO and control animals during the saline injection period. Interestingly, a pattern of decreased nocturnal behavior persisted after acute morphine exposure, which is consistent with the idea that the locomotor activation associated with morphine is acquired rather than innate (Kalivas and Duffy, 1987).

Examining the activity traces across experimental days, we noticed that as mice proceeded through the chronic morphine paradigm, mouse activity became increasingly entrained to each morphine injection (Figures 3.1 and S7). Not only was the activity entrained to these injections, but their horizontal locomotor activity appeared to increase over the course of the chronic morphine paradigm (Figures 3.1 and S7). A similar effect has been reported in rats, wherein fentanyl-treated rats' locomotion remained entrained to the drug infusion even after cessation of drug treatment (Gillman et al., 2009). Drug-induced hyperlocomotion (often referred to as behavioral activation) is a well-established phenomenon associated with rewarding properties of opioids and other drugs of abuse (Kalivas and Duffy, 1987; Robinson and Berridge, 1993). While this phenomenon was first described 50 years ago (Babbini and Davis, 1972), our data are the first to suggest that ipRGCs contribute to this acquired drug-related behavior.

To concentrate on the peak effect of morphine on horizontal activity, we specifically analyzed ZT 1, ZT 2, ZT 13, and ZT 14 (2–3 h) after daily injections at ZT 0 and ZT 12. Analysis of ZT 1, ZT 2, ZT 13, and ZT 14 revealed no differences between genotypes or experimental days during the light (ZT 1 & ZT 2) or dark (ZT 13 & ZT 14) phases post injection

with vehicle and acute morphine (Figures 3.2 and S7). However, after subchronic and chronic morphine exposure, differences began to emerge. Consistent with past findings (Tian et al., 1997; Sora and Li, 2001; Contarino et al., 2002; Yoo et al., 2003), MKO mice did not acquire morphine-induced behavioral sensitization following chronic exposure and thus exhibited reduced post-injection locomotor activity compared with age-matched McKO and control animals (Figures 3.2 and S7). This corroborates past experiments that have demonstrated the necessity of MORs for the acquisition of morphine-induced locomotor activation (Tian et al., 1997; Sora and Li, 2001; Contarino et al., 2002; Yoo et al., 2003). Surprisingly, MKO mice increased their locomotor activity between ZT 18 and ZT 23 following prolonged, but not acute, morphine treatment. This is even more interesting when we consider that after 6–12 h post injection, the morphine would have been systemically degraded (Bergum et al., 2022a). This effect could result from a circadian activity shift mediated by morphine's weak activity at the δ-opioid receptor (as δ-opioid receptor agonism has been shown to induce circadian phase shifts in rodents) (Byku and Gannon, 2000; Andersen et al., 2003). Intriguingly, only control mice appeared to acquire morphine-induced behavioral sensitization (compared with saline baselines), while McKO littermates did not (Figure S7). Moreover, control animals showed increased post-injection horizontal activity following 6 and 10 days of chronic morphine treatment in the light phase but not the dark phase (Figure 3.2). This suggests that MORs expressed by ipRGCs might only play a role in morphine-induced behavioral activation during the light phase. Light has been shown to suppress locomotor activity in an ipRGC-dependent manner via both clock-dependent and clock-independent pathways (Lupi et al., 2008; LeGates et al., 2014; Rupp et al., 2019). Crucially, the MOR agonist DAMGO reduced light-evoked ipRGC firing via specific ionic currents (Cleymaet et al., 2019), and morphine has been shown to accumulate in the mouse retina

following chronic systemic injection (Bergum et al., 2022a). Thus, morphine that accumulates in the retina could suppress the light-evoked ipRGC firing. MOR-mediated suppression of ipRGC activity could thus decrease light-mediated activation of sleep-promoting neurons in the brain's sleep and circadian centers to increase activity in nocturnal animals (Lupi et al., 2008; Rupp et al., 2019). While morphine certainly acts on other circadian, arousal, and reward centers within the brain to elicit behavioral sensitization/activation (Eacret et al., 2020), to our knowledge, this study provides the first behavioral evidence that MORs expressed by ipRGCs are involved in morphine-related behavioral sensitization.

3.3.2 Systemic Morphine Affects Thermoregulation via MORs Expressed by ipRGCs

Thermoregulation is an important physiological process that allows the body to properly function (Morrison and Nakamura, 2011). Circadian changes in body temperature in rodents are thought to correlate tightly with those of locomotor activity (Refinetti, 1999). Morphine has been shown to differentially alter body temperature depending on the dose (Rawls and Benamar, 2011; Koek, 2014). Importantly, activation of specific ipRGC subtypes has been linked to acute and circadian light-induced reductions in body temperature (Rupp et al., 2019). While circadian body temperature changes can sometimes precede circadian locomotor activity changes, typically, body temperature rhythms closely resemble circadian activity rhythms (Weinert and Waterhouse, 1998; Refinetti, 1999). In mammals, both body temperature and locomotor activity are higher during the active phase and lower during the inactive phase (Weinert and Waterhouse, 1998). While the two are not necessarily linked (Refinetti, 1999), locomotor activity can increase body temperature and thus mask the circadian body temperature rhythmicity (Weinert and Waterhouse, 1998). Thus, it is important to consider that morphine-induced changes in body temperature could be affected by its locomotor effects. Diurnal variations in body temperature

were conserved across all genotypes and experimental days (Figure S9). Specifically, control, McKO, and MKO mice all exhibited decreased average body temperature in the light phase across the morphine treatment regimen (Figure S8). Consistent with the activity data, extended morphine exposure reduced diurnal temperature amplitude in control and McKO mice but not MKO mice (Figure S8). Importantly, control and McKO mice only exhibited body temperature reductions in the dark phase following chronic morphine exposure (Figure S8). Notably, control mice had increased body temperature relative to McKO animals during subchronic and chronic morphine exposure (Figure 3.3). These data suggest that MORs expressed by ipRGCs play a role in the morphine-related body temperature changes in the dark phase but not the light phase. While these data are difficult to interpret, they indicate that MORs expressed by ipRGCs might play a role in morphine-induced alterations in body temperature regulation.

High doses of systemic morphine are known to induce robust body temperature decreases upon acute exposure (Baker and Meert, 2003; Rawls and Benamar, 2011). Although many studies have examined morphine-induced hypothermia, the exact mechanism underlying this phenomenon remains unresolved (Rawls and Benamar, 2011). Some rodent studies have suggested that the hypothermic effects of high-dose morphine are mediated by the κ-opioid receptor (Chen et al., 1996), which could explain the slight decrease in body temperature we observed on Morphine Day 10 (relative to saline) in the dark phase (Figure 3.4). However, the observation that the post-injection body temperature of MKO mice remained largely unaffected by vehicle/morphine treatment strongly implicates MORs in morphine-induced hypothermia.

In the dark phase, control mice and McKO littermates exhibited significant reductions in post-injection body temperatures following acute morphine exposure (relative to saline controls) (Figure 3.4A,B). Interestingly, McKO littermates showed little change in post-injection body

temperature throughout chronic morphine treatment (Figure 3.4B). Meanwhile, control mice exhibited reductions in morphine's hypothermic effect over the course of chronic treatment (in both phases) (Figure 3.4A). Based on these data, Control animals appeared to develop tolerance to the hypothermic effects of morphine. While past studies have reported tolerance to the hypothermic effects of morphine (Zarrindast et al., 2001), the mechanism by which this occurs remains largely unexplored. It is possible that chronic exposure reduces the hypothermic effect of morphine via MOR desensitization within the thermoregulatory pathway. However, upon concurrent examination of morphine's effect on body temperature and locomotor behavior across the chronic treatment paradigm, it appears to us that morphine-induced increases in behavioral activity across the paradigm might be driving a gradual body temperature increase. In other words, the return of post-injection body temperature (near saline levels) could be due to the heat that is produced by morphine-induced behavioral activation. In support of this idea, both the hypothermic effects and the locomotor-stimulating effects of morphine have been linked to the mesolimbic dopamine pathway (Kalivas and Duffy, 1987; Zarrindast and Zarghi, 1992; Becker et al., 2001; Baker and Meert, 2002; Le Marec et al., 2011; Koek et al., 2012). Moreover, opioid receptors in the preoptic area of the hypothalamus (POA) have been associated with both the wake-promoting and thermoregulatory properties of opioid drugs (Chen et al., 1996; Greco et al., 2008; Wang et al., 2013). Taken together, these findings suggest that a convergent mechanism underlies both morphine-induced behavioral sensitization and the progressive reductions in morphine-induced hypothermia.

3.3.3 Strengths and Limitations

To gain a clearer understanding of morphine's effect on circadian behavioral rhythms, we employed mini-telemetry devices to measure their horizontal locomotor activity and body

temperature 24 h/day for the duration of each trial. While this method does require surgery, it provides a more complete picture of the animal's locomotor behavior throughout the day when compared with traditional wheel-running experiments. First, wheel running is not able to record locomotor activity when mice are away from the wheel. Additionally, the inherent rewarding nature of wheel running (Novak et al., 2012) complicates the interpretation of the data when studying drugs of abuse such as morphine. To distill the morphine-specific effect on horizontal locomotor activity, we first treated the mice with saline for 5–6 days prior to morphine exposure. This helped the animals habituate to handling while also providing us with a behavioral baseline to compare to the drug treatment. Specifically, by comparing vehicle-injected animals to morphine-injected animals we controlled for any potential locomotor responses that the stress of handling and/or the i.p. injection itself might elicit.

While the current study uncovered a potentially novel contributor to morphine-induced behavioral sensitization, this study was not without limitations. First, the use of the Control/McKO line yielded mice with at least a 75% C57BL/6J background, while the MKO mice were completely backcrossed to the C57BL/6J background. Importantly, the control line has been shown to exhibit normal morphine-induced antinociception and develop antinociceptive tolerance (Weibel et al., 2013). Moreover, this mouse line acquires opioid-induced behavioral activation/sensitization and self-administers opioids (Severino et al., 2020). For the purposes of this study, the control/Mu^{fl} line functions normally with regard to opioid-related behavioral responses, and we thus felt it was acceptable to compare Control/McKO animals to age-matched MKO animals (despite minor differences in genetic background) (Weibel et al., 2013). Another potential limitation of our study was using the Cre-lox breeding strategy to generate McKOs where only ipRGCs are expected to lack MORs. Specifically, many *Opn4*-cre mouse

lines have been shown to express Cre in retinal ganglion cells other than ipRGCs (Ecker et al., 2010; Maloney et al., 2022). Consequently, other retinal neurons might lose functional MOR expression as a result of the cross between *Opn4*-cre mice and mice with a floxed version of the MOR. While *Opn4*-cre mice have been shown to label non-photosensitive retinal ganglion cells (Maloney et al., 2022), it is unlikely that potentially removing MORs from these retinal ganglion cells would have any significant effect on light-mediated regulation of behavior. For example, in aging rats, loss of ipRGCs and no other retinal ganglion cells correlates well with circadian rhythm impairments (Lax et al., 2016). Additionally, in a number of retinal diseases affected a variety of cell types, at the stages where alterations in circadian rhythms are detected, the misalignments have been positivity correlated with ipRGC loss (Lax et al., 2019). This further substantiates the role of ipRGCs in mediating circadian photoentrainment over other types of retinal neurons that might express Cre and/or MORs.

Interestingly, there is some evidence of *Opn4* expression outside of the mammalian retina. In humans, *Opn4* expression was detected in areas of the brain that express MORs. The most significant areas are the caudate, putamen, and nucleus accumbens (Moraes et al., 2021). Additionally, studies performed in C3H/HeNHsd rd/rd mice have indicated Opn4 expression in the hypothalamus and cerebellum (Flyktman et al., 2017). Thus, *Opn4*-driven Cre expression could reduce functional MOR in specific brain regions involved in morphine-induced changes in locomotor activity and temperature regulation. However, we have previously shown that McKO animals do not exhibit significant differences in MOR expression compared to control (Berezin et al., 2022). Additionally, mouse studies in C57BL6 mice have shown that MOR-expressing cells in these regions (specifically the caudate, putamen, nucleus accumbens, and cerebellum) do not also express *Opn4* and vice versa (Saunders et al., 2018). This suggests that brain regions

that are important for mediating morphine-induced locomotor activation would not have Cre-dependent decreases in MOR expression. Furthermore, our own validation of the McKO mouse line indicated that Cre expression was primarily restricted to cells in the retina (with minimal expression in the brain) (Figures S11 and S12). While experimental evidence points to the idea that Cre-dependent elimination of functional MOR expression occurs mostly within the retina, we acknowledge that the *Opn4*-cre mouse line could be functionally modulating MOR expression in a small subset of brain neurons that could affect morphine-driven behaviors.

Animal handling complications limited this study to assessing the effect of morphine on body temperature and locomotor activity in freely moving animals (see Materials and Methods). While we were not able to directly assess sleep/wake activity using EEG/EMG, telemetric locomotor activity monitoring has been shown to provide a reliable behavioral readout that correlates well with EEG/EMG-derived sleep/wake analysis in rodents (Storch et al., 2004). Lastly, the present experiments were performed using exclusively male mice to avoid any behavioral complications associated with the estrus cycle. Future studies should examine the contribution of MORs expressed by ipRGCs to potential sex-dependent differences in the effect of opioids on circadian behaviors. These studies in female animals are crucial given mounting evidence of sex-related differences in the responsiveness to opioid drugs in rodents and humans (Mogil et al., 2000; Zubieta et al., 2002; Craft et al., 2006).

3.4 Materials and Methods

3.4.1 Animals

Oprm1$^{fl/fl}$ (Mu^{fl}) breeders (Jackson Labs strain #030074) were generously provided by Dr. Brigitte Kieffer (Douglas Research Center, McGill University). Mu^{fl} mice have exons two and three of the MOR (*Oprm1*) gene flanked by a *loxP* site and were maintained on a 50%

C57BL/6J-50% 129Sv background for five generations before receipt (Weibel et al., 2013). Mice with Cre recombinase expressed upstream of the melanopsin (*Opn4*) promoter [Tg(*Opn4*-cre) SA9Gsat/Mmucd, #036544-UCD; *Opn4*-cre] were purchased from the Mutant Mouse Resource and Research Center (MMRRC) at the University of California, Davis. These *Opn4*-cre mice were backcrossed into a 100% C57BL/6J background prior to purchase and were maintained as hemizygotes (*Opn4*-cre +/−). MOR-conditional knockout (McKO) mice, in which ipRGCs lack functional MORs, were generated as described previously (Cleymaet et al., 2021; Berezin et al., 2022). In brief, Mu^{fl} and *Opn4*-cre mice were crossed to obtain McKO mice with the floxed *Oprm1* gene on both alleles and *Opn4*-cre on one allele. Thus, the result of this cross produced 50% Mu^{fl}/control: 50% McKO littermates. Notably, this Mu^{fl}/McKO line was maintained on a background containing at least 75% C57BL/6J and 25% 129Sv. In all experiments, Mu^{fl} littermates of McKO mice were used as controls. Mice lacking functional MORs globally (B6.129S2-Oprm1tm1Kff/J; MKO) were purchased from Jackson Labs (strain #007559) (Matthes et al., 1996). MKO mice were backcrossed to C57BL/6J mice for at least 12 generations prior to purchase.

For the validation of this McKO mouse line, we crossed McKO mice to *Opn4*-EGFP BAC-carrying mice (Tg(*Opn4*-EGFP)ND100Gsat/Mmucd strain, generated by the GENSAT project) (Cleymaet et al., 2019). To examine Cre expression within the brain, we used mice that had Cre recombinase under control of the *GAL* promoter (B6J.FVB(Cg)-Tg(*Gal*-cre)KI87Gsat/Mmucd; *Gal*-cre). These Gal-cre animals were crossed to Ai14 (Jackson Labs strain #007914) mice to express tdTomato following *GAL*-driven Cre-dependent recombination (*Gal*-cre-tdTomato).

Adult male animals (8–26 weeks) were housed under a 12-h light:12-h dark cycle (LD) cycle, with lights on at 7:00 a.m. (ZT 0) and lights off at 7:00 p.m. (ZT 12). They were fed standard chow and water ad libitum. All animals used in these studies were handled in compliance with the Institutional Animal Care and Use Committees of Colorado State University (Protocol 18-8395A, 28 January 2019) and in accordance with the ARVO Statement for the Use of Animals in Ophthalmic and Vision Research.

3.4.2 Morphine Treatment

Mice were weighed and injected with doses of sterile saline or 20 mg/kg of morphine i.p. (Morphine sulfate salt pentahydrate, Sigma-Aldrich, Saint Louis, MO, USA; Product Number: M8777, dissolved in sterile saline). The dosage of 20 mg/kg i.p. morphine is commonly used to assess analgesic tolerance in mice (Peart and Gross, 2004). Mice received two injections daily: one at light onset (ZT 0) and a second at light offset (ZT 12). Prior to morphine administration, mice were injected with sterile saline twice daily for 6–7 days (the corresponding figures show the last day). The chronic morphine treatment paradigm consisted of 12 days of twice daily 20 mg/kg of morphine (administered at ZT 0 and ZT 12), which was always proceeded by at least 5 days of twice daily saline injections on the same schedule (Bergum et al., 2022a). Mice were weighed prior to surgery (preceding the injections) to ensure accurate dosages.

3.4.3 Surgery and Telemetry Recordings

Adult male Mu^{fl}/control, McKO, and MKO mice were surgically implanted with mini-telemetry transmitters (HD-X02 or TA-F10, DSI) as previously described (Zhang et al., 2021; Berezin et al., 2022). In brief, mice were deeply anesthetized with isoflurane (5%) and fitted with a nose cone for continuous isoflurane delivery (1–5%). Core body temperature and respiratory rate were monitored throughout surgery. Transmitters were subcutaneously inserted in the dorsal

abdomen. For HD-X02transmitters, electromyograph (EMG) leads were inserted into the cheek muscles, and electroencephalogram (EEG) leads were placed into holes drilled into the skull (1.0 mm posterior to bregma, 1.0 mm left of midline; 2.0 mm posterior to bregma, 1.0 mm right of midline) and held in place with dental acrylic. After the incisions were sutured, mice received an injection of the non-steroidal anti-inflammatory drug (NSAID) OstiLox (3 mg/kg meloxicam, VetOne) and their status was recorded every 5 min for the first 30 min post-surgery. Mice continued to be monitored for three days in separate cages under a standard 12-h light:12-h dark cycle with lights on at 7:00 a.m. (ZT 0). After recovery, each cage was placed on a receiver (DSI), which relayed the telemetry signals to a computer for recording. It is important to note that handling the mice during our twice daily i.p. injection schedule resulted in loosening and/or breaking the EMG/EEG leads; therefore, our analysis was reduced to activity and body temperature measurements provided by both types of transmitters. The implanted transmitters recorded the horizontal movement/locomotor activity and body temperature of Mu^{fl}/control, McKO, and MKO mice in their home cages (Berezin et al., 2022). Activity, measured in arbitrary units (a.u.), was recorded each minute. Mice were considered inactive when no horizontal movement was recorded during that minute. Similarly, body temperature measurements, measured in °C, were recorded each minute of the experimental trial for each animal.

3.4.4 Immunohistochemistry

Adult male mice were deeply anesthetized with pentobarbital sodium (Fatal-Plus) and then perfused with 10% sucrose in 0.1 M phosphate-buffered saline (PBS) followed by 4% PFA in PBS. The eyes were enucleated and post-fixed in 4% PFA at RT for 25 min (eyes were puncture-fixed for 20 min before the retinas were dissected out in PBS and returned to the

fixative for an additional 5 min). Whole brains were removed and post-fixed in 4% PFA at 4 °C for at least 24 h and then cut into 100 μm sections on a Leica vibratome. Brain slices and whole-mount retinas were washed with PBS then placed in blocking solution (5% serum, 0.5% Triton-X-100 in 0.1 M PBS). Tissues were incubated in the rabbit anti-Cre antibody (1:500 Cell Signaling #15036) for approximately 24 h followed by the appropriate secondary antibody (Goat anti-Rabbit Alexa Fluor 647, ThermoFisher, Waltham, MA, USA). The tissues were stained with DAPI (GeneTex, Irvine, CA, USA) then mounted on Superfrost Plus microscope slides (Fisher Scientific, Hampton, NH, USA) in Vectashield Plus Antifade Mounting Medium (Vector Laboratories, Burlingame, CA, USA).

Tissues were imaged in 1 μm Z-stack increments on a LSM 900 confocal microscope (Carl Zeiss, Oberkochen, Germany) with a 40x oil-immersion objective. For all images, sequential scans at each wavelength were performed, and 4x averaging was performed to improve the signal-to-noise ratio. Automated image analysis was performed using Fiji (v1.53, (Schindelin et al., 2012)). In brief, after initial pre-processing (i.e., adjusting brightness and denoising), a median blur filter was applied to each channel, and the images were thresholded and converted to binary masks. The 3D Objects Counter plugin (Bolte and Cordelières, 2006) was used to count DAPI+, GFP+, and/or Cre+ objects in each mask. The accuracy of GFP+ cell counting was manually verified, and most large (>700 μm^2) DAPI+ cell clusters were manually watershed segmented using the 3D ROI Manager (Ollion et al., 2013). The “Measure” and “Colocalization” features of the 3D ROI Manager were used to calculate all objects’ numbers, volumes, and percent colocalization (Ollion et al., 2013).

3.4.5 Data and Statistical Analysis

Data are presented as mean ± standard error of the mean (SEM), as specified in figure captions. The data were analyzed using two-way (genotype x experimental day) or three-way (phase x genotype x experimental day) ANOVA. Some data were transformed to the square root scale to satisfy ANOVA assumptions. Data wrangling, visualizations, and analyses were performed using RStudio (version 4.0.0) with Holm–Bonferroni post hoc adjustments for all pairwise comparisons, and $p < 0.05$ was considered significant.

3.5 Conclusions

The results of this experiment established a potential link between MORs expressed by ipRGCs and opioid-induced locomotor sensitization. This finding is particularly surprising because most studies assessing the underlying mechanisms of morphine-induced behavioral activation/sensitization have focused on MOR expression within the mesolimbic dopamine reward circuit and not the photoentrainment pathway (Kalivas and Duffy, 1987; Becker et al., 2001; Zubieta et al., 2002; Cook, 2003; Smith et al., 2009; Le Marec et al., 2011; Severino et al., 2020). Behavioral sensitization and the positive-reinforcing effects of opioids have long been linked due to their concurrent temporal progression and overlapping neuroanatomical correlates (Wise and Bozarth, 1987; Tzschentke, 2001; Smith et al., 2009). Moreover, behavioral sensitization is considered to be a strong behavioral marker for addiction-associated behaviors (Robinson and Berridge, 1993; Le Marec et al., 2011). Thus, the findings presented here, in conjunction with past work from our lab, not only suggest a retinal contribution to opioid-induced circadian disruptions but also point to ipRGC's involvement in the mixed etiology of drug-related behaviors (Cleymaet et al., 2019; Berezin et al., 2022; Bergum et al., 2022a). While we are not suggesting that ipRGCs are a primary mediator of these opioid-induced effects, this

study presents ipRGCs a potentially novel target to ameliorate the effects of opioid-related sleep/wake disturbances.

Chapter 4 - μ-Opioid Receptors May Not Develop Cellular Tolerance at the Level of Solitary Intrinsically Photosensitive Retinal Ganglion Cells

4.1 Introduction

Opioids remain among the most effective analgesics for treating both moderate and severe pain (Rosenblum et al., 2008). Unfortunately, long-term opioid use is often associated with analgesic tolerance, drug dependence and sleep/wake problems (Contet et al., 2004; Williams et al., 2013; Huhn and Finan, 2021). While the mechanism underlying opioid tolerance and addiction have been extensively studied, no clear picture has emerged regarding the cellular mechanisms underlying these processes.

Tolerance is broadly defined as a reduction in drug efficacy following prolonged exposure (Williams et al., 2013). Analgesic tolerance has been linked to the development of cellular tolerance in cells within the pain pathway such as the periaqueductal grey (Bagley et al., 2005; Adhikary and Williams, 2022). Classically, cellular tolerance is tested by measuring reductions in MOR agonist-mediated effects on cells derived from opioid-treated animals compared to opioid-naïve animals (Christie et al., 1987; Connor et al., 1999; Bagley et al., 2005; Levitt and Williams, 2012; Adhikary and Williams, 2022). Most of these experiments use G protein-mediated activation of G protein-coupled inwardly-rectifying potassium channel (GIRK) currents (Christie et al., 1987; Levitt and Williams, 2012; Fox and Hentges, 2017; Adhikary and Williams, 2022) and/or inhibition of voltage-gated calcium currents as a cellular readout for MOR activation (Connor and Christie, 1998; Connor et al., 1999; Bagley et al., 2005; Johnson et al., 2006). Interestingly, there is no evidence of GIRK channel expression in ipRGCs (Figure 4.1), but it has been previously shown that DAMGO inhibits ipRGC activity via inhibition of

voltage-gated calcium channels (Cleymaet et al., 2019). Therefore, we decided to test tolerance at the cellular level by using MOR-mediated voltage-gated calcium channel inhibition as a measure of MOR activation. Results from this investigation revealed that no change in responsiveness to MOR agonists between cells derived morphine-treated and morphine-naïve mice. This suggests that ipRGCs may not develop tolerance to opioid drugs following chronic systemic exposure.

4.2 Results

4.2.1 Mouse ipRGCs Do Not Express Functional GIRK Channels

GIRKs are perhaps the best-established MOR effector and mediate the inhibitory effects of opioids in various parts of the brain (Christie et al., 1987; Bagley et al., 2005; Levitt and Williams, 2012; Fox and Hentges, 2017; Adhikary and Williams, 2022). Unfortunately, when we immunolabelled for GIRK2 in the retina of mice that express Enhanced Green Fluorescent Protein (EGFP) exclusively in M1-M3 subtypes (*Opn4*::EGFP, (Schmidt et al., 2008)) we could not detect GIRK2 protein (Figure 4.1B), while GIRK2 was robustly expressed in the ventral tegmental area (Figure 4.1A). Additionally, application of the GIRK-specific activator (VU0529331) did not induce characteristic whole-cell GIRK current in solitary ipRGCs during a voltage-ramp protocol (Figure 4.1C) (Kozek et al., 2019). Moreover, ipRGCs do not exhibit a strong hyperpolarization upon MOR agonist application (data not shown); further indicating that ipRGCs do not express functional GIRK channels (Cleymaet et al., 2019).

4.2.2 Solitary ipRGCs May Not Develop Tolerance at the Level of Voltage-gated Calcium Channels

To dissect how MOR agonists affect somatic whole cell voltage-gated calcium currents in ipRGCs, we cultured retinal neurons from adult *Opn4*::EGFP+ melanopsin reporter mice.

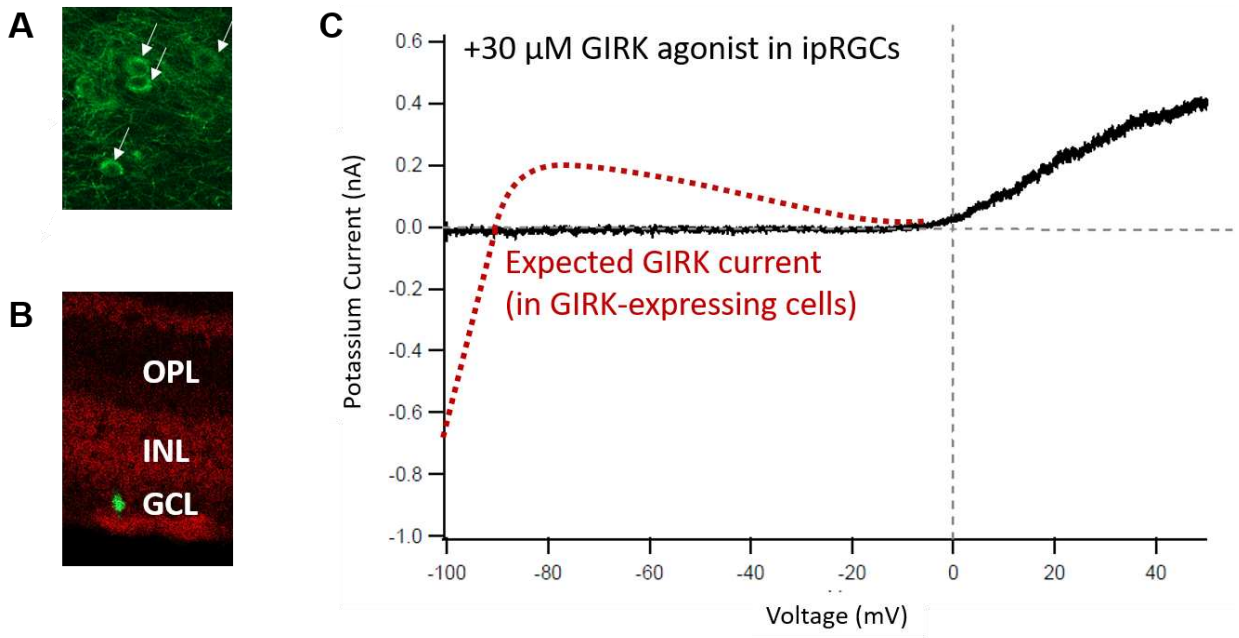

Figure 6.1 Opn4::EGFP+ ipRGCs do not express GIRK. (A) Single optical section shows robust GIRK2 expression (green) in the mouse ventral tegmental area. (B) Single optical section shows no GIRK2 expression (red) in Opn4::EGFP+ ipRGCs (green). (C) Application of maximal concentration of GIRK agonist (VU0529331) did not induce characteristic GIRK currents induced by a voltage-ramp in solitary ipRGCs.

Notably, *Opn4*::EGFP+ mice allowed us to target ipRGCs in a mixed acute retina culture. We then employed a cesium-based pipette solution along with an extracellular solution containing tetrodotoxin (TTX) to block potassium and sodium currents, respectively. Solitary ipRGCs were subjected to a depolarizing voltage-ramp protocol to measure whole-cell voltage-gated calcium currents. Using this protocol, we measured voltage-ramp evoked baseline whole-cell calcium currents in ipRGCs. We then introduced by 1 µM MOR selective agonist DAMGO into the extracellular bath solution and ran the same depolarizing voltage-ramp protocol. To verify the DAMGO-mediated inhibition of the whole-cell calcium current was not due to current rundown, we perfused 1 µM of the opioid antagonist naloxone to the extracellular bath solution and recorded a final ramp-evoked calcium current.

To determine if chronic morphine exposure reduces the ability of MOR agonists to inhibit voltage-gated calcium currents via inhibitory G proteins, these experiments were performed in enzymatically dissociated solitary ipRGCs derived from morphine-naïve and morphine-treated animals. Morphine treated mice were administered 20 mg/kg morphine twice

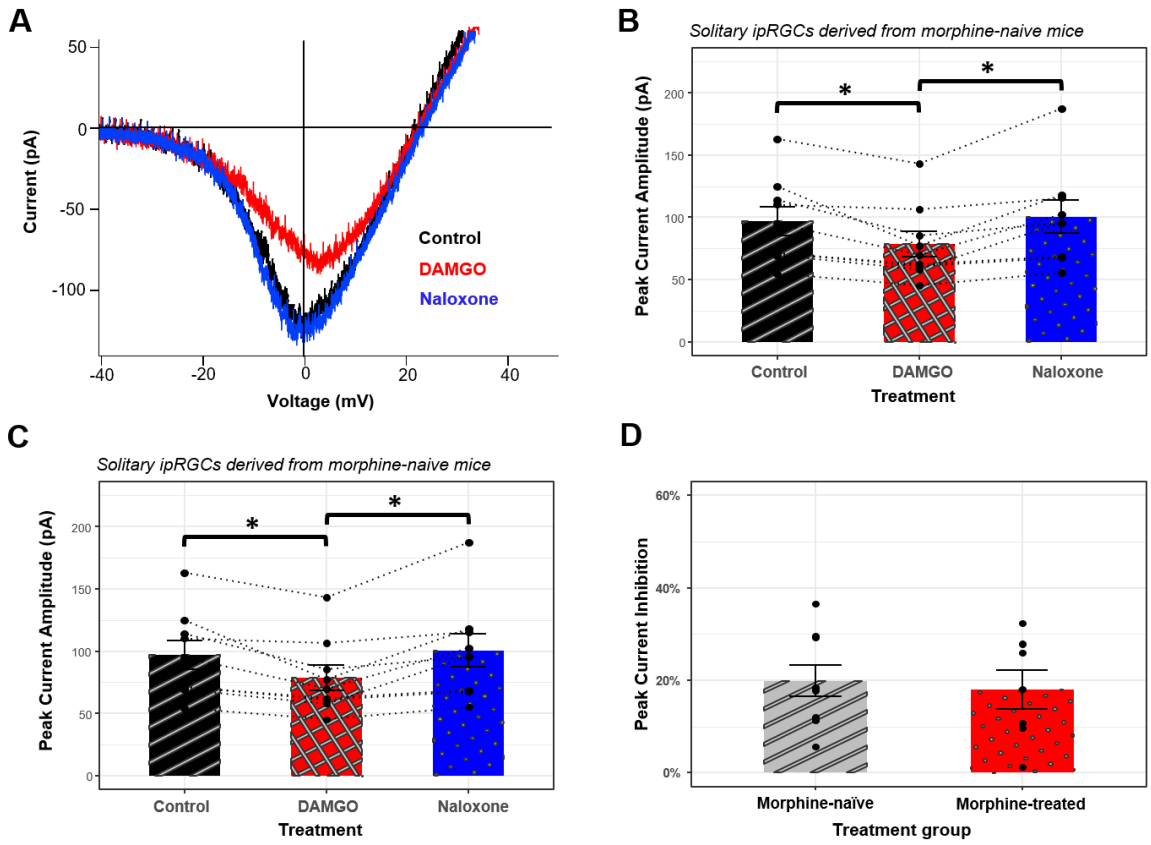

Figure 4.2 Solitary ipRGCs may not develop cellular tolerance following chronic morphine exposure at the level of whole cell Ca^{2+} currents. (A) Representative trace of ramp-evoked Ca^{2+} currents in a morphine-naïve enzymatically dissociated *Opn4*::EGFP+ ipRGC in control (black), 1 µM DAMGO (red) and 1 µM Naloxone treatment. (B) Cumulative data showing Ca^{2+} current amplitude plotted for morphine-naïve ipRGCs (n=9) in control, 1 µM DAMGO and 1 µM Naloxone. One-way ANOVA performed with a Tukey post hoc adjustment. (C) Cumulative data showing Ca^{2+} current amplitude plotted for morphine-treated ipRGCs (n=7) in control, 1 µM DAMGO and 1 µM Naloxone. One-way ANOVA performed with a Tukey post hoc adjustment (D) Comparison of DAMGO-mediated inhibition of peak Ca^{2+} current does not differ between ipRGCs derived from morphine-naïve vs. morphine treated mice. Independent samples t-test performed. Data presented as mean ± SEM, *=p<0.01.

daily for 6 days and retinas were dissected/dissociated one hour following the injection (Bergum et al., 2022b, 2022a). Importantly, solitary ipRGCs derived from morphine-treated animals were recorded up to 6 hours following the injection as tolerance is thought to persist for at least 6 hours following cessation of morphine exposure (Christie et al., 1987; Levitt and Williams, 2012; Adhikary and Williams, 2022).

Results show that the peak ramp-evoked calcium current was significantly reduced following 1 μM DAMGO treatment compared to control and antagonist treatment (1 μM naloxone), with no significant differences between ramp-evoked currents in control and naloxone treatment (Figure 4.2A). These findings confirm previous work from our lab that suggested DAMGO reversibly inhibited voltage-gated calcium currents in ipRGCs derived from morphine-naïve (n=9) mice (Figure 4.2B) (Cleymaet et al., 2019). Building on these findings, we performed similar whole-cell voltage clamp experiments on ipRGCs derived from mice that were chronically treated with morphine (n=7). These experiments yielded similar results to cells from animals with no exposure to morphine; with decreased ramp-evoked calcium currents following treatment with MOR agonist DAMGO (compared to control and naloxone treatment) (Figure 4.2C). Amazingly, when we compared the percent of DAMGO-mediated inhibition of the peak calcium current, no significant differences existed between cells derived from morphine naïve versus morphine-treated animals (Figure 4.2D, $p= 0.6934$). These results indicate that MOR-mediated inhibition of voltage gated calcium channels in solitary ipRGCs does not develop tolerance following chronic morphine administration. Results from these experiments suggest that solitary ipRGCs may not develop cellular tolerance following repeated morphine exposure.

4.3 Discussion

While the efficacy of opioid drugs in producing analgesic tolerance reduced following protracted use, opioid-related sleep/wake disturbances persist and even worsen throughout the course of opioid treatment (Kay, 1975; Hsu et al., 2012; Fathi et al., 2020; Huhn and Finan, 2021). Thus, it appears that chronic opioid users do *not* develop tolerance to the effect of opioids on sleep/wake behaviors. Previous studies from our lab pointed to a potential role for MOR expressing ipRGCs in opioid-related sleep/wake disruption (Cleymaet et al., 2019; Bergum et al., 2022c, 2022b), however the cellular and molecular correlates for this persistent drug-induced circadian disturbance have yet to be thoroughly investigated. The findings of these experiments point to the idea that either MORs expressed by ipRGCs do not develop opioid tolerance or the MOR-effector coupling in ipRGCs is different. Thus, MOR expressing ipRGC may be a potential mediator of the persistent sleep/wake problems that are characteristic of long-term opioid use.

4.3.1 The Effect of Chronic Morphine on MORs Expressed by ipRGCs

Experiments have attempted to link the development of cellular tolerance to analgesic tolerance for decades (Christie et al., 1987; Williams et al., 2013; Adhikary and Williams, 2022). Typically, GIRK currents have been used as a reliable cellular readout for MOR activation (Christie et al., 1987; Levitt and Williams, 2012; Fox and Hentges, 2017; Adhikary and Williams, 2022). However, the lack of GIRK expression in ipRGCs (Figure 6.1) meant that we were forced to use an alternative MOR effector as an electrophysiological readout for MOR activation. Researchers investigating cellular tolerance development in the periaqueductal gray (PAG) ran into a similar problem with functional GIRK expression in only a subset of neurons (and small currents in the neurons that did functionally express the GIRK channel) (Bagley et al.,

2005; Connor et al., 2015). These researchers used MOR-mediated inhibition of voltage-gated calcium channels as an alternative, yet reliable readout for MOR function (Connor and Christie, 1998; Bagley et al., 2005; Connor et al., 2015). Indeed, inhibition of whole cell calcium currents is mediated by the $\beta\gamma$ subunits of inhibitory G proteins and thus provides a relatively direct measure of MOR-effector coupling (Williams et al., 2001; Connor et al., 2015). As previous work from our lab revealed that DAMGO inhibited whole cell calcium currents (Cleymaet et al., 2019), we employed MOR-inhibition of voltage-dependent calcium channels as a functional readout for MOR activation (Figure 6.2).

Past experiments examining cellular tolerance via MOR-induced inhibition of voltage-gated calcium channels included whole cell electrophysiology performed in expression systems as well as in dissociated neuronal cultures and brain slice preparations (Kennedy and Henderson, 1991; Connor et al., 1999, 2015; Bagley et al., 2005). Indeed, morphine-treated cells in culture as well as those derived from morphine-treated animals appeared to develop tolerance at the level of voltage-dependent calcium channels (Kennedy and Henderson, 1991; Connor et al., 1999, 2015, 2015; Bagley et al., 2005; Johnson et al., 2006). Notably, these studies recorded from both dissociated neurons and slice preparations from the PAG, locus coeruleus as well as the trigeminal ganglion; all of which are regions associated with pain and/or pain modulation. Amazingly, MORs expressed by ipRGCs do not appear to develop tolerance following chronic exposure to morphine (in terms of the MOR-mediated inhibition of the voltage-dependent calcium current). This is especially significant when we consider that voltage-gated calcium channels not only play a role in the opioid-mediated effect on intracellular signaling, but are also an important component of the melanopsin signaling cascade (Hartwick et al., 2007). In fact, it is thought that voltage-gated calcium channel activity is responsible for sustained ipRGC firing in

response to light (Cleymaet et al., 2019). Thus, the approximately 20% reduction we see in whole cell calcium current in response to 1 μM DAMGO could significantly impact the ability of ipRGCs to fire spikes in response to environmental light stimuli *in vivo*. Importantly, morphine not only persists, but accumulates in the mouse retina following chronic systemic exposure (Bergum et al., 2022a). Given that MOR-mediated inhibition of calcium influx remains unaffected by chronic morphine, it follows that chronic MOR activation from opioid drugs accumulating in the retina would persistently inhibit ipRGC firing (especially in response to light). Thus, we believe that persistent opioid-mediated inhibition of ipRGC might contribute to the sleep/wake dysregulation commonly associated with chronic opioid use.

4.3.2 Strengths and Limitations

This study was carefully designed so that we could reliably assay MOR activation in ipRGCs using a well-established and physiologically relevant effector as a readout. Furthermore, the MOR-mediated inhibition was reversible by naloxone, confirming that the effect was indeed due to MOR activation (rather than current rundown over the course of each recording). While these experiments provided some compelling data, it is important to note some of the more significant limitations and pitfalls associated with this study.

While it is tempting to label MORs expressed by ipRGCs as resistant to opioid tolerance, there are still a number of factors that must be considered. Firstly, the use of MOR-mediated inhibition of voltage-gated calcium channels only provides a readout of MOR activation by looking at one effector. While we were unable to record GIRK currents from solitary ipRGCs (even following intravitreal injection of a Cre-dependent virus containing the GIRK channel, as in Marcott et al., 2014), it has been shown that MOR activation shifts the activation threshold of voltage-gated potassium currents (Cleymaet et al., 2019). Unfortunately, we were unable to

reliably reproduce this data in solitary ipRGCs derived from untreated mice and thus could not test if this MOR-mediated effect was altered following chronic systemic exposure to morphine (data not shown). Many of the previously published recordings that examined the MOR-induced shift in voltage-gated potassium current activation supplemented the culture media (by including ciliary growth factor, brain derived neurotrophic factor and forskolin) which may be crucial for the intracellular signaling cascade that is thought to mediate the MOR effect on the whole cell potassium current (Cleymaet et al., 2019). Additionally, the MOR-mediated shift in voltage-gated potassium current activation is highly variable and less robust than the MOR-induced inhibition of voltage-gated calcium channels. Future experiments could focus on how MORs affect cyclic adenosine monophosphate (cAMP) signaling in ipRGCs as the enzymatic activity of adenylate cyclase is inhibited by the α subunit of $G_{o/i}$ proteins (Williams et al., 2001).

While examining voltage-gated currents to assess MOR activation is common and well accepted, the most compelling experiments would assess how MOR activation alters the firing activity of ipRGCs. We have previously shown that DAMGO can suppress light-evoked firing in ipRGCs using multielectrode array and loose-patch recording methods (Cleymaet et al., 2019). However, the blue light used to visualize the GFP+ ipRGCs would instantaneously light-adapt the retina (Schmidt et al., 2008), thus, we were unable to perform similar experiments that examined ipRGC light response. Despite this, we attempted to record ipRGC activity in both cell-attached and current clamp modes, to examine the effect of MOR activation on baseline and current-evoked ipRGC firing. In cell attached mode, we reliably recorded extracellular spikes from acutely dissociated ipRGCs, however, the shifting baseline throughout each recording made it difficult to determine a drug effect (data not shown). Similarly, in current clamp mode, the declining health of the cells prevented us from reproducibly recording a DAMGO effect on

current-evoked action potential firing (data not shown). Due to the invasive nature of the whole cell patch clamp technique, using multielectrode array to perform these experiments might produce more reliable results.

Finally, it is important to note that these findings were performed on enzymatically dissociated ipRGCs. These dissociated neurons are often devoid of any processes which makes them fundamentally different from patching on ipRGCs in retinal slice and/or whole mount preparations. Acutely dissociated ipRGCs lack synaptic inputs from neighboring cells which is advantageous when attempting to ascertain a direct somatic effect of a drug on whole cell ipRGC currents without the use of an expensive synaptic blocking cocktail. With that said, enzymatically and physically isolating these neurons provides only a limited picture of how opioids will affect these neurons *in vivo*. Indeed, the MOR-mediated inhibition of calcium currents might differ in the processes compared to the soma. Low efficiency agonists such as morphine failed to activate GIRK currents in dissociated locus coeruleus neurons, while increasing potassium conductance in brain slice preparations (Ingram et al., 1997). Thus, moving forward it is important to perform similar experiments from MOR-expressing ipRGCs in whole mount retinal preparations.

4.4 Materials and Methods

4.4.1 Animals

The mice used in this study were of the transgenic Tg(Opn4-EGFP)ND100Gsat/Mmucd strain, generated by the GENSAT project. This strain carries a bacterial artificial chromosome (BAC) in which the melanopsin (*Opn4*) promoter drives expression of enhanced green fluorescent protein (EGFP); these mice are referred to as *Opn4*::EGFP (Schmidt et al., 2008; Cleymaet et al., 2019). This study employed adult male and female animals for the experiments.

Opn4::EGFP mice anesthetized with isoflurane and euthanized via cervical dislocation. Adult male and female animals (8+ weeks) were housed under a 12-h light:12-h dark cycle (LD) cycle, with lights on at 7:00 a.m. (ZT 0) and lights off at 7:00 p.m. (ZT 12). They were fed standard chow and water ad libitum. All animals used in these studies were handled in compliance with the Institutional Animal Care and Use Committees of Colorado State University (Protocol 18-8395A, 28 January 2019) and in accordance with the ARVO Statement for the Use of Animals in Ophthalmic and Vision Research.

4.4.2 Morphine Treatment

Mice were weighed and injected with 20 mg/kg doses of morphine i.p. (Morphine sulfate salt pentahydrate, Sigma-Aldrich, Saint Louis, MO, USA; Product Number: M8777, dissolved in sterile saline) as previously described (Bergum et al., 2022b, 2022a). Specifically, the chronic morphine treatment paradigm consisted of 5 days of twice daily 20 mg/kg morphine (administered at ZT 0 and ZT 12), followed by a final 20 mg/kg i.p. injection at ZT 0 (McLane et al., 2017).

4.4.3 Patch-clamp Recording Solutions

For isolation of I_{K+} in whole-cell voltage-clamp (Figure 4.1C), a K-gluconate based internal solution was used. This solution contained (in mM) the following: 110 K-gluconate, 7 phosphocreatine-di(tris) salt, 10 L-ascorbic acid, 2 EGTA, 3 Mg-ATP, 0.5 Na-GTP, 20 KCl, 10 HEPES, 2 QX 314, pH 7.2 (adjusted with KOH) and osmolarity of 290 ± 5 mOsmol. For I_{Ca2+} recordings, a Cs-gluconate based internal solution was used that contained (in mM) the following: 100 Cs-gluconate, 10 phosphocreatine-di(tris) salt, 10 L-ascorbic acid, 2 EGTA, 3 Mg-ATP, 0.5 Na-GTP, 10 tetraethylammonium chloride, 0.1 CaCl2, 10 NaCl, pH 7.2 (adjusted with CsOH) and osmolarity of 295 ± 5 mOsmol, and the extracellular solution was supplemented

with 5 mM $CaCl_2$ (Hu et al., 2013; Cleymaet et al., 2019). The standard extracellular solution was Ames' medium (US Biological), with osmolarity of 300 ± 10 mOsmol constantly gassed with 95% O2 / 5% CO2. [D-Ala2, MePhe4, Gly-ol5]-enkephalin (DAMGO), Naloxone hydrochloride and QX 314 were obtained from Tocris Bioscience (Bristol, UK). Tetrodotoxin (TTX) obtained from Alomone Labs (Jerusalem, Israel). Other salts or chemicals were purchased from Sigma (St. Louis, MO).

4.4.4. Dissociated ipRGC preparation for whole cell recording

Solitary ipRGCs were enzymatically dissociated from *Opn4*::EGFP mouse retina as previously described (Meyer-Franke et al., 1995; Van Hook and Berson, 2010; Cleymaet et al., 2019). In brief, eyes were enucleated and hemisected posterior to the limbus; the lens and vitreous humor were removed. Retinas were detached in dark from the retinal pigmented epithelium and incubated for 15 min at 37°C in a papain solution (10 U/ml, Worthington; Lakewood, NJ). After rinsing in a papain free solution, manual trituration was performed with a large-bore Pasteur pipette and dissociated cells were plated on poly-d-lysine/laminin coated coverslips (Corning™BioCoat™; Bedford, MA) followed by >2 hours incubation in MACS® NeuroMedium without L-Glutamine (Miltenyi Biotech; Auburn, CA). The medium was supplemented with MACS® NeuroBrew-21, antibiotics (100 u/ml penicillin and 100 µg/ml streptomycin) and Gibco™ GlutaMAX™ Supplement (ThermoFischer, Waltham, MA, USA). Coverslips were transferred to a perfusion chamber mounted on an upright microscope (Akioskop 2 FS plus, Zeiss) and superfused at 2–5 ml/min with 300 ± 10 mOsmol bicarbonate buffered Ames' medium (US Biological; Swampscott, MA) constantly gassed with 95% O_2 / 5% CO_2. Coverslips were viewed through a 40x water immersion objective, infrared differential contrast, and an infrared CCD camera with 2.5 pre-magnification (XC-75; Sony, Japan)

connected to a Camera Controller C2741–62 (Hamamatsu; Japan), which directed output to a 19” monitor (Westinghouse; Santa Fe Springs, CA). Dissociation yielded a mixture of retinal neurons from which M1 ipRGCs were identified based on their large size (~10 μm) and bright green fluorescence. Cells derived from morphine-treated animals were recorded <6 hours following euthanasia; as tolerance persists up to 6 hours following cessation of morphine exposure (Christie et al., 1987; Levitt and Williams, 2012; Adhikary and Williams, 2022).

4.4.5 Whole cell voltage-clamp recordings from dissociated, solitary ipRGCs

A horizontal puller (model p-97, Sutter; Novato, CA) was used to pull patch pipettes of 5–15 MΩ from 1.5-mm-diameter, thick-walled borosilicate glass (World Precision Instruments; Sarasota, FL). The pipettes were subsequently coated with dental wax (Cavex; Netherlands) to minimize stray pipette capacitance. Whole-cell voltage-clamp recordings were made from dissociated ipRGC somas using an EPC-10 USB patch-clamp amplifier and Patchmaster software (version 2.3; HEKA) at room temperature during daytime. Membrane current and voltage data were filtered at 3 kHz. Recordings with leak >50 pA at −70 mV holding potential and/or series resistance (Rs) >50 MΩ at any time during the recording were terminated and excluded from analysis. Similarly, if the Rs changed more than 10% during the recording, data was not considered for further analysis. The holding current to set the holding potential at −70 mV at break in was determined in voltage-clamp mode. Voltage-gated potassium current (I_{K+}) and voltage-gated calcium current (I_{Ca2+}) was evoked by a voltage-clamp ramp protocol that lasted 2 seconds and extended from −100 to 50 mV (sampled at 5 kHz).

4.4.6 Data and Statistical Analysis

Data were analyzed off-line using IgorPro software (version 5.03; Wavemetrics) as previously described in (Tooker et al., 2013). Voltage-clamp ramp were leak-subtracted and

normalized to the peak to analyze the Ca^{2+} or K^{+} current. The leak subtraction procedure consisted of extrapolating the slope of the line between −100 mV and −60 mV. The estimated leak current was subtracted from the raw value providing the "pure" I_{Ca2+} or I_{K+}. Normalized, leak-subtracted ramp-evoked I_{Ca2+} I-V curves were fit using the following Boltzmann equation: $I = 1 / \{ 1 + \exp[(V - V_{1/2}) / S]\}$, where $V_{1/2}$ is the half-activation potential and S is the slope of the voltage dependency.

Data are presented as mean ± standard error of the mean (SEM) as specified in figure captions. The data were analyzed using a one-way ANOVA or unpaired t-test; performed using RStudio (version 4.0.0) with Tukey's post hoc adjustments for all pairwise comparisons, and $p < 0.05$ was considered significant.

4.5 Conclusions

The findings from the above investigation provides interesting data suggesting the MORs expressed by ipRGCs could be resistant to tolerance development at a cellular level. These results in consort with past work from our lab support the idea that retinal MORs could contribute to opioid-related sleep/wake problems (Cleymaet et al., 2019; Bergum et al., 2022b, 2022a). Indeed, morphine has been shown to accumulate in the retina following systemic exposure (Bergum et al., 2022a), which can have implications on non-image forming visual functions including PLR and regulation of sleep/wake behaviors (LeGates et al., 2014; Cleymaet et al., 2021; Bergum et al., 2022b). This study suggests that MOR function following chronic opioid exposure may not desensitize in ipRGCs. Therefore, it appears that ipRGC firing is persistently altered by retinal opioid accumulation could have a significant impact on ipRGC signaling that is crucial for regulating sleep/wake activity. Given that persistent sleep/wake dysfunction is a hallmark of long-term opioid use (Kay, 1975; Hsu et al., 2012; Huhn and Finan,

2021), the present study offers MORs expressed by ipRGCs a potential molecular correlate for chronic opioid-induced sleep/wake disturbances.

Chapter 5 – Discussion

Despite evidence that chronic opioid use results in persistent sleep/wake disturbances, the exact mechanism by which this occurs remains poorly understood. Due to the lack of a significant opioid-related visual phenotype, the retina has not been the focus of investigations into the mechanism of opioid-induced sleep and circadian dysfunction. Although opioids have been reported to alter pupil size and PLR in humans and rodents (Pickworth et al., 1990, 1991; Grace et al., 2010; Cleymaet et al., 2021), only recently have people turned to ipRGCs as a potential source of opioid-related sleep/wake disturbances. Indeed, ipRGCs are crucial regulators of non-image forming visual functions including PLR and circadian photoentrainment (LeGates et al., 2014). While past research has provided a great framework on which to build a case for a retinal contribution to opioid-induced sleep/wake problems (Mistlberger and Holmes, 1999; Byku and Gannon, 2000; Meijer et al., 2000; Vansteensel et al., 2005; Eacret et al., 2020; Huhn and Finan, 2021), this investigation provides strong evidence that support the idea that ipRGCs contribute to opioid-related sleep/wake dysfunction. Here, we will review the results of the present investigation and contextualize these results in the context of opioids and sleep/wake regulation.

5.1 The Role of Endogenous Retinal Opioid Signaling in Sleep/Wake Regulation

To better understand how exogenous opioid compounds like morphine might dysregulate retinal opioid signaling, it is first important to examine the endogenous role of opioid signaling in terms of sleep/wake regulation. Early work done in the retina revealed an opposing role for local dopaminergic and opioidergic signaling in the tuning of retinal processing to light/dark adapted conditions (Dubocovich and Weiner, 1983; Boelen et al., 1994). Our studies performed

in the mouse retina corroborate this idea as increases in β-endorphin as well as *POMC* mRNA (the β-endorphin precursor) expression in the retina were evident during the dark phase (Berezin et al., 2022). Importantly, our group has shown that choline acetyltransferase (ChAT)+ cholinergic amacrine cells express POMC and are likely the main source of retinal β-endorphin (Gallagher et al., 2010). In a follow-up study, we found that β-endorphin+ ChaT+ amacrine cells were increased in the dark which suggests that β-endorphin release is enhanced in the dark phase. Additionally, alterations in retinal opioid signaling have been linked to alterations in sleep and circadian behavior in mice. In line with the immunohistochemical evidence, mini telemetry data showed that McKO mice (lacking the MOR exclusively in ipRGCs) exhibited reduced locomotor activity and decreased wakefulness/increased sleep in the dark phase compared to wild type animals (Berezin et al., 2022). Importantly, McKO mice did not exhibit any significant changes in circadian photoentrainment (ie. remained nocturnal). When we consider that ipRGC spiking is interpreted by the mammalian brain as environmental light (Do, 2019), it appears that endogenous β-endorphin release in the dark phase functions to suppress ipRGC firing via the MOR. Indeed, ipRGCs have been shown to fire spontaneous spikes in the dark (Zhao et al., 2014; Do, 2019) and the resting membrane potential of ipRGCs is depolarized (about -40 mV for the M1 subtype) which means opioid-induced suppression of ipRGC activity could have a significant impact on the amount of ipRGC-dependent signal that reaches the brain's sleep/wake centers (Lucas and Schmidt, 2019). In this way, it appears that MOR signaling in ipRGCs plays a functional role in sleep/wake homeostasis rather than sleep induction. These findings are consistent with the idea that retinal opioid signaling is involved in tuning ipRGC firing to regulate proper sleep/wake behavior in mice.

Mice are nocturnal animals with light acting as s very strong signal for sleep induction and homeostasis (Altimus et al., 2008; Güler et al., 2008; Lupi et al., 2008; Tsai et al., 2009). The role of retinal opioid signaling in regulating dark-phase wakefulness behavior in mice has been outlined, however it is important to consider the neuromodulator that is often associated with light in the retina: dopamine. Dopamine has been shown to directly modulate ipRGC activity as well as to be dependent on light for its release (Van Hook et al., 2012; Vuong et al., 2015; Munteanu et al., 2018). Past research has shown that dopaminergic amacrine cells (DACs) appear to release dopamine upon illumination (Doyle et al., 2002; Witkovsky, 2004) to enhance ipRGC activity via the D1 dopamine receptor (D1R) (Van Hook et al., 2012). Enhanced ipRGC activity is in turn interpreted by the mouse brain as a robust signal for sleep. In the retina, dopamine appears to be an opposing modulatory force to opioids in terms of the regulation of ipRGC activity.

To dive into the reciprocal neuromodulatory effects of dopamine and opioid signaling in the retina, we must also examine how these neurotransmitters regulate each other's release. While there is some evidence of dopamine inhibiting the release of the endogenous opioid peptide enkephalin in the chicken retina, these studies have not been replicated in mammalian models (Boelen et al., 1994). However, enkephalin was shown to negatively regulate dopamine release in the rabbit retina (Dubocovich and Weiner, 1983). These findings informed work from our group which sought to examine the role of opioid signaling in the mouse inner retina. To follow up on this study, our group identified that DACs express both MORs and DORs (Gallagher et al., 2012). As MORs and DORs bind preferentially to endogenous β-endorphin and enkephalin (Kieffer, 1995), it follows that this interaction within DAC synaptic terminals underlies the opioid-dependent suppression of dopamine release (Dubocovich and Weiner,

1983). Importantly, this suggests that in the dark β-endorphin can effectively blunt dopamine mediated excitation via D1Rs on ipRGCs, providing an indirect signal for the suppression of ipRGC activity. When we consider that β-endorphin also directly suppresses ipRGC activity via MORs in the dark, the importance of endogenous opioid signaling within the inner retina

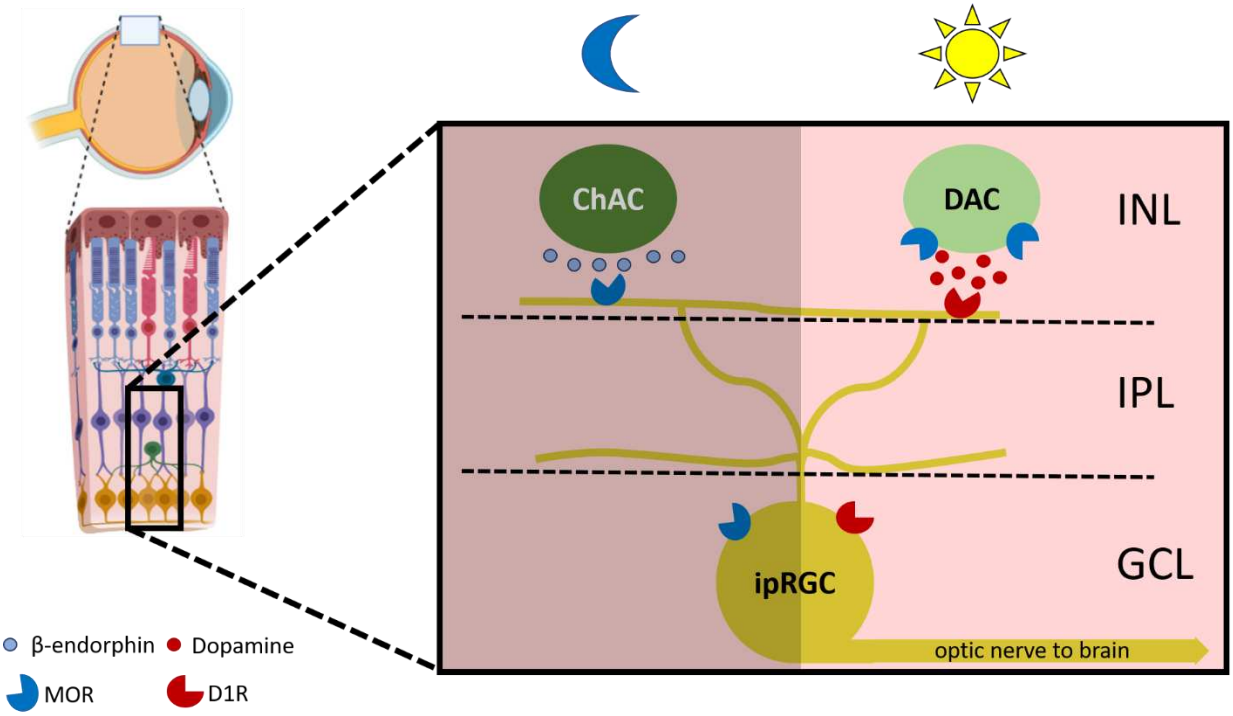

Figure 5.1 Dopamine and opioid signaling within the inner retina tunes photosensitive retinal ganglion cell activity to modulate sleep/wake behavior. Cholinergic amacrine cells (ChACs) release β-endorphin onto retinal μ-opioid receptors (MORs) to suppress intrinsically photosensitive retinal ganglion cell (ipRGC) activity during the dark phase. Contrastingly, DACs release dopamine which binds to D1 dopamine receptors (D1R) on ipRGCs to promote ipRGC firing during the light period. Abbreviations: Ganglion cell layer (GCL); Inner nuclear layer (INL) Inner plexiform layer (IPL).

becomes even more evident (Berezin et al., 2022). Taken together, β-endorphin, through both pre- and postsynaptic means, can suppress ipRGC activity to enhance the strength of the dark signal that is transmitted to the sleep/circadian centers in the brain. In turn, the brain will interpret low ipRGC firing activity (in the dark) as a strong signal to promote wakefulness and

behavioral activity. The proposed roles of dopamine and opioid signaling within the inner retina are detailed in Figure 5.1.

5.2 Exogenous Opioid-mediated Disruption of the Non-image Forming Visual Circuit in the Inner Retina

Now that we have established the role of neuromodulation within the inner retina in the context of sleep/wake regulation, we can examine how chronic morphine might alter both opioid and dopamine signaling within ipRGCs. Based on recent findings from our lab, morphine appears to accumulate in the retina following repeated systemic exposure (Bergum et al., 2022a). While the morphine content of the retina samples in this manuscript might include vitreous humor (VH), given the proximity of the VH to the ipRGCs in the ganglion cell layer of the retina it is almost certain that morphine will be able to act on MORs expressed by ipRGCs. Morphine mediated activation of MORs on the cell surface of ipRGCs can signal to downstream effectors to the suppress ipRGC activity via inhibition of voltage-gated calcium channels and shifting the activation of voltage-dependent potassium (as well as by inhibiting adenylate cyclase activity) (Williams et al., 2013; Cleymaet et al., 2019). Moreover, morphine in the inner retina will likely inhibit the release of dopamine from DACs presynaptic to ipRGCs. In this way, morphine can act both pre- and postsynaptically to reduce ipRGC activity independent of the endogenous opioid peptides in the retina. While morphine does accumulate following chronic systemic exposure, it also appears to have a longer half-life in the retina compared to the brain (Bergum et al., 2022a). This means that chronic morphine exposure might lead to sustained activation of MORs within this retinal microcircuit. In fact, sustained and/or repeated activation of MORs often leads to rapid receptor desensitization and/or tolerance (Williams et al., 2013). Indeed, multiple MOR effectors (including, but not limited to GIRKs, adenylate cyclase and voltage-

gated calcium channels) exhibit adaptations that are associated with chronic opioid exposure (Williams et al., 2001, 2013; Adhikary and Williams, 2022). In our hands, we failed to see any functional changes in MOR-mediated inhibition of voltage-gated calcium currents following chronic morphine exposure. While future work should focus on how chronic MOR activation affects adenylate cyclase/cAMP signaling within ipRGCs, data from this investigation does suggest that MORs expressed by ipRGCs might be resistant to developing tolerance (at the cellular level). This finding differs from similar experiments performed in brain neurons (PAG, locus coeruleus and trigeminal ganglion) that showed reduced MOR-mediated inhibition of whole cell calcium currents following chronic morphine exposure (Connor et al., 1999, 2015; Johnson et al., 2006). The implications of the lack of cellular tolerance development are interesting to consider as it suggests that ipRGCs do not employ cellular adaptations to suppress overactive MOR signaling. Physiologically, this suggests that morphine-treated animals have ipRGCs that are tonically inhibited by persistent morphine deposited in the retina. While this is an interesting observation, the current study lacks the depth needed to form a meaningful mechanistic explanation for an apparent lack of cellular tolerance development in ipRGCs.

Given that ipRGCs are not the only cell type in the inner retina that express MORs, we can surmise that morphine accumulation would also effect MOR-expressing DACs that release dopamine onto ipRGCs. Based on our model, morphine could persistently inhibit dopamine release into the inner retina; suppressing a light-related neuromodulatory signal associated with ipRGC activation. However, MORs are also somatic and no visual deficits have been reported as the result of opioid use. Morphine-mediated suppression of DAC-ipRGC dopamine signaling could thus magnify the inhibitory effect that morphine has on ipRGCs via a presynaptic mechanism. Given that presynaptic MORs tend not to desensitize following prolonged activation

(Pennock et al., 2012), it is tempting to speculate that MORs expressed on the axon terminals of DACs may also not reduce their signaling efficiency following chronic exposure to morphine. Future work will have to confirm this speculation about MORs expressed by DACs, however further investigation into MORs expressed by ipRGC might provide valuable information regarding their seeming lack of functional adaptations following continuous activation. Taken together, retinal morphine can both directly (via MORs expressed by ipRGCs) and indirectly (via inhibition of DAC) reduce ipRGC activity, effectively diluting the light information that is transmitted to the brain via ipRGCs. In this way, the morphine that persists in the retina following chronic treatment can obscure the brain's ability to entrain to the environmental light/dark cycle, which could underlie some of the sleep/wake problems that are associated with long-term opioid use.

5.3 The Role of Retinal MORs in Opioid-induced Sleep/Wake Problems

When looking at the behavioral data in Chapter 3, it is still unclear the exact role that MORs expressed by ipRGCs play in opioid-related sleep/wake problems. While we did perform an extensive behavioral study to try and disentangle ipRGC involvement with regard to opioid-related circadian changes, this investigation revealed a surprising behavioral sensitization phenotype without providing a clear mechanistic understanding of exactly how opioids perturb sleep (via ipRGCs). Similar to past rodent studies (Kosobud et al., 2007; Gillman et al., 2009), we saw that mice shifted their entrainment from light to the drug injection over the course of the morphine treatment paradigm. This is consistent with reports that individuals with substance use disorders tend to have circadian disruptions that are associated with habitual drug taking (Hasler et al., 2012; Tamura et al., 2021). The psychomotor stimulant theory of addiction links drug-induced behavioral sensitization to central reward circuitry (Kalivas and Duffy, 1987; Wise and

Bozarth, 1987). Given this link, results from Chapter 3 suggest that MORs expressed by ipRGC might be involved in both circadian regulation as well as addiction-related behaviors (Bergum et al., 2022b). While this is an intriguing finding, it still leaves many questions as to the functional contribution of MOR expressing ipRGCs to opioid-related sleep/wake dysfunction.

Both rodent and human studies have shown that substance use can lead to circadian disruption, indeed, individuals with substance use disorders experience significant delays in sleep/wake phase which often manifests as insomnia and daytime sleepiness (Meijer et al., 2000; Vansteensel et al., 2005; Roehrs and Roth, 2015; Chakravorty et al., 2018; Rhon, 2019; Baldassarri et al., 2020). Based on past research that highlighted the importance of ipRGCs on circadian entrainment to environmental light cues (especially in the context of hormonal, mood and cognitive regulation) (LeGates et al., 2014), one would expect that opioids within the retina would alter photoentrainment. Indeed, light-mediated circadian phase shifts were blocked in rodents that have been administered opioid drugs (Meijer et al., 2000; Vansteensel et al., 2005). Specifically, we anticipated that persistent opioid-mediated inhibition of ipRGC function might cause animals to drift into free running; mimicking the circadian phenotype observed in enucleated mice (Foster et al., 1991) as well as in animals wherein ipRGC have been selectively ablated (Güler et al., 2008). While retinal opioid accumulation may not be sufficient to completely block ipRGC-dependent light input to hypothalamic sleep/circadian centers, it is likely that the reported opioid-induced circadian disturbances seen in rodents are at least partially mediated by MORs expressed by ipRGCs. Our schedule of morphine administration entrained mouse behavioral activity to morphine injections, which masked regular circadian behavior entrained by light (for nocturnal mice). Importantly, MORs expressed by ipRGCs exerted a more significant effect in this “re-entrainment” process during the light phase, which is consistent with

light-induced activity of ipRGCs. Future experiments utilizing osmotic pumps and/or morphine pellets may provide valuable information regarding the role of retinal MOR signaling and its contribution to opioid-induced circadian changes.

5.4 Conclusions

The findings from the current investigation provide strong pharmacokinetic and pharmacodynamic evidence for the contribution of MOR-expressing ipRGCs to chronic opioid-induced sleep/wake dysfunction. The selective accumulation of morphine in the mouse retina in conjunction with evidence suggesting that MORs expressed by ipRGCs might be resistant to tolerance development indicate that MORs expressed by ipRGCs are continuously signaling throughout chronic morphine treatment. Given the significant role that ipRGCs play in circadian sleep/wake regulation, it follows that persistent opioid-mediated suppression of ipRGC would alter sleep and circadian behaviors in mammals. Behavioral studies in rodents corroborate this idea, as opioid drugs have been shown to shift the photic regulation of circadian phase. Indeed, MOR agonists can serve as a light-independent signal for circadian entrainment. While there are a plethora of sleep/circadian centers in the brain that express the MOR and likely contribute to opioid-mediated alterations in sleep/wake behaviors, this investigation supports the idea that retinal MORs also play a role.

Recently, the link between opioid use and sleep/wake dysfunction has gained interest from researchers and clinicians (Eacret et al., 2020; Huhn and Finan, 2021). In fact, disrupted sleep/wake cycles have recently been appreciated as not just a hallmark of opioid use disorders, but also as a therapeutic target to improve clinical outcomes in patients undergoing long-term opioid treatment (Chakravorty et al., 2018; Huhn and Finan, 2021). The evidence from this investigation positions MORs expressed by ipRGCs as a promising therapeutic target for treating

opioid-related sleep/wake dysfunction. Indeed, the retina represents a unique CNS structure that is far more accessible for targeted therapeutics than sleep/circadian centers in the brain. Moreover, focal application of drugs into the retina could be administered concurrently with opioids; hopefully improving sleep/wake function in patients without interfering with the therapeutic benefits of the opioid drugs.

References

Adachi H, Tominaga H, Maruyama Y, Yoneda K, Maruyama K, Yoshii K, Kinoshita S, Nakano M, Tashiro K (2015) Stage-specific reference genes significant for quantitative PCR during mouse retinal development. Genes Cells 20:625–635.

Adhikary S, Williams JT (2022) Cellular Tolerance Induced by Chronic Opioids in the Central Nervous System. Front Syst Neurosci 16:937126.

Altimus CM, Güler AD, Villa KL, McNeill DS, LeGates TA, Hattar S (2008) Rods-cones and melanopsin detect light and dark to modulate sleep independent of image formation. Proc Natl Acad Sci USA 105:19998–20003.

Andersen G, Christrup L, Sjøgren P (2003) Relationships Among Morphine Metabolism, Pain and Side Effects During Long-Term Treatment: An Update. Journal of Pain and Symptom Management 25:18.

Andersen JM, Ripel Å, Boix F, Normann PT, Mørland J (2009) Increased Locomotor Activity Induced by Heroin in Mice: Pharmacokinetic Demonstration of Heroin Acting as a Prodrug for the Mediator 6-Monoacetylmorphine in Vivo. J Pharmacol Exp Ther 331:153–161.

Aquilante CL, Letrent SP, Pollack GM, Brouwer KLR (2000) Increased Brain P-glycoprotein in morphine tolerant rats. 66:5.

Aranda ML, Schmidt TM (2021) Diversity of intrinsically photosensitive retinal ganglion cells: circuits and functions. Cell Mol Life Sci 78:889–907.

Babbini M, Davis WM (1972) Time-dose relationships for locomotor activity effects of morphine after acute or repeated treatment. British Journal of Pharmacology 46:213–224.

Bagley EE, Chieng BCH, Christie MJ, Connor M (2005) Opioid tolerance in periaqueductal gray neurons isolated from mice chronically treated with morphine: Opioid tolerance in PAG. British Journal of Pharmacology 146:68–76.

Baker A, Meert T (2003) Morphine and d-Amphetamine Nullify Each Others' Hypothermic Effects in Mice. Pharmacology & Toxicology 92:64–70.

Baker AK, Meert TF (2002) Functional Effects of Systemically Administered Agonists and Antagonists of μ, δ, and κ Opioid Receptor Subtypes on Body Temperature in Mice. J Pharmacol Exp Ther 302:1253–1264.

Baldassarri SR, Beitel M, Zinchuk A, Redeker NS, Oberleitner DE, Oberleitner LMS, Carrasco D, Madden LM, Lipkind N, Fiellin DA, Bastian LA, Chen K, Yaggi HK, Barry DT (2020) Correlates of sleep quality and excessive daytime sleepiness in people with opioid use disorder receiving methadone treatment. Sleep Breath 24:1729–1737.

Becker A, Grecksch G, Kraus J, Peters B, Schroeder H, Schulz S, Höllt V (2001) Loss of locomotor sensitisation in response to morphine in D1 receptor deficient mice. Naunyn-Schmiedeberg's Archives of Pharmacology 363:562–568.

Benyamin R (2008) Opioid Complications and Side Effects. Pain Phys 2s;11:S105–S120.

Berezin C-T, Bergum N, Luchini KA, Curdts S, Korkis C, Vigh J (2022) Endogenous opioid signaling in the retina modulates sleep/wake activity in mice. Neurobiology of Sleep and Circadian Rhythms 13:100078.

Bergum N, Berezin C-T, Dooley G, Vigh J (2022a) Morphine Accumulates in the Retina Following Chronic Systemic Administration. Pharmaceuticals 15:527.

Bergum N, Berezin C-T, King CM, Vigh J (2022b) μ-Opioid Receptors Expressed by Intrinsically Photosensitive Retinal Ganglion Cells Contribute to Morphine-Induced Behavioral Sensitization. IJMS 23:15870.
Bergum N, Berezin C-T, Vigh J (2022c) A retinal contribution to opioid-induced sleep disorders? Front Neurosci 16:981939.
Bévalot F, Cartiser N, Bottinelli C, Fanton L, Guitton J (2016) Vitreous humor analysis for the detection of xenobiotics in forensic toxicology: a review. Forensic Toxicol 34:12–40.
Bhargava HN, Villar VM, Rahmani NH, Larsen AK (1992) Distribution of morphine in brain regions, spinal cord and serum following intravenous injection to morphine tolerant rats. Brain Research 595:228–235.
Boelen MK, Wellard J, Dowton M, Morgan IG (1994) Endogenous dopamine inhibits the release of enkephalin-like immunoreactivity from amacrine cells of the chicken retina in the light. Brain Research 645:240–246.
Boix F, Andersen JM, Mørland J (2013) Pharmacokinetic modeling of subcutaneous heroin and its metabolites in blood and brain of mice: Blood/brain pharmacokinetic modeling of subcutaneous heroin in mice. Addiction Biology 18:1–7.
Bolte S, Cordelières FP (2006) A guided tour into subcellular colocalization analysis in light microscopy. J Microsc 224:213–232.
Boström E, Hammarlund-Udenaes M, Simonsson USH (2008) Blood–Brain Barrier Transport Helps to Explain Discrepancies in *In Vivo* Potency between Oxycodone and Morphine. Anesthesiology 108:495–505.
Byku M, Gannon RL (2000) Opioid induced non-photic phase shifts of hamster circadian activity rhythms. Brain Research 873:189–196.
Byku M, Legutko R, Gannon RL (2000) Distribution of δ opioid receptor immunoreactivity in the hamster suprachiasmatic nucleus and intergeniculate leaflet. Brain Research 857:1–7.
Chakravorty S, Vandrey RG, He S, Stein MD (2018) Sleep Management Among Patients with Substance Use Disorders. Medical Clinics of North America 102:733–743.
Chapy H, Saubaméa B, Tournier N, Bourasset F, Behar-Cohen F, Declèves X, Scherrmann J-M, Cisternino S (2016) Blood-brain and retinal barriers show dissimilar ABC transporter impacts and concealed effect of P-glycoprotein on a novel verapamil influx carrier: Drug efflux/influx at brain and retina barriers. British Journal of Pharmacology 173:497–510.
Chaves C, Gómez-Zepeda D, Auvity S, Menet M-C, Crété D, Labat L, Remião F, Cisternino S, Declèves X (2016) Effect of Subchronic Intravenous Morphine Infusion and Naloxone-Precipitated Morphine Withdrawal on P-gp and Bcrp at the Rat Blood–Brain Barrier. Journal of Pharmaceutical Sciences 105:350–358.
Chaves C, Remiao F, Cisternino S, Decleves X (2017) Opioids and the Blood-Brain Barrier: A Dynamic Interaction with Consequences on Drug Disposition in Brain. CN 15 Available at: http://www.eurekaselect.com/152146/article [Accessed March 22, 2022].
Cheatle MD, Webster LR (2015) Opioid Therapy and Sleep Disorders: Risks and Mitigation Strategies. Pain Med 16:S22–S26.
Chen S-K, Badea TC, Hattar S (2011) Photoentrainment and pupillary light reflex are mediated by distinct populations of ipRGCs. Nature 476:92–95.
Chen X-H, Geller EB, Kim DeRiel J, Liu-Chen L-Y, Adler MW (1996) Antisense confirmation of μ- and κ-opioid receptor mediation of morphine's effects on body temperature in rats. Drug and Alcohol Dependence 43:119–124.

Christie MJ, Williams JT, North RA (1987) Cellular mechanisms of opioid tolerance: studies in single brain neurons. Mol Pharmacol 32:633–638.
Chrobok AI, Krause D, Winter C, Plörer D, Martin G, Koller G, Adorjan K, Canolli M, Adam R, Wagner EM, Peles E, Paul D, Vogel T, Pogarell O (2020) Sleeping Patterns in Patients with Opioid Use Disorder: Effects of Opioid Maintenance Treatment and Detoxification. Journal of Psychoactive Drugs 52:203–210.
Cleymaet AM, Berezin C-T, Vigh J (2021) Endogenous Opioid Signaling in the Mouse Retina Modulates Pupillary Light Reflex. IJMS 22:554.
Cleymaet AM, Gallagher SK, Tooker RE, Lipin MY, Renna JM, Sodhi P, Berg D, Hartwick ATE, Berson DM, Vigh J (2019) μ-Opioid Receptor Activation Directly Modulates Intrinsically Photosensitive Retinal Ganglion Cells. Neuroscience 408:400–417.
Connor M, Bagley EE, Chieng BC, Christie MJ (2015) β-Arrestin-2 knockout prevents development of cellular μ-opioid receptor tolerance but does not affect opioid-withdrawal-related adaptations in single PAG neurons: Arrestin knockout and opioid tolerance in PAG. Br J Pharmacol 172:492–500.
Connor M, Borgland SL, Christie MJ (1999) Continued morphine modulation of calcium channel currents in acutely isolated locus coeruleus neurons from morphine-dependent rats: Morphine closes calcium channels. British Journal of Pharmacology 128:1561–1569.
Connor M, Christie MJ (1998) Modulation of Ca^{2+} channel currents of acutely dissociated rat periaqueductal grey neurons. The Journal of Physiology 509:47–58.
Contarino A, Picetti R, Matthes HW, Koob GF, Kieffer BL, Gold LH (2002) Lack of reward and locomotor stimulation induced by heroin in μ-opioid receptor-deficient mice. European Journal of Pharmacology 446:103–109.
Contet C, Filliol D, Matifas A, Kieffer BL (2008) Morphine-induced analgesic tolerance, locomotor sensitization and physical dependence do not require modification of mu opioid receptor, cdk5 and adenylate cyclase activity. Neuropharmacology 54:475–486.
Contet C, Kieffer BL, Befort K (2004) Mu opioid receptor: a gateway to drug addiction. Current Opinion in Neurobiology 14:370–378.
Cook C (2003) The modulatory actions of dopamine D2/3 agonists and antagonists on the locomotor-activating effects of morphine and caffeine in mice. Pharmacology Biochemistry and Behavior 75:363–371.
Craft RM, Clark JL, Hart SP, Pinckney MK (2006) Sex differences in locomotor effects of morphine in the rat. Pharmacology Biochemistry and Behavior 85:850–858.
Cutler DJ, Mundey MK, Mason R (1999) Electrophysiological effects of opioid receptor activation on Syrian hamster suprachiasmatic nucleus neurones in vitro. Brain Research Bulletin 50:119–125.
Dagenais C, Graff CL, Pollack GM (2004) Variable modulation of opioid brain uptake by P-glycoprotein in mice. Biochemical Pharmacology 67:269–276.
Dahlström BE, Paalzow LK (1975) Pharmacokinetics of morphine in plasma and discrete areas of the rat brain. Journal of Pharmacokinetics and Biopharmaceutics 3:293–302.
Deboer T (2018) Sleep homeostasis and the circadian clock: Do the circadian pacemaker and the sleep homeostat influence each other's functioning? Neurobiology of Sleep and Circadian Rhythms 5:68–77.
Díaz-Coránguez M, Ramos C, Antonetti DA (2017) The inner blood-retinal barrier: Cellular basis and development. Vision Research 139:123–137.

Dimsdale JE, Norman D, DeJardin D, Wallace M (2007) The Effect of Opioids on Sleep Architecture. Journal of Clinical Sleep Medicine 3:4.
Do MTH (2019) Melanopsin and the Intrinsically Photosensitive Retinal Ganglion Cells: Biophysics to Behavior. Neuron 104:205–226.
Doyle SE, McIvor WE, Menaker M (2002) Circadian rhythmicity in dopamine content of mammalian retina: role of the photoreceptors: Dopamine rhythms in RCS rat retina. Journal of Neurochemistry 83:211–219.
Dubocovich ML, Weiner N (1983) Enkephalins modulate [3H]dopamine release from rabbit retina in vitro. J Pharmacol Exp Ther 224:634–639.
Eacret D, Veasey SC, Blendy JA (2020) Bidirectional Relationship between Opioids and Disrupted Sleep: Putative Mechanisms. Mol Pharmacol 98:445–453.
Ecker JL, Dumitrescu ON, Wong KY, Alam NM, Chen S-K, LeGates T, Renna JM, Prusky GT, Berson DM, Hattar S (2010) Melanopsin-Expressing Retinal Ganglion-Cell Photoreceptors: Cellular Diversity and Role in Pattern Vision. Neuron 67:49–60.
Erbs E, Faget L, Scherrer G, Matifas A, Filliol D, Vonesch J-L, Koch M, Kessler P, Hentsch D, Birling M-C, Koutsourakis M, Vasseur L, Veinante P, Kieffer BL, Massotte D (2015) A mu–delta opioid receptor brain atlas reveals neuronal co-occurrence in subcortical networks. Brain Struct Funct 220:677–702.
Fathi HR, Yoonessi A, Khatibi A, Rezaeitalab F, Rezaei-Ardani A (2020) Crosstalk between Sleep Disturbance and Opioid Use Disorder: A Narrative Review. Addiction & Health 12:140–158.
Flyktman A, Jernfors T, Manttari S, Nissila J, Timonen M, Saarela S (2017) Transcranial Light Alters Melanopsin and Monoamine Production in Mouse (*Mus musculus*) Brain. J Neurol Res 7:39–45.
Foster RG, Provencio I, Hudson D, Fiske S, De Grip W, Menaker M (1991) Circadian photoreception in the retinally degenerate mouse (rd/rd). J Comp Physiol A 169:39–50.
Fox PD, Hentges ST (2017) Differential Desensitization Observed at Multiple Effectors of Somatic μ-Opioid Receptors Underlies Sustained Agonist-Mediated Inhibition of Proopiomelanocortin Neuron Activity. J Neurosci 37:8667–8677.
Gallagher SK, Anglen JN, Mower JM, Vigh J (2012) Dopaminergic amacrine cells express opioid receptors in the mouse retina. Vis Neurosci 29:203–209.
Gallagher SK, Witkovsky P, Roux MJ, Low MJ, Otero-Corchon V, Hentges ST, Vigh J (2010) β-Endorphin expression in the mouse retina. J Comp Neurol 518:3130–3148.
Garnaat SL, Weisberg RB, Uebelacker LA, Herman DS, Bailey GL, Anderson BJ (2017) The overlap of sleep disturbance and depression in primary care patients treated with buprenorphine. Substance Abuse 38:450–454.
Georgescu D, Zachariou V, Barrot M, Mieda M, Willie JT, Eisch AJ, Yanagisawa M, Nestler EJ, DiLeone RJ (2003) Involvement of the Lateral Hypothalamic Peptide Orexin in Morphine Dependence and Withdrawal. J Neurosci 23:3106–3111.
Gharavi R, Hedrich W, Wang H, Hassan HE (2015) Transporter-Mediated Disposition of Opioids: Implications for Clinical Drug Interactions. Pharm Res Available at: http://link.springer.com/10.1007/s11095-015-1711-5 [Accessed March 22, 2022].
Gillman AG, Leffel JK, Kosobud AEK, Timberlake W (2009) Fentanyl, but not haloperidol, entrains persisting circadian activity episodes when administered at 24- and 31-h intervals. Behavioural Brain Research 205:102–114.

Glaser AM, Reyes-Vázquez C, Prieto-Gómez B, Burau K, Dafny N (2012) Morphine administration and abrupt cessation alter the behavioral diurnal activity pattern. Pharmacology Biochemistry and Behavior 101:544–552.

Gong Q-L, Hedner J, Bjran R, Hedner T (1992) Morphine-3-glucuronide may functionally antagonize morphine-6-glucuronide induced antinociception and ventilatory depression in the rat. Pain 48:249–255.

Gottås A, Arnestad M, Halvorsen PS, Bachs LC, Høiseth G (2016) Pharmacokinetics of heroin and its metabolites in vitreous humor and blood in a living pig model. Forensic Toxicol 34:277–285.

Grace PM, Stanford T, Gentgall M, Rolan PE (2010) Utility of saccadic eye movement analysis as an objective biomarker to detect the sedative interaction between opioids and sleep deprivation in opioid-naive and opioid-tolerant populations. J Psychopharmacol 24:1631–1640.

Greco M-A, Fuller PM, Jhou TC, Martin-Schild S, Zadina JE, Hu Z, Shiromani P, Lu J (2008) Opioidergic projections to sleep-active neurons in the ventrolateral preoptic nucleus. Brain Research 1245:96–107.

Groenendaal D, Freijer J, de Mik D, Bouw MR, Danhof M, de Lange ECM (2007) Population pharmacokinetic modelling of non-linear brain distribution of morphine: influence of active saturable influx and P-glycoprotein mediated efflux: PK modelling of active BBB transport of morphine. British Journal of Pharmacology 151:701–712.

Guillot E, de Mazancourt P, Durigon M, Alvarez J-C (2007) Morphine and 6-acetylmorphine concentrations in blood, brain, spinal cord, bone marrow and bone after lethal acute or chronic diacetylmorphine administration to mice. Forensic Science International 166:139–144.

Güler AD, Ecker JL, Lall GS, Haq S, Altimus CM, Liao H-W, Barnard AR, Cahill H, Badea TC, Zhao H, Hankins MW, Berson DM, Lucas RJ, Yau K-W, Hattar S (2008) Melanopsin cells are the principal conduits for rod–cone input to non-image-forming vision. Nature 453:102–105.

Gupta K, Chen C, Lutty GA, Hebbel RP (2019) Morphine promotes neovascularizing retinopathy in sickle transgeneic mice. Blood Advances 3:1073–1083.

Haddad-Tóvolli R, Dragano NRV, Ramalho AFS, Velloso LA (2017) Development and Function of the Blood-Brain Barrier in the Context of Metabolic Control. Front Neurosci 11:224.

Hallinan R, Elsayed M, Espinoza D, Veillard A-S, Morley KC, Lintzeris N, Haber P (2019) Insomnia and excessive daytime sleepiness in women and men receiving methadone and buprenorphine maintenance treatment. Substance Use & Misuse 54:1589–1598.

Hamabe W, Maeda T, Kiguchi N, Yamamoto C, Tokuyama S, Kishioka S (2007) Negative Relationship Between Morphine Analgesia and P-Glycoprotein Expression Levels in the Brain. J Pharmacol Sci 105:353–360.

Handal M, Grung M, Skurtveit S, Ripel Å, Mørland J (2002) Pharmacokinetic differences of morphine and morphine-glucuronides are reflected in locomotor activity. Pharmacology Biochemistry and Behavior 73:883–892.

Harris G, Wimmer M, Randallthompson J, Astonjones G (2007) Lateral hypothalamic orexin neurons are critically involved in learning to associate an environment with morphine reward. Behavioural Brain Research 183:43–51.

Harris GC, Wimmer M, Aston-Jones G (2005) A role for lateral hypothalamic orexin neurons in reward seeking. Nature 437:556–559.
Hartwell EE, Pfeifer JG, McCauley JL, Moran-Santa Maria M, Back SE (2014) Sleep disturbances and pain among individuals with prescription opioid dependence. Addictive Behaviors 39:1537–1542.
Hartwick ATE, Bramley JR, Yu J, Stevens KT, Allen CN, Baldridge WH, Sollars PJ, Pickard GE (2007) Light-Evoked Calcium Responses of Isolated Melanopsin-Expressing Retinal Ganglion Cells. J Neurosci 27:13468–13480.
Hasler BP, Smith LJ, Cousins JC, Bootzin RR (2012) Circadian rhythms, sleep, and substance abuse. Sleep Medicine Reviews 16:67–81.
Hattar S, Kumar M, Park A, Tong P, Tung J, Yau K-W, Berson DM (2006) Central projections of melanopsin-expressing retinal ganglion cells in the mouse. J Comp Neurol 497:326–349.
Hecht A, Schiorring E (1979) Behavioral effects of low and high acute doses of morphine in solitary mice. Psychopharmacology 64:73–79.
Hellemans J, Mortier G, De Paepe A, Speleman F, Vandesompele J (2007) qBase relative quantification framework and software for management and automated analysis of real-time quantitative PCR data. Genome Biol 8:R19.
Hosoya K, Tachikawa M (2009) Inner Blood-Retinal Barrier Transporters: Role of Retinal Drug Delivery. Pharm Res 26:2055–2065.
Hsu W-Y, Chiu N-Y, Liu J-T, Wang C-H, Chang T-G, Liao Y-C, Kuo P-I (2012) Sleep quality in heroin addicts under methadone maintenance treatment. Acta Neuropsychiatr 24:356–360.
Hu C, Hill DD, Wong KY (2013) Intrinsic physiological properties of the five types of mouse ganglion-cell photoreceptors. Journal of Neurophysiology 109:1876–1889.
Huhn AS, Finan PH (2021) Sleep Disturbance as a Therapeutic Target to Improve Opioid Use Disorder Treatment. Experimental and Clinical Psychopharmacology:1064–1297.
Husain S, Abdul Y, Crosson CE (2012) Preservation of Retina Ganglion Cell Function by Morphine in a Chronic Ocular-Hypertensive Rat Model. Invest Ophthalmol Vis Sci 53:4289.
Husain S, Potter DE, Crosson CE (2009) Opioid Receptor-Activation: Retina Protected from Ischemic Injury. Invest Ophthalmol Vis Sci 50:3853.
Ingram S, Wilding TJ, McCleskey EW, Williams JT (1997) Efficacy and Kinetics of Opioid Action on Acutely Dissociated Neurons. Mol Pharmacol 52:136–143.
Itoh T, Murai S, Yoshida H, Masuda Y, Saito H, Chen CH (1987) Effects of methamphetamine and morphine on the vertical and horizontal motor activities in mice. Pharmacology Biochemistry and Behavior 27:193–197.
James MH, Stopper CM, Zimmer BA, Koll NE, Bowrey HE, Aston-Jones G (2019) Increased Number and Activity of a Lateral Subpopulation of Hypothalamic Orexin/Hypocretin Neurons Underlies the Expression of an Addicted State in Rats. Biological Psychiatry 85:925–935.
Johnson EE, Chieng B, Napier I, Connor M (2006) Decreased μ-opioid receptor signalling and a reduction in calcium current density in sensory neurons from chronically morphine-treated mice. British Journal of Pharmacology 148:947–955.
Kalivas PW, Duffy P (1987) Sensitization to repeated morphine injection in the rat: possible involvement of A10 dopamine neurons. J Pharmacol Exp Ther 241:204–212.

Kalvass JC, Olson ER, Cassidy MP, Selley DE, Pollack GM (2007) Pharmacokinetics and Pharmacodynamics of Seven Opioids in P-Glycoprotein-Competent Mice: Assessment of Unbound Brain EC $_{50,u}$ and Correlation of in Vitro, Preclinical, and Clinical Data. J Pharmacol Exp Ther 323:346–355.

Karinen R, Andersen JM, Ripel A, Hasvold I, Hopen AB, Morland J, Christophersen AS (2009) Determination of Heroin and Its Main Metabolites in Small Sample Volumes of Whole Blood and Brain Tissue by Reversed-Phase Liquid Chromatography-Tandem Mass Spectrometry. Journal of Analytical Toxicology 33:345–350.

Kay DC (1975) Human sleep during chronic morphine intoxication. Psychopharmacologia 44:117–124.

Kennedy C, Henderson G (1991) Mu-opioid receptor inhibition of calcium current: development of homologous tolerance in single SH-SY5Y cells after chronic exposure to morphine in vitro. Mol Pharmacol 40:1000–1005.

Kerdelhue B, Karteszi M, Pasqualini C, Reinberg A, Mezey E, Palkovits M (1983) Circadian variations in β-endorphin concentrations in pituitary and in some brain nuclei of the adult male rat. Brain Research 261:243–248.

Kieffer BL (1995) Recent advances in molecular recognition and signal transduction of active peptides: Receptors for opioid peptides. Cell Mol Neurobiol 15:615–635.

Kieffer BL, Evans CJ (2009) Opioid receptors: From binding sites to visible molecules in vivo. Neuropharmacology 56:205–212.

Koch CE, Leinweber B, Drengberg BC, Blaum C, Oster H (2017) Interaction between circadian rhythms and stress. Neurobiology of Stress 6:57–67.

Koek W (2014) Effects of repeated exposure to morphine in adolescent and adult male C57BL/6J mice: age-dependent differences in locomotor stimulation, sensitization, and body weight loss. Psychopharmacology 231:1517–1529.

Koek W, France CP, Javors MA (2012) Morphine-induced motor stimulation, motor incoordination, and hypothermia in adolescent and adult mice. Psychopharmacology 219:1027–1037.

Kosobud AEK, Gillman AG, Leffel JK, Pecoraro NC, Rebec GV, Timberlake W (2007) Drugs of Abuse Can Entrain Circadian Rhythms. The Scientific World JOURNAL 7:203–212.

Kozek KA, Du Y, Sharma S, Prael FJ, Spitznagel BD, Kharade SV, Denton JS, Hopkins CR, Weaver CD (2019) Discovery and Characterization of VU0529331, a Synthetic Small-Molecule Activator of Homomeric G Protein-Gated, Inwardly Rectifying, Potassium (GIRK) Channels. ACS Chem Neurosci 10:358–370.

L. Mercer S, Coop A (2011) Opioid Analgesics and P-Glycoprotein Efflux Transporters: A Potential Systems-Level Contribution to Analgesic Tolerance. CTMC 11:1157–1164.

Latif Z-H, Šaltyte Benth J, Solli KK, Opheim A, Kunoe N, Krajci P, Sharma-Haase K, Tanum L (2019) Anxiety, Depression, and Insomnia Among Adults With Opioid Dependence Treated With Extended-Release Naltrexone vs Buprenorphine-Naloxone: A Randomized Clinical Trial and Follow-up Study. JAMA Psychiatry 76:127.

Lax P, Esquiva G, Fuentes-Broto L, Segura F, Sánchez-Cano A, Cuenca N, Pinilla I (2016) Age-related changes in photosensitive melanopsin-expressing retinal ganglion cells correlate with circadian rhythm impairments in sighted and blind rats. Chronobiology International 33:374–391.

Lax P, Ortuño-Lizarán I, Maneu V, Vidal-Sanz M, Cuenca N (2019) Photosensitive Melanopsin-Containing Retinal Ganglion Cells in Health and Disease: Implications for Circadian Rhythms. IJMS 20:3164.
Le Marec T, Marie-Claire C, Noble F, Marie N (2011) Chronic and intermittent morphine treatment differently regulates opioid and dopamine systems: a role in locomotor sensitization. Psychopharmacology 216:297–303.
LeGates TA, Fernandez DC, Hattar S (2014) Light as a central modulator of circadian rhythms, sleep and affect. Nat Rev Neurosci 15:443–454.
Letrent SP, Polli JW, Humphreys JE, Pollack GM, Brouwer KR, Brouwer KLR (1999) P-glycoprotein-mediated transport of morphine in brain capillary endothelial cells. Biochemical Pharmacology 58:951–957.
Levitt ES, Williams JT (2012) Morphine Desensitization and Cellular Tolerance Are Distinguished in Rat Locus Ceruleus Neurons. Mol Pharmacol 82:983–992.
Li JY, Schmidt TM (2018) Divergent projection patterns of M1 ipRGC subtypes. J Comp Neurol 526:2010–2018.
Li Y, Faiz A, Moshage H, Schubert R, Schilling L, Kamps JA (2021) Comparative transcriptome analysis of inner blood-retinal barrier and blood–brain barrier in rats. Sci Rep 11:12151.
Li Y, van den Pol AN (2008) μ-Opioid Receptor-Mediated Depression of the Hypothalamic Hypocretin/Orexin Arousal System. Journal of Neuroscience 28:2814–2819.
Liu L, Liu X (2019) Roles of Drug Transporters in Blood-Retinal Barrier. In: Drug Transporters in Drug Disposition, Effects and Toxicity (Liu X, Pan G, eds), pp 467–504 Advances in Experimental Medicine and Biology. Singapore: Springer Singapore. Available at: http://link.springer.com/10.1007/978-981-13-7647-4_10 [Accessed March 22, 2022].
Livak KJ, Schmittgen TD (2001) Analysis of Relative Gene Expression Data Using Real-Time Quantitative PCR and the 2−ΔΔCT Method. Methods 25:402–408.
Lötsch J (2005) Opioid Metabolites. Journal of Pain and Symptom Management 29:10–24.
Lucas JA, Schmidt TM (2019) Cellular properties of intrinsically photosensitive retinal ganglion cells during postnatal development. Neural Dev 14:8.
Lucas RJ, Douglas RH, Foster RG (2001) Characterization of an ocular photopigment capable of driving pupillary constriction in mice. Nat Neurosci 4:621–626.
Lucas RJ, Hattar S, Takao M, Berson DM, Foster RG, Yau K-W (2003) Diminished Pupillary Light Reflex at High Irradiances in Melanopsin-Knockout Mice. Science 299:245–247.
Lupi D, Oster H, Thompson S, Foster RG (2008) The acute light-induction of sleep is mediated by OPN4-based photoreception. Nat Neurosci 11:1068–1073.
Ma Y, Miracca G, Yu X, Harding EC, Miao A, Yustos R, Vyssotski AL, Franks NP, Wisden W (2019) Galanin Neurons Unite Sleep Homeostasis and α2-Adrenergic Sedation. Current Biology 29:3315-3322.e3.
Maloney R, Quattrochi L, Yoon J, Souza R, Berson D (2022) Efficacy and Specificity of Melanopsin Reporters for Retinal Ganglion Cells. Neuroscience. Available at: http://biorxiv.org/lookup/doi/10.1101/2022.04.26.489554 [Accessed September 30, 2022].
Mansour A, Fox CA, Burke S, Meng F, Thompson RC, Akil H, Watson SJ (1994a) Mu, delta, and kappa opioid receptor mRNA expression in the rat CNS: An in situ hybridization study. J Comp Neurol 350:412–438.

Mansour A, Fox CA, Thompson RC, Akil H, Watson SJ (1994b) Mu-Opioid receptor mRNA expression in the rat CNS: comparison to mu-receptor binding. Brain Research 643:245–265.
Marcott PF, Mamaligas AA, Ford CP (2014) Phasic Dopamine Release Drives Rapid Activation of Striatal D2-Receptors. Neuron 84:164–176.
Maskell PD, Albeishy M, De Paoli G, Wilson NE, Seetohul LN (2016) Postmortem redistribution of the heroin metabolites morphine and morphine-3-glucuronide in rabbits over 24 h. Int J Legal Med 130:519–531.
Maskell PD, Wilson NE, Seetohul LN, Crichton ML, Beer LJ, Drummond G, De Paoli G (2019) Postmortem tissue distribution of morphine and its metabolites in a series of heroin-related deaths. Drug Test Anal 11:292–304.
Matthes HWD, Maldonadot R, Simonin F, Valverdet O, Slowet S, Kitchen I, Befort K, Dierich A, Le Meur M, Dolle P, Tzavara E, Hanoune J, Roques BP, Kieffer BL (1996) Loss of morphine-induced analgesia, reward effect and withdrawal symptoms in mice lacking the mu-Opioid-receptor gene. Nature 383:819–823.
Matzeu A, Martin-Fardon R (2020) Targeting the Orexin System for Prescription Opioid Use Disorder. Brain Sciences 10:226.
McLane VD, Bergquist I, Cormier J, Barlow DJ, Houseknecht KL, Bilsky EJ, Cao L (2017) Long-term morphine delivery via slow release morphine pellets or osmotic pumps: Plasma concentration, analgesia, and naloxone-precipitated withdrawal. Life Sciences 185:1–7.
McQuay H (1999) Opioids in pain management. THE LANCET 353:4.
Meijer JH, Ruijs ACJ, Albus H, van de Geest B, Duindam H, Zwinderman AH, Dahan A (2000) Fentanyl, a mu-opioid receptor agonist, phase shifts the hamster circadian pacemaker. Brain Research 868:135–140.
Meyer-Franke A, Kaplan MR, Pfieger FW, Barres BA (1995) Characterization of the signaling interactions that promote the survival and growth of developing retinal ganglion cells in culture. Neuron 15:805–819.
Mistlberger RE, Holmes MM (1999) Morphine-induced activity attenuates phase shifts to light in C57BL/6J mice. Brain Research 829:113–119.
Mogil JS, Chesler EJ, Wilson SG, Juraska JM, Sternberg WF (2000) Sex differences in thermal nociception and morphine antinociception in rodents depend on genotype. Neuroscience & Biobehavioral Reviews 24:375–389.
Moraes MN, de Assis LVM, Provencio I, Castrucci AM de L (2021) Opsins outside the eye and the skin: a more complex scenario than originally thought for a classical light sensor. Cell Tissue Res 385:519–538.
Moreton JE, Roehrs T, Khazan N (1976) Drug Self-Administration and Sleep-Awake Activity in Rats Dependent on Morphine, Methadone, or/-Alpha-Acetylmethadol. :5.
Morrison S F, Nakamura K (2011) Central neural pathways for thermoregulation. Front Biosci 16:74.
Muindi F, Zeitzer JM, Heller HC (2014) Retino-hypothalamic regulation of light-induced murine sleep. Front Syst Neurosci 8 Available at: http://journal.frontiersin.org/article/10.3389/fnsys.2014.00135/abstract [Accessed April 29, 2022].
Munteanu T, Noronha KJ, Leung AC, Pan S, Lucas JA, Schmidt TM (2018) Light-dependent pathways for dopaminergic amacrine cell development and function. eLife 7:e39866.

Novak CM, Burghardt PR, Levine JA (2012) The use of a running wheel to measure activity in rodents: Relationship to energy balance, general activity, and reward. Neuroscience & Biobehavioral Reviews 36:1001–1014.
Ochiai W, Kaneta M, Nagae M, yuzuhara A, Li X, Suzuki H, Hanagata M, Kitaoka S, Suto W, Kusunoki Y, Kon R, Miyashita K, Masukawa D, Ikarashi N, Narita M, Suzuki T, Sugiyama K (2016) Mice with neuropathic pain exhibit morphine tolerance due to a decrease in the morphine concentration in the brain. European Journal of Pharmaceutical Sciences 92:298–304.
Oldendorf WH (1977) The blood-brain barrier. Experimental Eye Research 25:177–190.
Ollikainen E, Aitta-aho T, Koburg M, Kostiainen R, Sikanen T (2019) Rapid analysis of intraperitoneally administered morphine in mouse plasma and brain by microchip electrophoresis-electrochemical detection. Sci Rep 9:3311.
Ollion J, Cochennec J, Loll F, Escudé C, Boudier T (2013) TANGO: a generic tool for high-throughput 3D image analysis for studying nuclear organization. Bioinformatics 29:1840–1841.
Pačesová D, Novotný J, Bendová Z (2016) The Effect of Chronic Morphine or Methadone Exposure and Withdrawal on Clock Gene Expression in the Rat Suprachiasmatic Nucleus and AA-NAT Activity in the Pineal Gland. Physiol Res:517–525.
Pačesová D, Volfová B, Červená K, Hejnová L, Novotný J, Bendová Z (2015) Acute morphine affects the rat circadian clock via rhythms of phosphorylated ERK1/2 and GSK3β kinases and *P er1* expression in the rat suprachiasmatic nucleus: Morphine affects ERK1/2, GSK3β and *Per1* in the SCN. Br J Pharmacol 172:3638–3649.
Pacifici R, di Carlo S, Bacosi A, Pichini S, Zuccaro P (2000) Pharmacokinetics and cytokine production in heroin and morphine-treated mice. International Journal of Immunopharmacology 22:603–614.
Palus K, Chrobok L, Kepczynski M, Lewandowski MH (2017) Enkephalin and neuropeptide-Y interaction in the intergeniculate leaflet network, a part of the mammalian biological clock. Neuroscience 343:10–20.
Pasternak GW, Pan Y-X (2013) Mu Opioids and Their Receptors: Evolution of a Concept Sibley DR, ed. Pharmacol Rev 65:1257–1317.
Peart JN, Gross GJ (2004) Morphine-Tolerant Mice Exhibit a Profound and Persistent Cardioprotective Phenotype. Circulation 109:1219–1222.
Peckham EM, Traynor JR (2006) Comparison of the Antinociceptive Response to Morphine and Morphine-Like Compounds in Male and Female Sprague-Dawley Rats. J Pharmacol Exp Ther 316:1195–1201.
Pennock RL, Dicken MS, Hentges ST (2012) Multiple Inhibitory G-Protein-Coupled Receptors Resist Acute Desensitization in the Presynaptic But Not Postsynaptic Compartments of Neurons. Journal of Neuroscience 32:10192–10200.
Penson R (2000) Randomized placebo-controlled trial of the activity of the morphine glucuronides. Clinical Pharmacology & Therapeutics 68:667–676.
Pickworth WB, Bunker E, Welch P, Cone E (1991) Intravenous buprenorphine reduces pupil size and the light reflex in humans. Life Sciences 49:129–138.
Pickworth WB, Lee H, Fudala PJ (1990) Buprenorphine-induced pupillary effects in human volunteers. Life Sciences 47:1269–1277.
Rawls S M, Benamar K (2011) Effects of opioids, cannabinoids, and vanilloids on body temperature. Front Biosci S3:822.

Rees KA, Pounder DJ, Osselton MD (2013) Distribution of opiates in femoral blood and vitreous humour in heroin/morphine-related deaths. Forensic Science International 226:152–159.
Refinetti R (1999) Relationship between the daily rhythms of locomotor activity and body temperature in eight mammalian species. American Journal of Physiology-Regulatory, Integrative and Comparative Physiology 277:R1493–R1500.
Rhon DI (2019) Comorbid Insomnia and Sleep Apnea areAssociated with Greater Downstream HealthCare Utilization and Chronic Opioid Use afterArthroscopic Hip Surgery. Pain Phys 4:E351–E360.
Riazi-Esfahani M, Kiumehr S, Asadi-Amoli F, Dehpour AR (2009) Effects of intravitreal morphine administered at different time points after reperfusion in a rabbit model of ischemic retinopathy. Retina 29:262–268.
Riazi-Esfahani M, Kiumehr, S, Asadi-Amoli F, Lashay AR, Dehpour AR (2008) Morphine Pretreatment Provides Histologic Protection against Ischemia-Reperfusion Injury in Rabbit Retina. Retina 28.
Robinson TE, Berridge KC (1993) The neural basis of drug craving: an incentive-sensitization theory of addiction. Brain Research Reviews 18:247–291.
Roehrs T, Hyde M, Blaisdell B, Greenwald M, Roth T (2006) Sleep Loss and REM Sleep Loss are Hyperalgesic. Sleep 29:145–151.
Roehrs TA, Roth T (2015) Sleep Disturbance in Substance Use Disorders. Psychiatric Clinics of North America 38:793–803.
Rook E, Huitema A, Brink W, Ree J, Beijnen J (2006) Pharmacokinetics and Pharmacokinetic Variability of Heroin and its Metabolites: Review of the Literature. CCP 1:109–118.
Rosen IM, Aurora RN, Kirsch DB, Carden KA, Malhotra RK, Ramar K, Abbasi-Feinberg F, Kristo DA, Martin JL, Olson EJ, Rosen CL, Rowley JA, Shelgikar AV, American Academy of Sleep Medicine Board of Directors (2019) Chronic Opioid Therapy and Sleep: An American Academy of Sleep Medicine Position Statement. Journal of Clinical Sleep Medicine 15:1671–1673.
Rosenblum A, Marsch LA, Joseph H, Portenoy RK (2008) Opioids and the treatment of chronic pain: Controversies, current status, and future directions. Experimental and Clinical Psychopharmacology 16:405–416.
Rupp AC, Ren M, Altimus CM, Fernandez DC, Richardson M, Turek F, Hattar S, Schmidt TM (2019) Distinct ipRGC subpopulations mediate light's acute and circadian effects on body temperature and sleep. eLife 8:e44358.
Sanches LR, Seulin SC, Leyton V, Bismara Paranhos BAP, Pasqualucci CA, Munoz DR, Osselton MD, Yonamine M (2012) Determination of Opiates in Whole Blood and Vitreous Humor: A Study of the Matrix Effect and an Experimental Design to Optimize Conditions for the Enzymatic Hydrolysis of Glucuronides. Journal of Analytical Toxicology 36:162–170.
Saper CB, Fuller PM, Pedersen NP, Lu J, Scammell TE (2010) Sleep State Switching. Neuron 68:1023–1042.
Saunders A, Macosko EZ, Wysoker A, Goldman M, Krienen FM, de Rivera H, Bien E, Baum M, Bortolin L, Wang S, Goeva A, Nemesh J, Kamitaki N, Brumbaugh S, Kulp D, McCarroll SA (2018) Molecular Diversity and Specializations among the Cells of the Adult Mouse Brain. Cell 174:1015-1030.e16.

Sawant OB, Horton AM, Zucaro OF, Chan R, Bonilha VL, Samuels IS, Rao S (2017) The Circadian Clock Gene Bmal1 Controls Thyroid Hormone-Mediated Spectral Identity and Cone Photoreceptor Function. Cell Reports 21:692–706.
Sawe J, Kager L, Svensson Eng J, Rane A (1985) Oral morphine in cancer patients: in vivo kinetics and in vitro hepatic glucuronidation. British Journal of Clinical Pharmacology 19:495–501.
Schaefer CP, Tome ME, Davis TP (2017) The opioid epidemic: a central role for the blood brain barrier in opioid analgesia and abuse. Fluids Barriers CNS 14:32.
Schindelin J, Arganda-Carreras I, Frise E, Kaynig V, Longair M, Pietzsch T, Preibisch S, Rueden C, Saalfeld S, Schmid B, Tinevez J-Y, White DJ, Hartenstein V, Eliceiri K, Tomancak P, Cardona A (2012) Fiji: an open-source platform for biological-image analysis. Nat Methods 9:676–682.
Schmidt TM, Chen S-K, Hattar S (2011) Intrinsically photosensitive retinal ganglion cells: many subtypes, diverse functions. Trends in Neurosciences 34:572–580.
Schmidt TM, Taniguchi K, Kofuji P (2008) Intrinsic and Extrinsic Light Responses in Melanopsin-Expressing Ganglion Cells During Mouse Development. Journal of Neurophysiology 100:371–384.
Scott KS, Oliver JS (1999) Vitreous Humor as an Alternative Sample to Blood for the Supercritical Fluid Extraction of Morphine and 6-Monoacetylmorphine. Med Sci Law 39:77–81.
Serdarevic M, Osborne V, Striley CW, Cottler LB (2017) The association between insomnia and prescription opioid use: results from a community sample in Northeast Florida. Sleep Health 3:368–372.
Severino AL, Mittal N, Hakimian JK, Velarde N, Minasyan A, Albert R, Torres C, Romaneschi N, Johnston C, Tiwari S, Lee AS, Taylor AM, Gavériaux-Ruff C, Kieffer BL, Evans CJ, Cahill CM, Walwyn WM (2020) μ-Opioid Receptors on Distinct Neuronal Populations Mediate Different Aspects of Opioid Reward-Related Behaviors. eNeuro 7:ENEURO.0146-20.2020.
Sherin JE, Elmquist JK, Torrealba F, Saper CB (1998) Innervation of Histaminergic Tuberomammillary Neurons by GABAergic and Galaninergic Neurons in the Ventrolateral Preoptic Nucleus of the Rat. J Neurosci 18:4705–4721.
Sheth S, Holtsman M, Mahajan G (2018) Major Opioids in Pain Management. In: Essentials of Pain Medicine, pp 373-384.e2. Elsevier. Available at: https://linkinghub.elsevier.com/retrieve/pii/B9780323401968000425 [Accessed March 22, 2022].
Simmons Z, Erickson LD, Hedges D, Kay DB (2020) Insomnia Is Associated With Frequency of Suicidal Ideation Independent of Depression: A Replication and Extension of Findings From the National Health and Nutrition Examination Survey. Front Psychiatry 11:561564.
Smith MA, Greene-Naples JL, Lyle MA, Iordanou JC, Felder JN (2009) The Effects of Repeated Opioid Administration on Locomotor Activity: I. Opposing Actions of μ and κ Receptors. J Pharmacol Exp Ther 330:468–475.
Sora I, Li X-F (2001) Mu Opiate Receptor Gene Dose Effects on Different Morphine Actions: Evidence for Differential in vivo mu Receptor Reserve. Neuropsychopharmacology 25:14.

Storch C, Höhne A, Holsboer F, Ohl F (2004) Activity patterns as a correlate for sleep–wake behaviour in mice. Journal of Neuroscience Methods 133:173–179.
Struys MMRF, Sahinovic M, Lichtenbelt BJ, Vereecke HEM, Absalom AR (2011) Optimizing intravenous drug administration by applying pharmacokinetic/pharmacodynamic concepts. British Journal of Anaesthesia 107:38–47.
Szkeley JI, Miglecz E, Ronai Z (1980) Biphasic Effects of a Potent Enkephalin Analogue (D-Met2,ProS)-Enkephalinamide and Morphine on Locomotor Activity in Mice. Psychopharmacology 71:299–301.
Tamura EK, Oliveira-Silva KS, Ferreira-Moraes FA, Marinho EAV, Guerrero-Vargas NN (2021) Circadian rhythms and substance use disorders: A bidirectional relationship. Pharmacology Biochemistry and Behavior 201:173105.
Thannickal TC, John J, Shan L, Swaab DF, Wu M-F, Ramanathan L, McGregor R, Chew K-T, Cornford M, Yamanaka A, Inutsuka A, Fronczek R, Lammers GJ, Worley PF, Siegel JM (2018) Opiates increase the number of hypocretin-producing cells in human and mouse brain and reverse cataplexy in a mouse model of narcolepsy. Sci Transl Med 10:eaao4953.
Tian M, Broxmeyer HE, Fan Y, Lai Z, Zhang S, Aronica S, Cooper S, Bigsby RM, Steinmetz R, Engle SJ, Mestek A, Pollock JD, Lehman MN, Jansen HT, Ying M, Stambrook PJ, Tischfield JA, Yu L (1997) Altered Hematopoiesis, Behavior, and Sexual Function in mu Opioid Receptor–deficient Mice. Journal of Experimental Medicine 185:1517–1522.
Tierno A, Fiore P, Gannon RL (2002) Delta opioid inhibition of light-induced phase advances in hamster circadian activity rhythms. Brain Research 937:66–73.
Tooker RE, Lipin MY, Leuranguer V, Rozsa E, Bramley JR, Harding JL, Reynolds MM, Vigh J (2013) Nitric Oxide Mediates Activity-Dependent Plasticity of Retinal Bipolar Cell Output via S-Nitrosylation. J Neurosci 33:19176–19193.
Tripathi R, Rao R, Dhawan A, Jain R, Sinha S (2020) Opioids and sleep – a review of literature. Sleep Medicine 67:269–275.
Tsai JW, Hannibal J, Hagiwara G, Colas D, Ruppert E, Ruby NF, Heller HC, Franken P, Bourgin P (2009) Melanopsin as a Sleep Modulator: Circadian Gating of the Direct Effects of Light on Sleep and Altered Sleep Homeostasis in Opn4−/− Mice Foster RG, ed. PLoS Biol 7:e1000125.
Tsujino N, Sakurai T (2013) Role of orexin in modulating arousal, feeding, and motivation. Front Behav Neurosci 7 Available at: http://journal.frontiersin.org/article/10.3389/fnbeh.2013.00028/abstract [Accessed April 27, 2022].
Tzschentke TM (2001) Pharmacology and behavioral pharmacology of the mesocortical dopamine system. Progress in Neurobiology 63:241–320.
van Dorp ELA, Romberg R, Sarton E, Bovill JG, Dahan A (2006) Morphine-6-Glucuronide: Morphine's Successor for Postoperative Pain Relief? Anesthesia & Analgesia 102:1789–1797.
Van Hook MJ, Berson DM (2010) Hyperpolarization-Activated Current (Ih) in Ganglion-Cell Photoreceptors Taylor WR, ed. PLoS ONE 5:e15344.
Van Hook MJ, Wong KY, Berson DM (2012) Dopaminergic modulation of ganglion-cell photoreceptors in rat: Dopamine and ipRGCs. European Journal of Neuroscience 35:507–518.

Vandesompele J, Preter KD, Roy NV, Paepe AD (2002) Accurate normalization of real-time quantitative RT-PCR data by geometric averaging of multiple internal control genes. Genome Biology 3:1–12.
Vansteensel MJ, Deboer T, Dahan A, Meijer JH (2003) Differential Responses of Circadian Activity Onset and Offset Following GABA-ergic and Opioid Receptor Activation. J Biol Rhythms 18:297–306.
Vansteensel MJ, Magnone MC, van Oosterhout F, Baeriswyl S, Albrecht U, Albus H, Dahan A, Meijer JH (2005) The opioid fentanyl affects light input, electrical activity and *Per* gene expression in the hamster suprachiasmatic nuclei. European Journal of Neuroscience 21:2958–2966.
Viscusi ER, Viscusi AR (2020) Blood–brain barrier: mechanisms governing permeability and interaction with peripherally acting μ-opioid receptor antagonists. Reg Anesth Pain Med 45:688–695.
Volkow ND, Jones EB, Einstein EB, Wargo EM (2019) Prevention and Treatment of Opioid Misuse and Addiction: A Review. JAMA Psychiatry 76:208.
Vuong HE, Hardi CN, Barnes S, Brecha NC (2015) Parallel Inhibition of Dopamine Amacrine Cells and Intrinsically Photosensitive Retinal Ganglion Cells in a Non-Image-Forming Visual Circuit of the Mouse Retina. J Neurosci 35:15955–15970.
Wang Q, Yue X-F, Qu W-M, Tan R, Zheng P, Urade Y, Huang Z-L (2013) Morphine Inhibits Sleep-Promoting Neurons in the Ventrolateral Preoptic Area Via Mu Receptors and Induces Wakefulness in Rats. Neuropsychopharmacol 38:791–801.
Weibel R, Reiss D, Karchewski L, Gardon O, Matifas A, Filliol D, Becker JAJ, Wood JN, Kieffer BL, Gaveriaux-Ruff C (2013) Mu Opioid Receptors on Primary Afferent Nav1.8 Neurons Contribute to Opiate-Induced Analgesia: Insight from Conditional Knockout Mice Cunha TM, ed. PLoS ONE 8:e74706.
Weinert D, Waterhouse J (1998) Diurnally Changing Effects of Locomotor Activity on Body Temperature in Laboratory Mice. Physiology & Behavior 63:837–843.
Williams JT, Christie MJ, Manzoni O (2001) Cellular and Synaptic Adaptations Mediating Opioid Dependence. Physiological Reviews 81:299–343.
Williams JT, Ingram SL, Henderson G, Chavkin C, von Zastrow M, Schulz S, Koch T, Evans CJ, Christie MJ (2013) Regulation of μ -Opioid Receptors: Desensitization, Phosphorylation, Internalization, and Tolerance Dolphin AC, ed. Pharmacol Rev 65:223–254.
Wise RA, Bozarth MA (1987) A psychomotor stimulant theory of addiction. Psychol Rev 94:469–492.
Witkovsky P (2004) Dopamine and retinal function. Doc Ophthalmol 108:17–39.
Wu Z, Autry AE, Bergan JF, Watabe-Uchida M, Dulac CG (2014) Galanin neurons in the medial preoptic area govern parental behaviour. Nature 509:325–330.
Wyman J, Bultman S (2004) Postmortem Distribution of Heroin Metabolites in Femoral Blood, Liver, Cerebrospinal Fluid, and Vitreous Humor. Journal of Analytical Toxicology 28:260–263.
Yang J, Reilly B, Davis T, Ronaldson P (2018) Modulation of Opioid Transport at the Blood-Brain Barrier by Altered ATP-Binding Cassette (ABC) Transporter Expression and Activity. Pharmaceutics 10:192.

Yoo J-H, Yang E-M, Lee S-Y, Loh HH, Ho IK, Jang C-G (2003) Differential effects of morphine and cocaine on locomotor activity and sensitization in μ-opioid receptor knockout mice. Neuroscience Letters 344:37–40.

Yousif S, Saubaméa B, Cisternino S, Marie-Claire C, Dauchy S, Scherrmann J-M, Declèves X (2008) Effect of chronic exposure to morphine on the rat blood-brain barrier: focus on the P-glycoprotein. Journal of Neurochemistry 107:647–657.

Zarrindast M-R, Barghi-Lashkari S, Shafizadeh M (2001) The possible cross-tolerance between morphine- and nicotine-induced hypothermia in mice. Pharmacology Biochemistry and Behavior 68:283–289.

Zarrindast M-R, Zarghi A (1992) Morphine stimulates locomotor activity by an indirect dopaminergic mechanism: Possible D-1 and D-2 receptor involvement. General Pharmacology: The Vascular System 23:1221–1225.

Zhang Z, Beier C, Weil T, Hattar S (2021) The retinal ipRGC-preoptic circuit mediates the acute effect of light on sleep. Nat Commun 12:5115.

Zhao X, Stafford BK, Godin AL, King WM, Wong KY (2014) Photoresponse diversity among the five types of intrinsically photosensitive retinal ganglion cells: Light responses of melanopsin ganglion cells. The Journal of Physiology 592:1619–1636.

Zhou Y, Bendor J, Hofmann L, Randesi M, Ho A, Kreek MJ (2006) Mu opioid receptor and orexin/hypocretin mRNA levels in the lateral hypothalamus and striatum are enhanced by morphine withdrawal. Journal of Endocrinology 191:137–145.

Zong J, Pollack GM (2000) Morphine Antinociception Is Enhanced in mdr1a Gene-Deficient Mice. Pharmaceutical Research 17:749–753.

Zubieta J-K, Smith YR, Bueller JA, Xu Y, Kilbourn MR, Jewett DM, Meyer CR, Koeppe RA, Stohler CS (2002) μ-Opioid Receptor-Mediated Antinociceptive Responses Differ in Men and Women. Journal of Neuroscience 22:5100–5107.

Zuccaro P, Ricciarello R, Pichini S, Pacifici R, Altieri I, Pellegrini M, D'Ascenzo G (1997) Simultaneous Determination of Heroin, 6-Monoacetylmorphine, Morphine, and its Glucuronides by Liquid Chromatography-Atmospheric Pressure Ionspray-Mass Spectrometry. Journal of Analytical Toxicology 21:268–277.

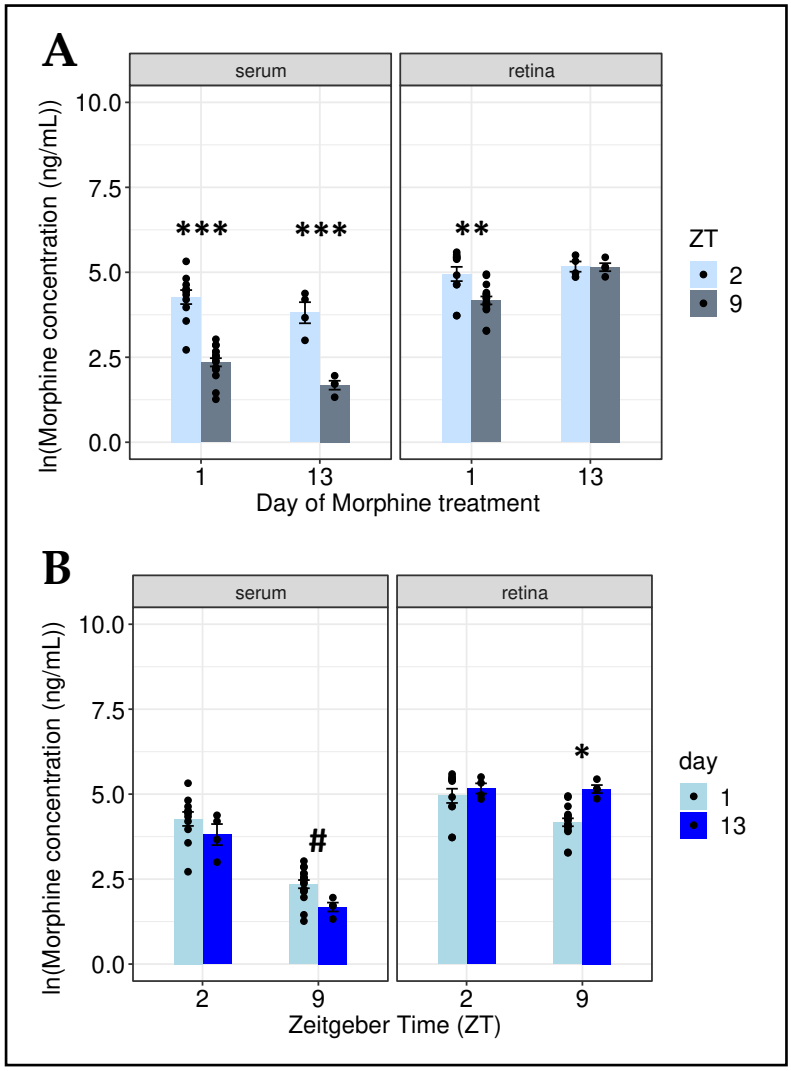

Figure S1. Morphine accumulates in the retina following chronic systemic exposure. (**A & B**) Morphine appears accumulate in the retina following 13 days of chronic morphine treatment, while the serum pharmacokinetics remain similar for samples collected at ZT 2 and ZT 9. Three-Way ANOVA with a Tukey post-hoc adjustment natural logarithmic (ln) scale. (#: $p<0.05$, *$p<0.001$, **$p<0.001$, ***=$p<0.0001$). Data presented as the mean ± SEM.

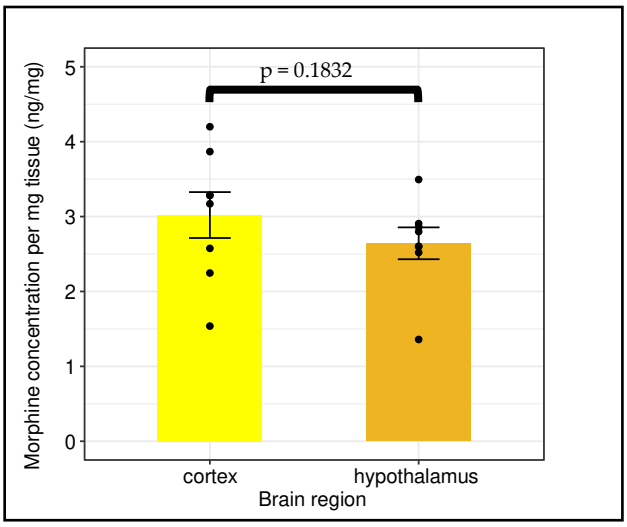

Figure S2. Morphine deposits similarly in different brain regions. Hypothalamus and cerebral cortex samples collected from the same mice show no difference in morphine deposition an hour (ZT 1) after a single 20 mg/kg i.p. morphine injection. Data presented as the mean ± SEM and assessed using a paired samples t-test (n=8).

Table S1. Primer and probe sequences for qRT-PCR experiments.

Target, GenBank accession number	Forward Primer (5'-3')	Reverse Primer (5'-3')	Probe Sequence (5'-3')
P-glycoprotein (Abcb1a), NM_011076.3	CAGCCAGCATTCTCCGTAATA	CCCAAGGATCAGAAACAACA	/FAM/CAGCGGCAG/ZEN/AACAGCAACTTGTTT/IABkFQ/
β-actin (Actb), NM_007393.5	GTCATCCATGGCGAACTGG	ACTGTCGAGTCGCGTCC	/HEX/CGTTGCCGG/ZEN/TCCACACCCGCCA/IABkFQ/
TATA box binding protein (Tbp), NM_013684.3	CCATGAAATAGTGATGCTGGGC	GGGTATCTGCTGGCGGTTT	/HEX/TGCGGTCGC/ZEN/GTCATTTTCTCCGCAGT/IABkFQ/

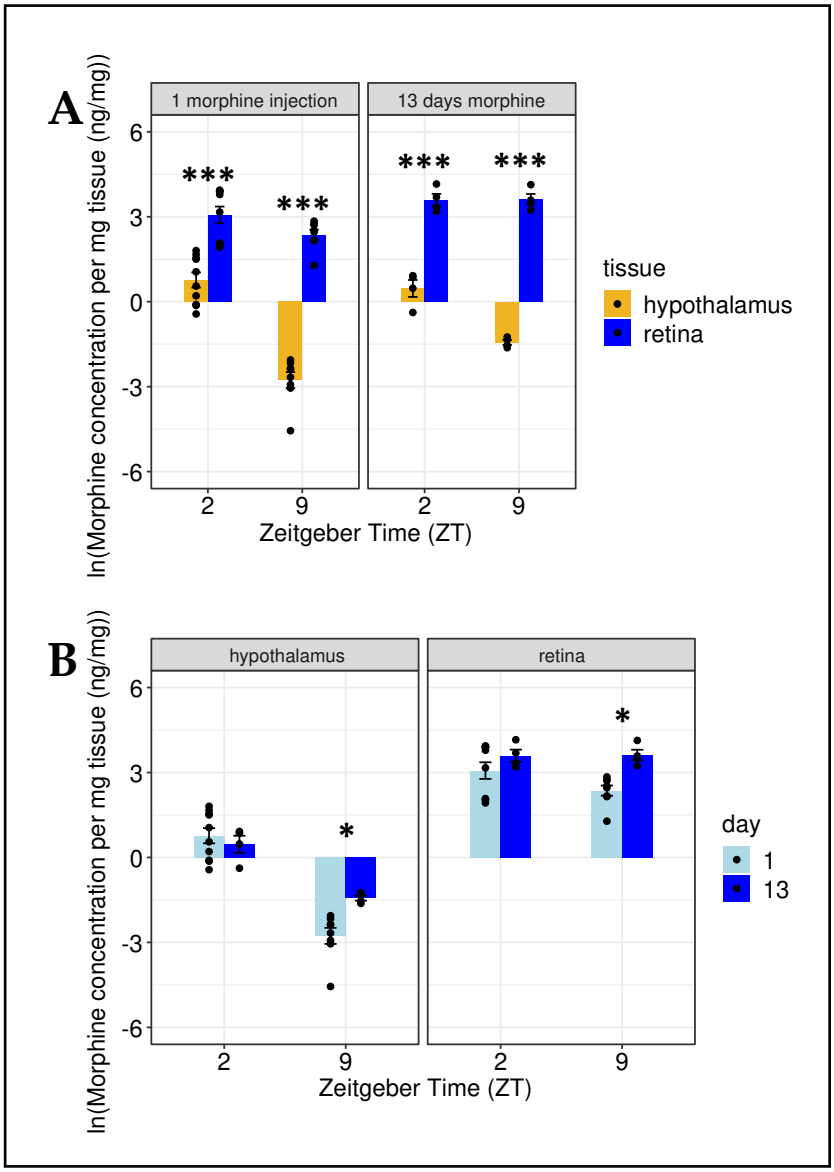

Figure S4. Morphine accumulates in the retina, but not the hypothalamus at ZT 2 and ZT 9**.** (**A**) Morphine concentrations exceed hypothalamic morphine concentrations at ZT 2 and ZT 9 following chronic morphine exposure (13 days morphine). (**B**) Morphine accumulates in the retina, but not the hypothalamus following chronic morphine exposure. Two-Way ANOVA with a Tukey post-hoc adjustment performed on natural logarithmic (ln) scale. Data presented as the mean ± SEM (#p<0.05, *p<0.01, **p<0.001, ***=p<0.0001).

Table S2. Matrix validation results for morphine LC-MS/MS.

Matrix	Accuracy	Precision	Range ng/ml	Calibration Model	Carryover	Interference	LOQ ng/ml	Stability
Retina	94-98 %	4.6-6.2%	20-5000	Linear	None	None	20	72h
Serum	87-105%	0.84-5.9%	0.5-1000	Linear	None	None	0.5	72h
Hypothalamus	94.2-108%	2.9-13.9%	0.2-50	Linear	None	None	0.2	72h

Table S3. Parameters and acceptance criteria for morphine LC-MS/MS matrix validation.

Parameter	Acceptance Criteria
Accuracy	Must not exceed +/- 20% at 3 concentrations
Precision	% CV must not exceed 20% at 3 concentrations
Calibration Model	Linear Range with R^2 greater than 0.99 (linear mode with 1/x weighting if appropriate fit)
Carryover	Carryover from highest calibrator to subsequent blank samples does not exceed 20% of signal of lowest calibrator
Interference Studies	No interfering signal form matrix, internal standards, standard, or other common drugs of abuse, OTC drugs, and prescription medications
Limit of Quantitation (LOQ)	Lowest concentration that meets accuracy and precision acceptance criteria
Processed Sample Stability	Length of time that analyte in extracted sample can be stored at room temperature on autosampler rack and meet accuracy and precision criteria

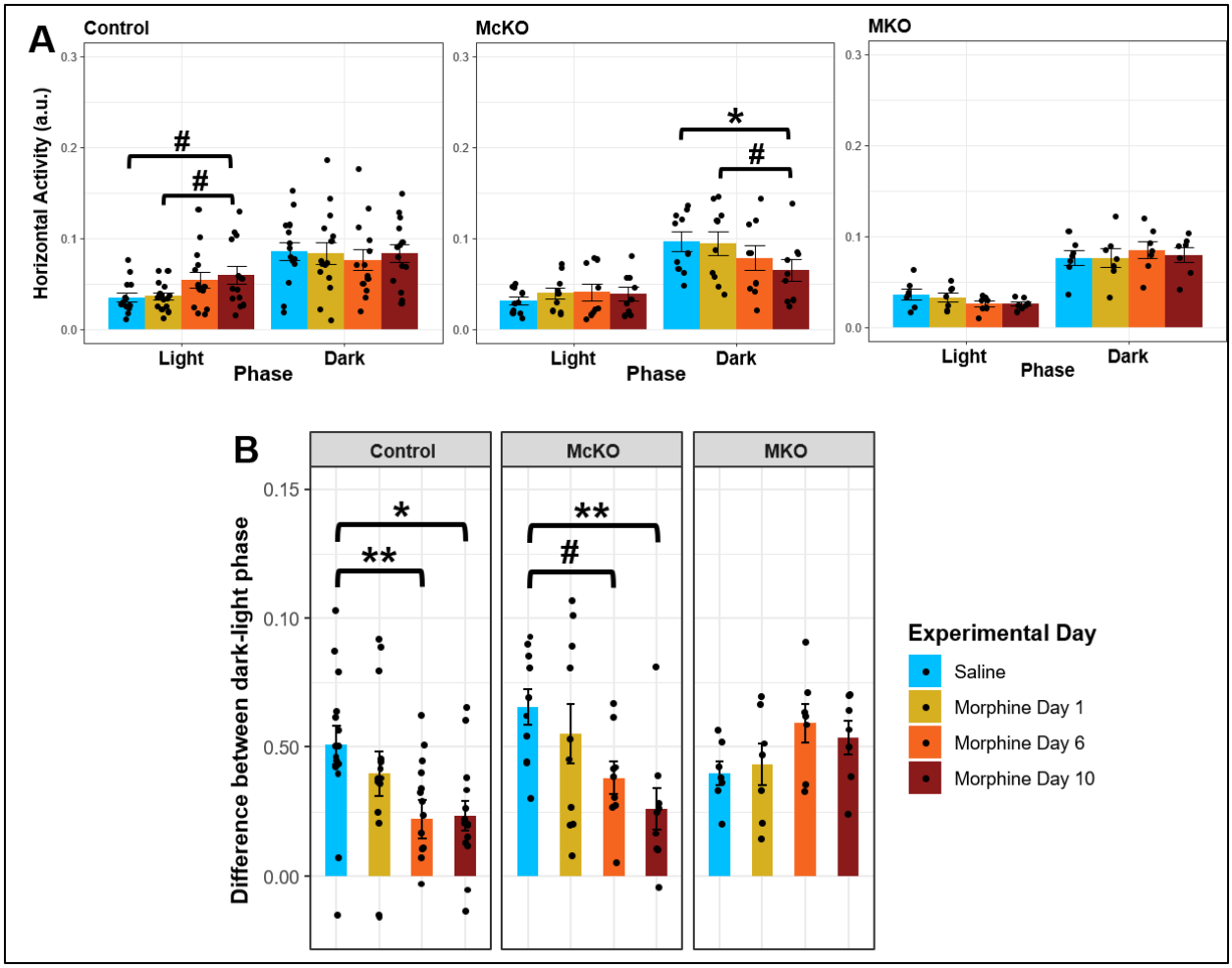

Figure S5. Prolonged, but not acute morphine decreases diurnal variations in circadian behavioral activity. **(A)** Control (n=14-15) mice increase their locomotor activity in the light phase, while McKO (n=9-10) littermates decrease their locomotor activity in the light phase following repeated morphine exposure (with no change in the MKO regardless of phase or experimental day) . Three-way ANOVA with a Holm-Bonferroni post-hoc adjustment performed on all pairwise comparisons. **(B)** Control and McKO mice exhibit a decrease in diurnal variations in circadian activity, whereas MKO (n=7) animals do not. Two-way ANOVA with a Holm-Bonferroni post-hoc adjustment performed on all pairwise comparisons (#p<0.05, *p<0.01, **p<0.001, ***=p<0.0001). Data presented as mean ± SEM.

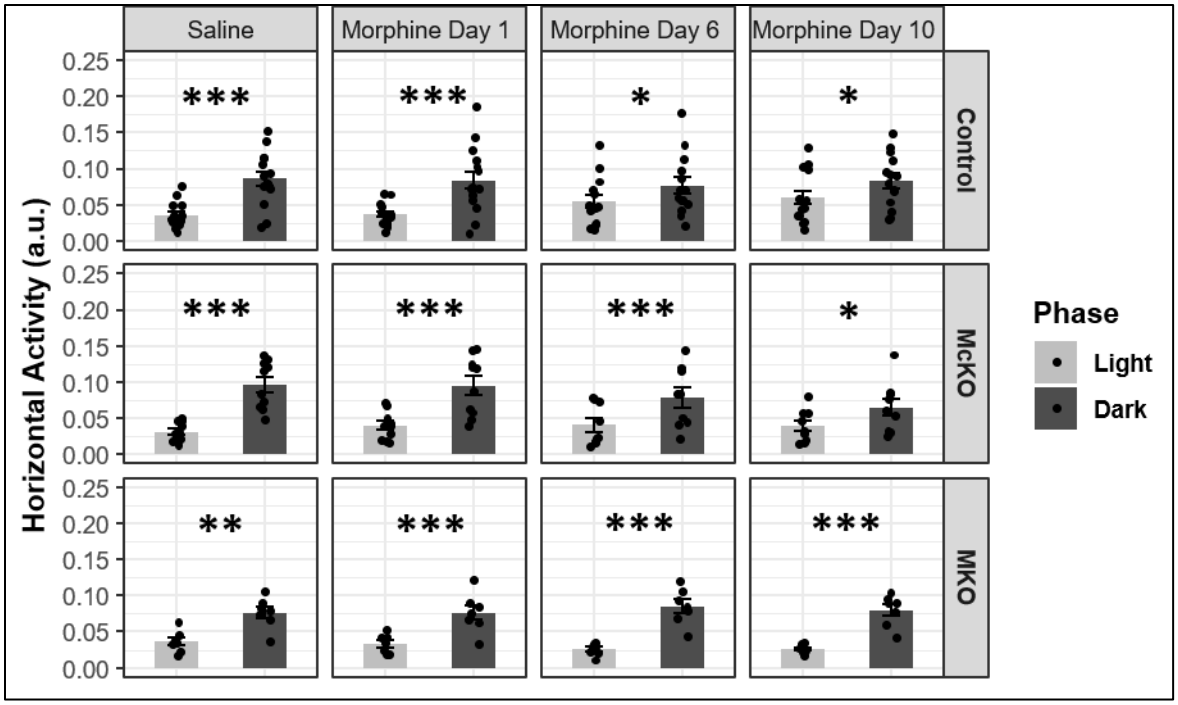

Figure S6. All genotypes retain normal behavioral activity patterns throughout the course of the morphine treatment paradigm. Three-way ANOVA by phase x genotype x experimental day (#p<0.05, *p<0.01, **p<0.001, ***=p<0.0001). Data presented as mean ± SEM.

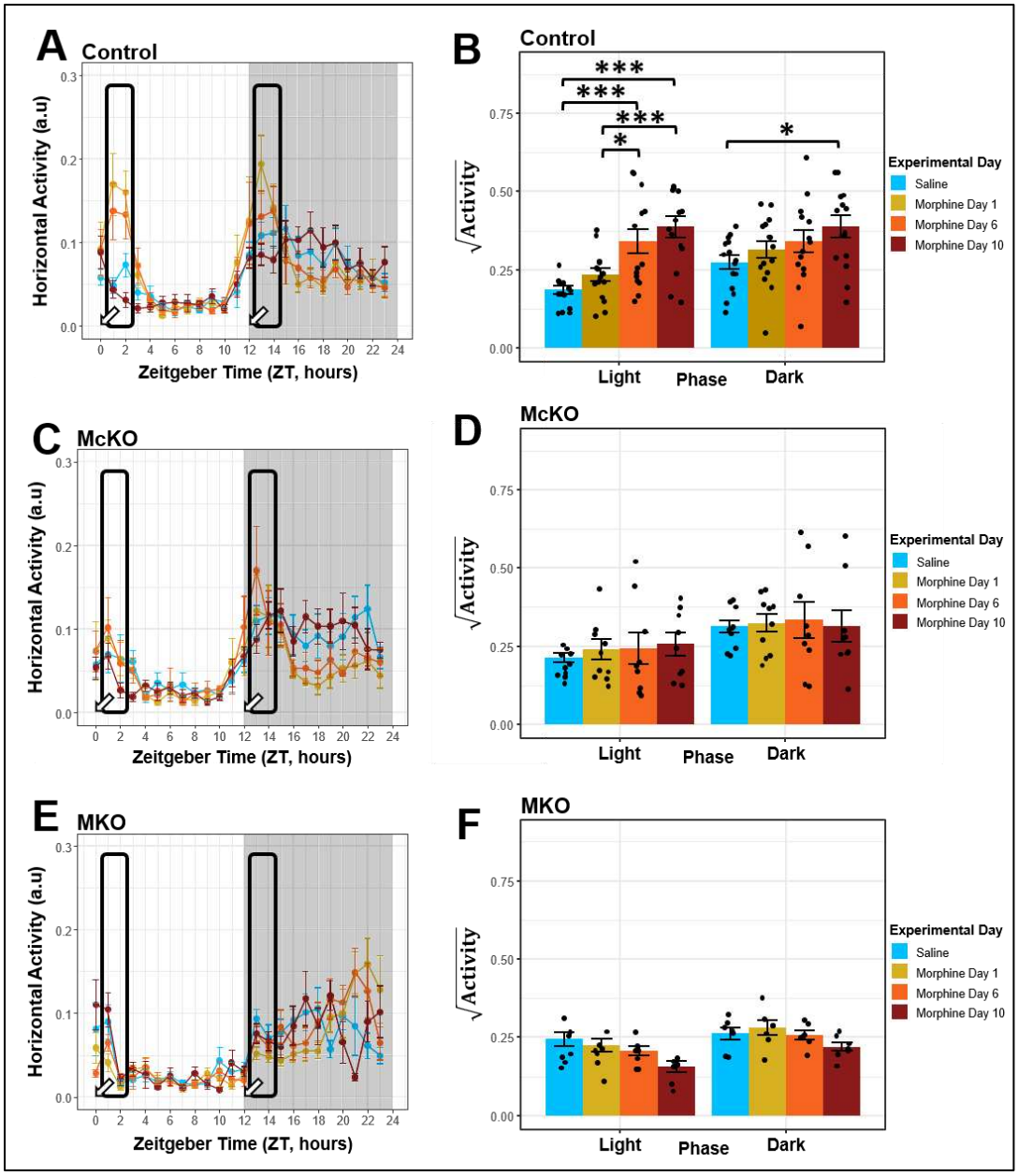

Figure S7. Protracted morphine exposure causes morphine-induced behavioral sensitization in Control, but not McKO or MKO mice. **(A)** & **(B)** Control mice (n=14-15) treated with chronic morphine exhibit morphine-induced behavioral activation 2-3 hours following a 20 mg/kg i.p. morphine injection at ZT0 and ZT12. **(C)** & **(D)** McKO mice (n=9-10) treated with morphine exhibit no change in morphine-induced behavioral activation 2-3 hours following a 20 mg/kg i.p. morphine injection at ZT0 and ZT12. (**E**) & (**F**) MKO mice (n=7) treated with morphine exhibit no morphine-induced behavioral activation 2-3 hours following a 20 mg/kg i.p. morphine injection at ZT0 and ZT12. Three-way ANOVA (phase x genotype x experimental day) with a Holm-Bonferroni post-hoc adjustment performed on all pairwise comparisons. (**p<0.001, ***=p<0.0001). Timing of injections indicated by the white arrows. Data presented as mean ± SEM.

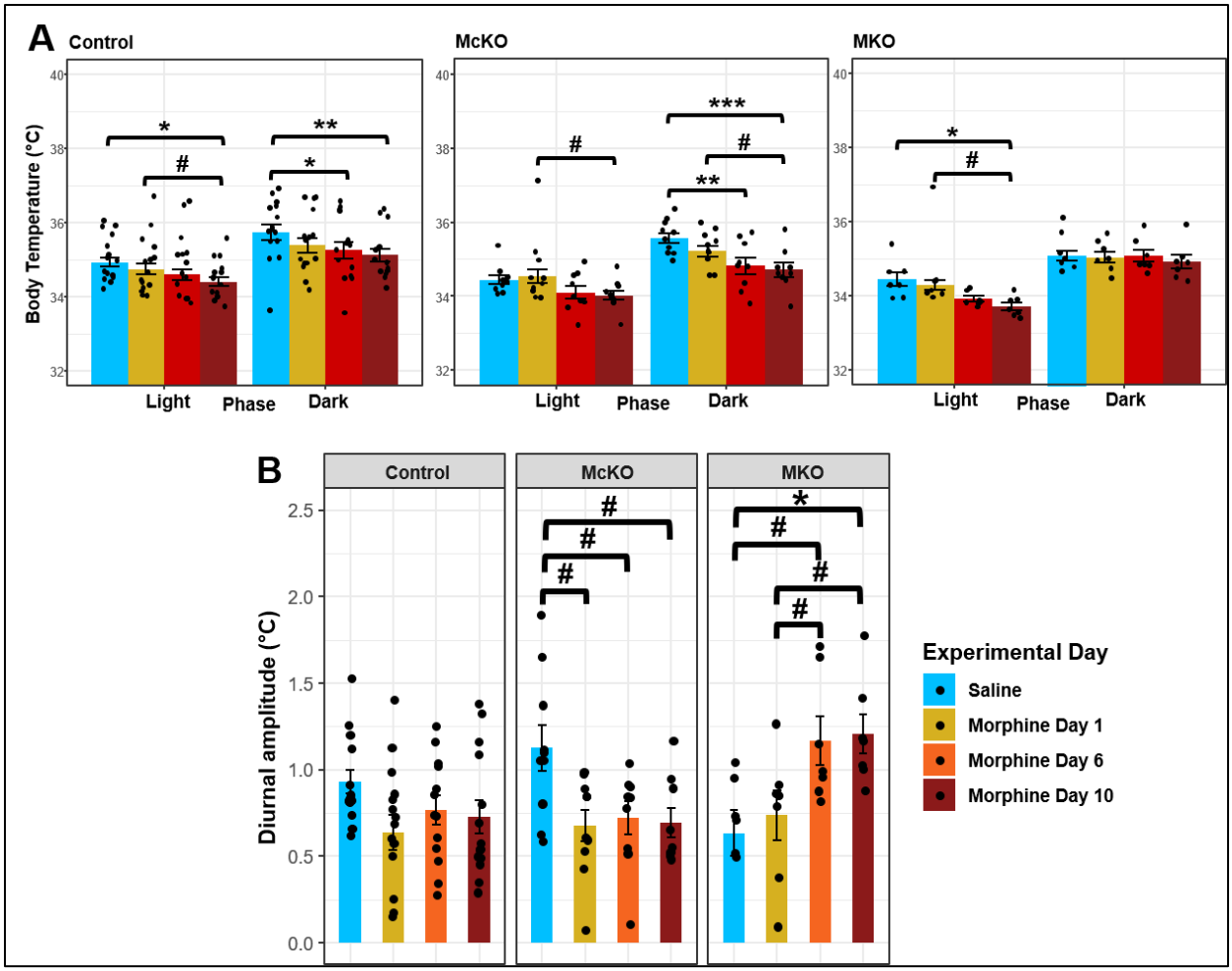

Figure S8. Prolonged, but not acute morphine decreases body temperature in control, McKO and MKO mice. **(A)** Mice treated with morphine for an extended period of time have decreases in average body temperature, except for MKO mice during the dark phase. Three-way ANOVA with a Holm-Bonferroni post-hoc adjustment performed on all pairwise comparisons. **(B)** Control (n=14-15) and McKO (n=9-10) mice exhibit a decrease in diurnal variations in body temperature following chronic morphine exposure, whereas KO (n=7) animals do not. Two-way ANOVA with a Holm-Bonferroni post-hoc adjustment performed on all pairwise comparisons (#p<0.05, *p<0.01, **p<0.001, ***=p<0.0001). Data presented as mean ± SEM.

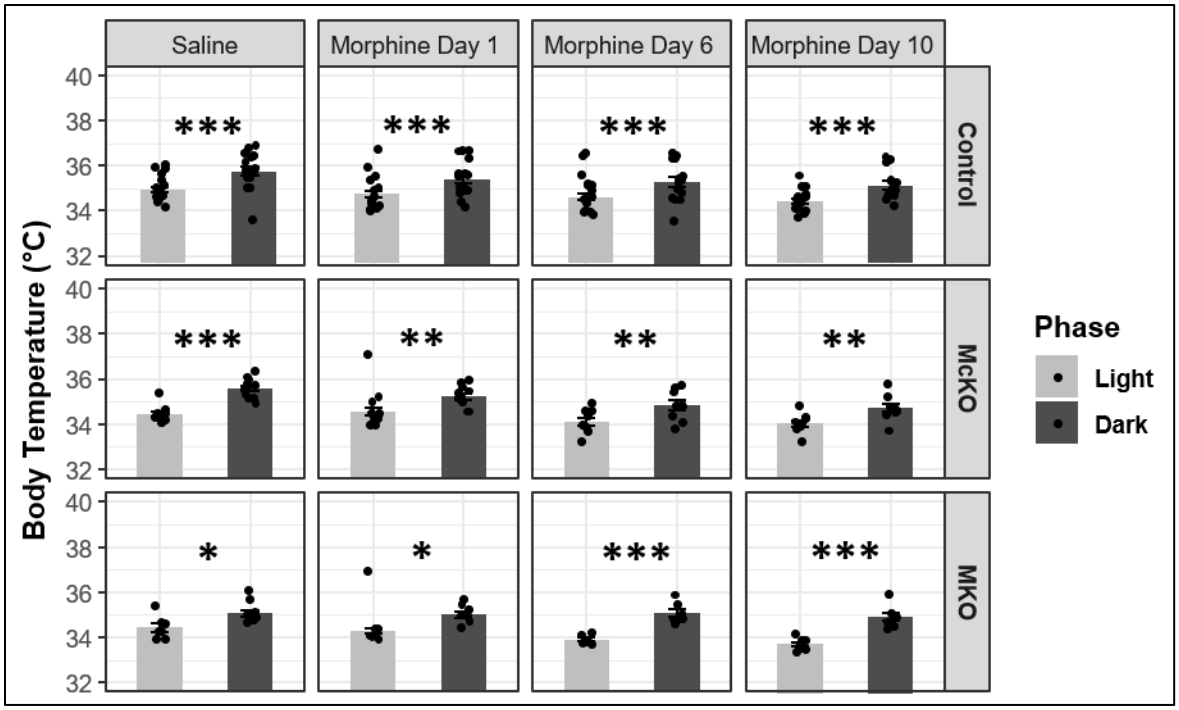

Figure S9. All genotypes retain normal body temperature patterns throughout the course of the morphine treatment paradigm. Three-way ANOVA by phase x genotype x experimental day (#p<0.05, *p<0.01, **p<0.001, ***=p<0.0001). Data presented as mean ± SEM.

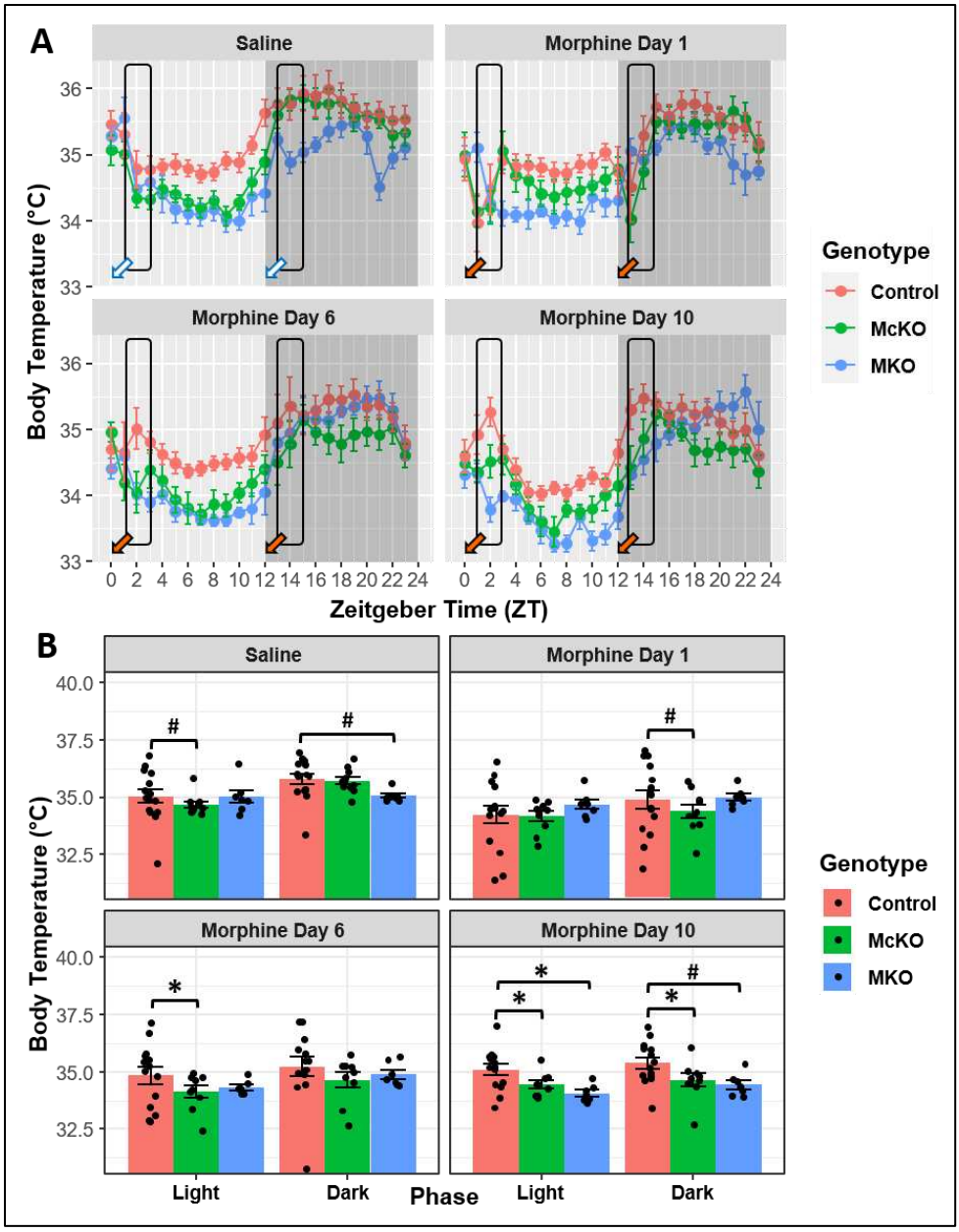

Figure S10. Mice that differentially express the MOR show body temperature changes in response to injections at different stages of a chronic morphine paradigm. **(A)** Following chronic morphine exposure, control (n=14-15) mice have a post-injection body temperature compared to McKO (n=9-10) littermates and age-matched MKO mice (n=7) following a 20 mg/kg i.p. morphine injection at ZT 0 and ZT 12. Arrows indicate time of i.p. injection with either saline (white arrows) or 20 mg/kg morphine (orange arrows). **(B)** Quantification of locomotor activity 2-3 hours following injections at ZT0 and ZT12. Three-way ANOVA with a Holm-Bonferroni post-hoc adjustment performed on all pairwise comparisons (#p<0.05, *p<0.01, **p<0.001, ***=p<0.0001). Data presented as mean ± SEM.

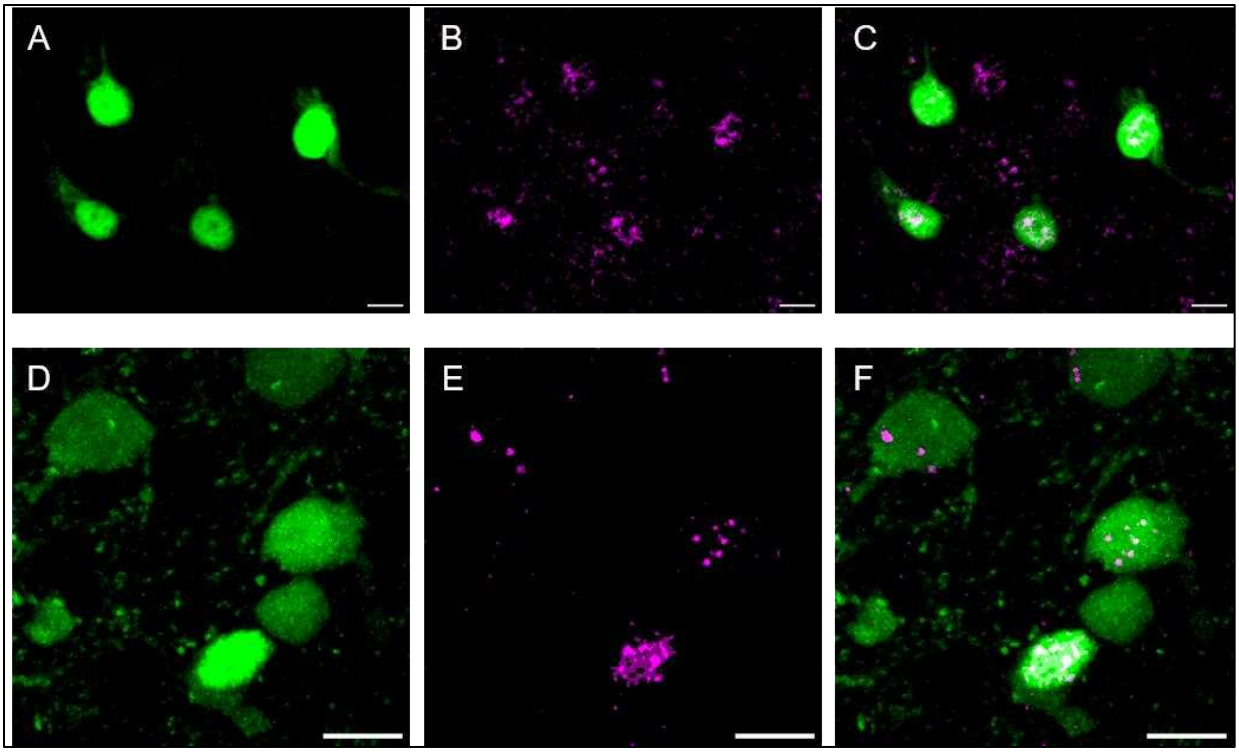

Figure S11. Positive controls show somatic Cre immunolabeling. (**A-C**) Whole-mount retina from a McKO x *Opn4*-EGFP mouse. **(A)** Native GFP signal, **(B)** Cre antibody labeling (psuedocolored), and **(C)** composite image of the maximum projection of all z-stacks containing the cells of interest. **(D-F**) *Gal*-cre-tdTomato brain slice containing the preoptic area of the hypothalamus. **(D)** Native tdTomato signal (pseudocolored), (**E**) Cre antibody labeling (psuedocolored), and **(F)** composite image of the maximum projection of all z-stacks containing the cells of interest. Scale bars = 10 μm.

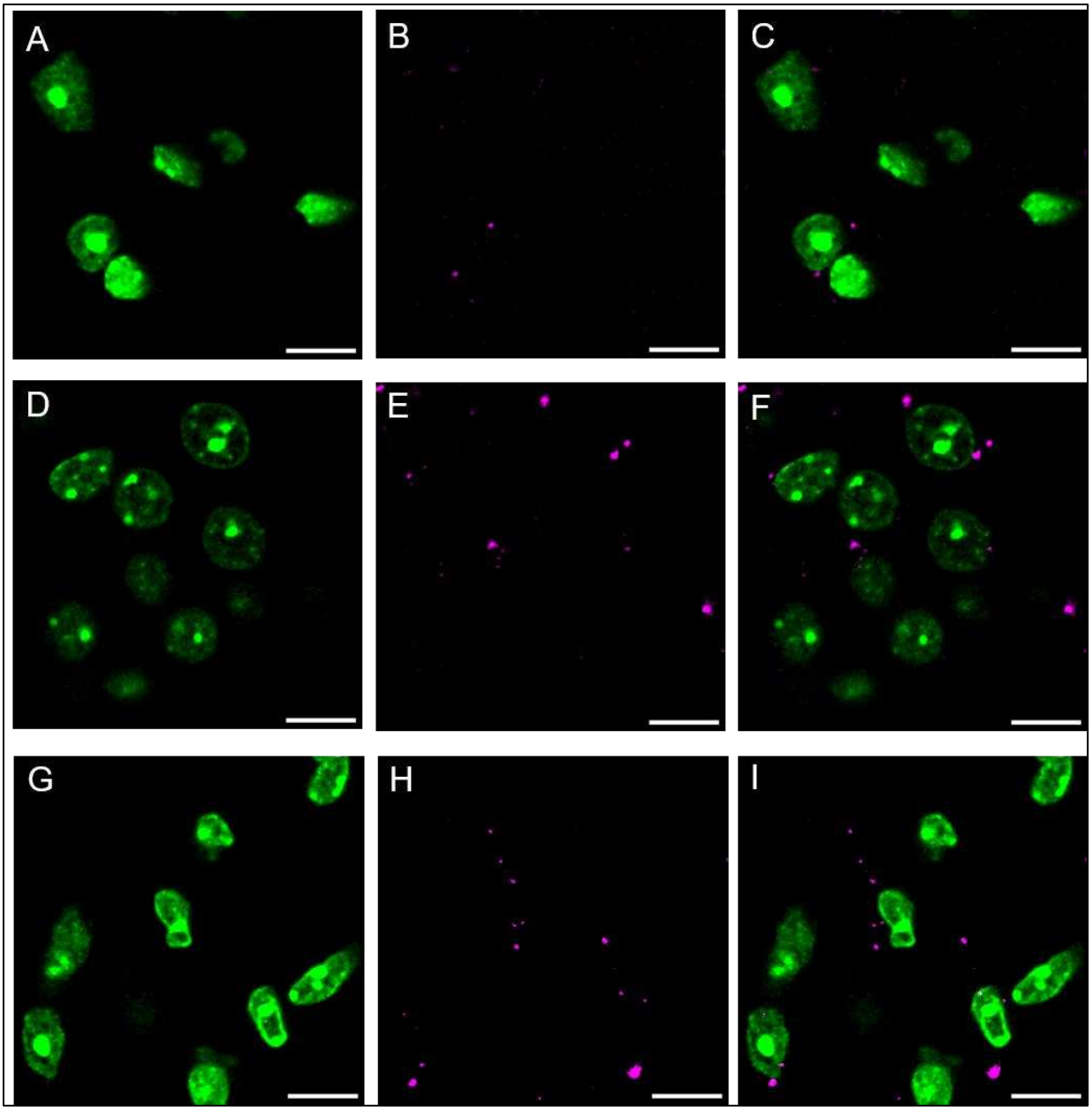

Figure S12. Cre immunolabeling in the McKO brain may originate from EGFP+ ipRGCs. Sections containing the ventrolateral preoptic area of the hypothalamus **(A-C)**, caudate putamen **(D-F)**, and paraventricular nucleus of the thalamus **(G-I)**. Single optical sections showing DAPI nuclear stain (pseudocolored) **(A, D, G)** and Cre antibody labeling **(B, E, H)**. Composite images of single optical sections **(C, F, I)** reveal Cre immunoreactivity primarily on the surface of (i.e. surrounding) cells. Scale bars = 10 μm